



Possibilities for gears with high efficiency which are able to stop in case of a power outage without any additional device

Diplomarbeit

zur Erlangung des akademischen Grades eines

Diplom-Ingenieur

in der Studienrichtung

Maschinenbau

eingereicht von

Philipp Schedl
0827019

an der Fakultät für Maschinenwesen und Betriebswissenschaften
betreut vom Institut für Konstruktionswissenschaften und Technische Logistik durch

Prof. Dr.-Ing. Michael Weigand

Vienna, September 2013

Philipp Schedl

uncorrected copy

Declaration of authorship

I hereby certify that this thesis has been composed by me and is based on my own work, unless stated otherwise. No other person's work has been used without due acknowledgement in this thesis. All references and verbatim extracts have been quoted, and all sources of information, including graphs and data sets, have been specifically acknowledged.

This paper was not previously presented to another examination board and has not been published.

(Date)

(Signature author)

Preface

The present work was done during my internship at the Otis Elevator Company. It was scientifically supported and supervised by the department for Engineering Design and Logistics Engineering of the technical university of Vienna.

My special thanks to for realizing this thesis goes to the following people.

Professor Michael Weigand, head of the department for Engineering Design and Logistics Engineering, for the interest and support of this thesis.

Mr. Alois Senger, center manager of Otis Elevator Company, for the initiation of this thesis.

Mr. Chan-jong Park, employee of Otis Elevator Company, for advices and guidance.

Furthermore all other colleagues of Otis Escalator Engineering Team Vienna for stimulating and pleasant working environment.

Philipp Schedl

September 2012

Abstract

In many drive systems gears are installed. It is common that these transmissions operate with high efficiencies. In some applications these gears should be self-locking additionally. This ensures that the gear is stopped in case of a failure at the motor side. This is necessary in order to reduce the risk of endangering human lives or goods in case of power outage and a brake failure. Because common self-locking gears have high power losses, often additional devices are in use. They are solely responsible for the self-locking. These devices require an increased design volume and construction costs. However they are taken into account to achieve a better efficiency and to decrease costs of operation.

In a global market the use of external devices occurs to additional problems. Many international companies are working with sub-firms thus to open up new markets. In these markets, it is increasingly difficult to maintain an overview of rules, regulations and laws. Sometimes this issue is abused to remove or to manipulate the mentioned external components.

Thereby the question arises how to create a gear which is able to stop only due to a fixed implemented geometry of the power transmitting parts. As a result most of the motor power can be used at the machine. Hence this geometry should be indispensable responsible for the power transmission as well as for the self-locking. That means if this geometry is removed the gear should not be able to perform the same task in the same scope.

The main aim of this master thesis is to find such a solution. Other (sub-)aims of this thesis are specified in a requirement list which is given by a company. Wherein must be noted that this list is valid for multiple applications in mechanical engineering.

Accordingly to the main aim of this master thesis, it has to be clarified if there is any possibility for a significant change of the efficiency performance of the gear only triggered by to the power flow direction.

To find possible solutions, common gears from the literature are selected (chapter 2) and calculated with Mathcad. In this master thesis, three kinds of gears are chosen. Self-locking helical gear (chapter 4), planetary gears in parallel connection (chapter 5) and linkage drives are subjects of investigation (chapter 6). In chapter 3 the influences to efficiencies of commonly used gears are researched generally.

If the calculations show, that it is possible to create self-locking, these models are modeled in a cad-software (Pro/Engineer). Subsequently they are tested in a multi body simulation, wherein it must be noted that these simulation is not part of this master thesis because it is not done of the same author as this thesis. Based on the simulation an analysis of the models is done with Mathcad, Matlab or gnuplot. With the findings of this analysis it is attempted to correct the disadvantages of these models.

This leads to new models which are evaluated with Excel to find out which model satisfies the requirement list best (chapter 7). The evaluation is done according to VDI guideline 2225, wherein the criteria for evaluation have been incorporated from the requirement list.

Kurzfassung

In vielen Antriebssystemen kommen Getriebe zur Anwendung. In den meisten Fällen sollen diese Getriebe hohe Wirkungsgrade aufweisen. Außerdem sollen diese Getriebe zusätzlich selbsthemmend wirken. Dadurch wird erreicht, dass die Last stillsteht, sobald der Antrieb ausfällt. Dies ist nötig um sicherzustellen, dass keine Menschen oder Güter zu Schaden kommen wenn die Leistungsversorgung ausfällt und Bremsen schadhaft sind. Da sich, die in der Literatur bekannten selbsthemmenden Getriebe durch hohe Verluste auszeichnen, werden oftmals zusätzliche Komponenten verwendet. Diese sind ausschließlich für die Selbsthemmung des Getriebes verantwortlich. Durch den Einbau von solchen zusätzlichen Komponenten steigen in der Regel das Bauvolumen und die Produktkosten. Allerdings werden höhere Wirkungsgrade erzielt und damit die Betriebskosten gesenkt.

Mit der Verwendung von zusätzlichen Einbauten entstehen in einem globalen Markt weitere Probleme. Viele internationale Konzerne vertreiben ihre Produkte in einigen Ländern über Subfirmen. Für den Mutterkonzern ist es damit zunehmend schwierig den Überblick über ihre Produkte und die damit verbundenen Haftungen und Gewährleistungen zu bewahren. In einigen Fällen wird dies ausgenutzt um die erwähnten zusätzlichen Komponenten zu entfernen oder zu manipulieren.

Dadurch entsteht die Frage wie ein Getriebe konzipiert sein müsste, welches nur durch eine fix implementierte Geometrie an den leistungsübertragenden Bauteilen, Selbsthemmung erzeugt und dennoch wenig Antriebsleistung vernichtet. Demnach soll die erwähnte Geometrie sowohl für die Leistungsübertragung des Getriebes als auch für die Selbsthemmung verantwortlich sein. Das bedeutet wenn diese Geometrie entfernt oder geändert wird ist das Getriebe nicht mehr in der Lage dieselbe Aufgabe im selben Umfang zu realisieren.

Das Ziel dieser Diplomarbeit ist es ein Konzept für ein derartiges Getriebe zu finden. Durch eine von einer Firma vorgegebene Anforderungsliste sind andere (Sub-)Ziele vorgegeben. Wobei festgehalten werden muss, dass diese Liste für zahlreiche Anwendungen im Maschinenbau Gültigkeit hat.

Entsprechend der Aufgabenstellung gilt es in dieser Diplomarbeit zu Klären, ob nur durch die Richtung des Leistungsflusses verursacht (d.h. ohne zusätzliche Bauteile), das Wirkungsverhalten eines Getriebes signifikant geändert werden kann.

Um mögliche Lösungen zu finden werden aus der Literatur geeignete Getriebe ausgewählt (Kapitel 2) und mit Mathcad berechnet. Insgesamt sind in dieser Arbeit drei Arten von Getrieben ausgewählt worden. Diese waren die selbsthemmende Schrägverzahnung (Kapitel 4), Planetengetriebe in Parallelschaltung (Kapitel 5) und der Kurbeltrieb (Kapitel 6). In Kapitel 3 sind die Einflüsse aus Wirkungsgrade von häufig angewendeten Getrieben möglichst allgemein untersucht worden.

Sollte die Berechnungen zeigen, dass Selbsthemmung möglich ist, werden diese Modelle mittels CAD-Software (Pro/Engineer) modelliert. Diese dienen dazu um das Verhalten der Getriebe in einer Mehrkörpersystem-Simulation zu testen. Hierbei muss erwähnt werden, dass diese Simulation nicht vom Autor dieser Diplomarbeit durchgeführt wird und dementsprechend auch nicht Teil dieser Arbeit ist. Auf Basis der Simulation wird mittels Mathcad, Matlab oder gnuplot eine Analyse der Modelle durchgeführt. Mit den Erkenntnissen dieser Analyse wird versucht die Nachteile dieser Getriebemodelle zu korrigieren.

Dies führt zu neuen Modellen, die beurteilt werden um herauszufinden welches Modell die Anforderungsliste am besten erfüllt (Kapitel 7). Die Beurteilung wird dabei mit Excel in Anlehnung an die VDI-Richtlinie 2225 durchgeführt. Wobei die Bewertungskriterien aus der Anforderungsliste übernommen werden.

Content

Declaration of authorship.....	i
Preface.....	ii
Abstract.....	iii
Kurzfassung	iv
Content	v
List of tables	vii
List of figures.....	viii
Nomenclature.....	x
Wording.....	xi
1 Introduction and statement of the problem.....	1
1.1 Definitions and theory of self-locking and self-braking as well as common solutions 1	
1.1.1 Distinction of self-locking and self-braking according to VDI.....	2
1.1.2 Theory of self-locking.....	2
1.1.3 Problems with self-locking gears	4
1.1.4 Common solutions for self-locking gears with high efficiency	4
1.2 Relationship between this thesis and the systematic design procedure.....	6
1.3 Requirement list in more detail	7
2 Procedure in this thesis and principle solutions	9
3 General examination of the efficiency of selected gears	14
3.1 Influences on the efficiency of gears with tooth system	14
3.2 Comparing efficiencies of selected gears	16
3.2.1 Worm gear	16
3.2.2 Crossed-helical gear.....	19
3.2.3 Spur gear, helical gear and also bevel gear	21
4 Self-locking helical gear	27
4.1 Basic idea how the self-locking should be generated	27
4.2 Procedure for realization of the self-locking geometry	28
4.2.1 Self-locking condition, its background and its analysis	28
4.2.2 Used calculation procedure in detail.....	29
4.2.3 General relationships in the design procedure of a self-locking helical gear	32
4.3 Comparison of the geometry with the fundamental law of gearing and with conventional procedure.....	33
4.3.1 Comparison of the geometry with the fundamental law of gearing	33
4.3.2 Comparison with conventional calculation procedure	34
4.4 Limits of this approach and attempts to change them.....	36
4.4.1 Limitations of the approach	36
4.4.2 Attempts to change the limits	39
4.5 Conclusion of the self-locking helical gear	45

5	Planetary gears in parallel connection	46
5.1	Short theory of planetary gears	46
5.1.1	Differentiation of planetary gears and conventional gears	46
5.1.2	Possible operational modes, gear ratios, rotational speeds and torques.....	48
5.1.3	Powers, power flow and efficiency of the planetary gears	49
5.1.4	Compound planetary gears	50
5.1.5	Self-locking Planetary gears	52
5.1.6	Limitations in design	56
5.2	Models of self-locking planetary gears in parallel connection	57
5.3	Conclusion of the self-locking planetary gears in parallel connection	64
6	Linkage drive.....	65
6.1	Short treatise of the theory of linkage drives.....	65
6.2	Possibility for self-locking	67
6.3	Created models.....	68
6.4	Conclusion of the linkage drive concept	71
7	Evaluation	72
7.1	Procedure of the evaluation accordingly to VDI 2225	72
7.2	Evaluation procedure in detail	74
8	Conclusion of the master thesis	83
	Literature	86
	Appendix.....	89
	A -Creating a cad-model	89
	B –Source code of the Matlab plot	92

List of tables

Table 1.1: Requirement list in detail	7
Table 5.1: Comparison of advantages and disadvantages of planetary gears	46
Table 5.2: Determination of the direction of the power flow (Bouchè, 1988, p.148)	50
Table 6.1: Possible designs of linkage drives (accordingly to Volmer, 1978a, p.137)	66
Table 7.1: Scale which is typical be used for paired comparison (Pahl, 2007, p.178)	73
Table 7.2: Example of a paired comparison	73
Table 7.3: Scale of VDI 2225 guideline (Pahl, 2007, p.172)	73
Table 7.4: Paired comparison in detail	75
Table 7.5: Evaluation of the self-locking helical gear	76
Table 7.6: Evaluation of the Wildhaber/Novikov self-locking gear	77
Table 7.7: Evaluation of the load sharing self-locking gear	77
Table 7.8: Evaluation of the planetary gear with improved connection	78
Table 7.9: Evaluation of the optimized planetary gear in parallel connection	79
Table 7.10: Evaluation of the planetary gear in parallel connection with Cyclo gear	79
Table 7.11: Evaluation of the Linkage drive	80
Table 7.12: Total utility of all concepts	82

List of figures

Figure 1a: Principle of the wedge sliding gear: non self-locking (left) and self-locking (left)	3
Figure 1b: General principle of wedge sliding gear: non self-locking (left) and self-locking (right)	3
Figure 1c: Freewheel (left; Hiersig, 1995, p.399), with forces (right; Wittel, 2011, p.449)	5
Figure 1d: Arrangement of self-locking worm gear with high efficiency (DE 3442138 A1, Fig.1)	5
Figure 1e: Systematic design procedure accordingly to VDI guideline 2222 (according to Pahl, 2007, p.198).....	6
Figure 2a: General approach of this thesis	9
Figure 2b: Selecting procedure in this thesis	10
Figure 2c: Self-locking differential arrangement: above from literature (Looman, 2009, p.412), below idea in this thesis	11
Figure 2d: Fluid transmission arrangement (left) and principle (right) (both: Looman, 2009, p.140)	12
Figure 2e: Linkage drive	12
Figure 2f: Friction drive	13
Figure 3a: Typical industrial gear	14
Figure 3b: Classification of gears according to position of axles (Ravi, 2011, p.187).....	16
Figure 3c: Worm gear (Künne, 2001, p.282)	17
Figure 3d: Power losses of the worm gear in case of driving worm.....	18
Figure 3e: Power losses of worm gear in case of driven worm wheel	19
Figure 3f: Crossed-helical gear (index 1 represents the pinion and index 2 represents the wheel) (Perović, 2002, p. 407)	20
Figure 3g: Power losses of the crossed-helical gear in case of driving pinion.....	21
Figure 3h: Trend of the friction coefficient across the line of action (Niemann, 2003, p.223)	23
Figure 3i: Typical trend of sliding velocity across the line of action (according to: Niemann, 2003, p.38)	23
Figure 3j: Transverse contact ratio $\varepsilon_{\alpha t}$ depending on the profile angle α_n in normal section.....	24
Figure 3k: Relationship of the profile angle in transverse section α_{wt} with the profile angle in normal section α_n (left ordinate) and with the helix angle β (right ordinate).....	25
Figure 3l: Power losses of spur gear and helical gear	26
Figure 4a: Self-locking helical gear (Kapelevich, 2013, p.182)	27
Figure 4b: Background of the self-locking condition.....	28
Figure 4c: Plot of the self-locking condition.....	29
Figure 4d: Parameter study of the design approach of the self-locking helical gear	32
Figure 4e: General Fundamental law of gearing (Phillips, 2003, p.42, left) and two dimensional gearing (Niemann, 2003, p.33, right)	33
Figure 4f: Restricted area of possible solutions (Niemann, 2003, p.67, left) and more possible solutions (Kapelevich, 2013, p.9, right).....	35
Figure 4g: First self-locking helical gear	36
Figure 4h: Overview of possible solutions to handle high axial forces (left: Dudley, 2012, p.12, right: Künne, 2001, p.271)	37
Figure 4i: Relationship of lubricant, material and average friction coefficient (Tabor, 1966, p.II.36)	38
Figure 4j: Basic idea of calculation the strength at the root	38
Figure 4k: Ideas to fix the issues of the self-locking helical gear	39
Figure 4l: Sketch of a conventional internal gear	39
Figure 4m: Model with increased teeth height.....	40
Figure 4n: Model (right) and basic idea to increase teeth height at the wheel (left)	41
Figure 4o: Wedge edge gear with crossed axis (Bouché, 1995, p.63)	41
Figure 4p: Wildhaber/Novikov tooth profiles (GB 266163 A, Fig.1)	42
Figure 4q: Model with Wildhaber/Novikov mesh	43
Figure 4r: Cyclone tooth profiles (Niemann, 2003, p.42)	43

Figure 4s: Hlebanja tooth profile (Niemann, 2003: p.43)	44
Figure 4t: Self-locking helical gear with load sharing	44
Figure 5a: Conventional (a) and planetary gearbox (b) (Müller, 1982, p.8)	47
Figure 5b: Typical planetary gear (Rohloff AG)	47
Figure 5c: Symbols of conventional gears (left) and planetary gears (right)	47
Figure 5d: Serial connection (left) and parallel connection (right) of planetary gears	51
Figure 5e: pdf plotted over a $i_{SL} - i_{su}$ plane	51
Figure 5f: Basic idea of self-locking planetary gears: normal operation (left) and self-locking (right) (Müller, 1998, p.51)	52
Figure 5g: Possible gear principles and there basic ratios (accordingly to Volmer, 1978b, p.18÷19) ..	53
Figure 5h: 3-dimensional plot of the self-locking condition	54
Figure 5i: Contour plot in the i_0 -efficiency plane	55
Figure 5j: Assembling condition (Volmer, 1978b, p.52)	56
Figure 5k: Limitation of the gear ratio	56
Figure 5l: Approach of self-locking planetary gears in parallel connection	57
Figure 5m: Self-locking helical gear and planetary gear parallel connection	58
Figure 5n: Models based on literature: Scheme (above; Bouchè, 1988, p.59÷60), from literature (middle) and improved efficiency (below)	59
Figure 5o: General description of the arrangement in three shaft operation mode	60
Figure 5p: Model with improved connection: Scheme (above) and model (below)	61
Figure 5q: Optimized planetary gear in parallel connection: Scheme (above) and model (below)	62
Figure 5r: Model which includes the Cyclo gear	63
Figure 6a: Comparison of the patent (below: modified from DE 10127676 A1, Fig. 1) with literature (above: accordingly to Volmer, 1978a, p.60)	68
Figure 6b: First model of the linkage drive	69
Figure 6c: Second model of the linkage drive	70
Figure 6d: Scheme of the linkage drive model	71
Figure 7a: Overview of the paired comparison	74
Figure 7b: Summary of the evaluation	81
Figure 8a: Evaluated models: Involute self-locking helical gear (a), Wildhaber/Novikov self-locking helical gear (b), Self-locking helical gear with load sharing (c), Planetary gear with improved connection (d), Optimized planetary gear (e), Planetary gear in parallel connection with a Cyclo gear (f) and Linkage drive (g)	84
Figure 9a: Assembling	89
Figure 9b: Model tree of the skeleton part (right) and skeleton part (left)	90
Figure 9c: Sketch of the measurement	91
Figure 9d: Pinion of the arrangement	91

Nomenclature

α	profile angel at the any diameter in transverse section
α_a	profile angel at the addendum diameter in transverse section
α_n	profile angel at the pitch diameter in normal section
α_f	profile angel at the pitch diameter in transverse section
α_{wt}	profile angel at the operating diameter in transverse section
β	helix angel
γ	gradient or wedge angel
$\varepsilon_{\alpha t}$	contact ratio in transverse section
η	efficiency or mesh efficiency
η_0	base efficiency
ν	profile angel at the intersecting of drive and coast flank in transverse section
ξ	dimensionless power losses
ρ	friction angel
Σ	sum of the helix angels
ρ_{a0}	fillet radius of the tool
A_s	back clearance
c_{min}	tip clearance
d	pitch diameter
d_a	addendum diameter
d_b	base diameter
d_r	root diameter
d_w	operating diameter
e	eccentricity
f	friction coefficient
F_{th}	resulting force at the tooth
h_{a0}	addendum height of the reference profile
h_{fp}	foot height of the reference profile
i_{24}	base ratio
i_{xy}	relative ratio
l	length of a linkage
l_f	lever to the forces
m	mass
n	rotational speed
N	number of teeth
P_{in}	input power
P_l	power losses
v_s	sliding velocity
w	mesh width
w_r	tooth with at the root
x_L	limit of x-shift
z_L	minimum number of teeth

Wording

addendum diameter.....	Kopfkreisdurchmesser
altscher protractor.....	Altscher Übertragungswinkel
assembling condition.....	Einbaubedingung
axial slide bearing.....	Axialgleitlager
back clearance.....	Rückenspiel
banging.....	Das Hämmern
base diameter.....	Grundkreisdurchmesser
benefit value.....	Nutzwert
branching position.....	Verzweigungsposition
carrier.....	Planetenträger
central wheel.....	Zentralrad
center of curvature.....	Krümmungsmittelpunkt
chattering.....	Das Rattern
circumference speed.....	Umfangsgeschwindigkeit
clamping roller.....	Klemmrolle
coast flank.....	Schubflanke
conveyor gears.....	Fördertechnikgetriebe
coupling power.....	Kupplungsleistung
dead-center position.....	Totpunktslage
division gear.....	Teilergetriebe
double rocker.....	Doppelschwinge
drag-link mechanism.....	Doppelkurbel
drive flank.....	Zugflanke
engagement point.....	Eingriffspunkt
freewheel.....	Freilauf
fundamental law of gearing.....	Verzahnungsgesetz
guide wheel.....	Leitrad
heart treading.....	Wärmebehandlung
immersion depth.....	Eintauchtiefe
injection lubrication.....	Einspritzschmierung
line of action.....	Eingriffslinie
load balancing.....	Lastausgleich
mesh width.....	Zahnbreite
middle diameter.....	gemittelter Durchmesser
mulit-disk clutch.....	Lamellenkupplung
no-load loss.....	Leerlaufverlust
normal section.....	Normalschnitt
operating diameter.....	Wälzkreisdurchmesser
paired comparison.....	paarweiser Verleich
parallel crankshaft gear.....	Parallelkurbelgetriebe
partial benefit value.....	Teilnutzwert
pitch diameter.....	Teilkreisdurchmesser
point of action.....	Eingriffspunkt
power division.....	Leistungsteilung
power summation.....	Leistungssummierung

prismatic joint.....	Schubgelenk
rack.....	Zahnstange
rack and pinion gearing.....	Triebstockverzahnung
radial clearance.....	Radialspiel
radial slide bearing.....	Radialgleitlager
radius of curvature.....	Krümmungsradius
rattling.....	Das Klappern
rest state.....	Ruhezustand
rolling circle.....	Rollkreis
rolling power.....	Wälzleistung
root diameter.....	Fußkreisdurchmesser
rotational speed.....	Drehzahl
splash lubrication.....	Tauchschmierung
strength of the root.....	Zahnfußspannung
summation gear.....	Summiergetriebe
swivel joint.....	Drehgelenk
technical contradiction.....	technischer Widerspruch
three shaft operation mode.....	Dreiwellenbetrieb
tip diameter.....	Spitzkreisdurchmesser
tooth breakage.....	Zahnbruch
transverse section.....	Strinschnitt
two shaft operation mode.....	Zweiwellenbetrieb
Vickers hardness.....	Vickershärte
weighting factor.....	Gewichtungsfaktor
worm wheel.....	Schneckenrad
x-shift.....	Profilverschiebung
x-tooth system.....	Radpaar mit Profilverschiebung

1 Introduction and statement of the problem

In mechanical engineering gears are often used to change the allocated dynamic and kinematic variables. For safety reasons, it is often desirable/required that these gears have characteristics which bring the whole application to stop in case of power outage. These characteristics are called self-locking or self-braking. If this can be realized with the power-transmitting parts, in most of the cases this leads to a decrease in the efficiency of the gear. If standards, guidelines or customers require high efficiency of the application the self-locking/self-braking is commonly achieved with additional parts.

Nowadays, many companies operate internationally and sometimes with sub-firms. It is not always easy for them to keep track of all of their products and the related guarantees. Sometimes it happens that products of sub-firms are manipulated in the mentioned additional parts. In case of damage often follows a long legal dispute, in which must be clarified who is liable for the consequences. During this clarification process high costs and a loss of image of the original company can be caused. To prevent such cases, solutions are required where the power transmitting gears realize the self-locking/self-braking and yet a high efficiency while operation is available.

To find such a solution is the main aim of this master thesis. Secondary objectives of interest are:

- driving in both direction,
- silent operation,
- high gear ratio (approximately 100),
- outside diameter as less as possible,
- transmitting high torques (above 1000 Nm)
- overall efficiency above 90% and
- parallel or coaxial axis.

In the following chapter self-locking and self-braking are defined, problems which may occur with self-locking gears are described and common solutions are given.

1.1 Definitions and theory of self-locking and self-braking as well as common solutions

Because of the reasons mentioned above, one of the main requirements of this thesis, it is to find a small self-locking gear with high efficiency while operation. The following chapter describes self-locking as it is defined in the literature, gives two common designs, the relationship of this thesis to the systematic design procedure and in the end, the requirement list will be specified and discussed in more detail.

1.1.1 Distinction of self-locking and self-braking according to VDI

In VDI guideline 2158 definitions of self-locking and self-braking are given as follows.

Self-locking: *“A transmission is self-locking when it is able to produce in the rest state any large forces or moments acting on the retarded element H which causes frictional forces in the gear, which inhibit at least one element which is placed in the power flow direction, so that no movement is possible.”* (Hinrichsen, 2007, p.7)¹

Self-braking: *“A transmission is self-braking, if any size of external forces and moments in the running state acting at the inhibited element H, generate power losses at the elements in the power chain, which are, averaged over time, greater as the power which is supplied through element H. It comes to a stop, if the power which is supplied by element A is zero averaged over time.”* (Hinrichsen, 2007, p.7)¹

This means that self-locking and self-braking describe the ability to get a gear to stop when the motor power is suddenly reduced. In such a state, two cases have to be distinguished.

- Inertial driving
In this case, the inertia is driving the gear on the output shaft in the same direction as before the reduction of motor power.
- Backdriving
In this case, the load is driving the gear on the output shaft in the opposite direction as before the failure.

In both cases the former output shaft becomes input shaft and vice versa. Thus the power flow in the gear changes direction.

Accordingly to the definitions above it can be argued that the definition of self-braking includes more applications than the definition of self-locking. This is because of the occurrence of friction in the rest state. This leads to a more strictly definition of the self-locking as the self-braking. As a result it can be argued that any self-braking gear also performs self-locking. Contrariwise any self-locking gear is not necessarily executing self-braking.

1.1.2 Theory of self-locking

From the literature it is known that commonly wedge sliding gears, worm gears, planetary gears, crossed-helical gears and screwing transmissions are predestined to perform self-locking. This does not mean that other gears for example spur gears are not able to create self-locking with high efficiency.

For many of the aforementioned gears the wedge sliding gear provides the basis. Thus this principle is researched in the following (see figure 1a).

¹ Translation by the author of this master thesis

In **figure 1a** it is visible that the output force F_{out} , acts against the wedge. This leads to an output power with negative sign which shows that the power is leaving the mechanism.

In the self-locking case this is not possible. Therefore an additional force would be necessary to move the output wedge. This can be achieved by decreasing the wedge angle γ_{out} below the friction angle ρ . In this special case the relationship between the two wedge angles can be presented as $\gamma_{out} + \gamma_{in} = \pi/2$.

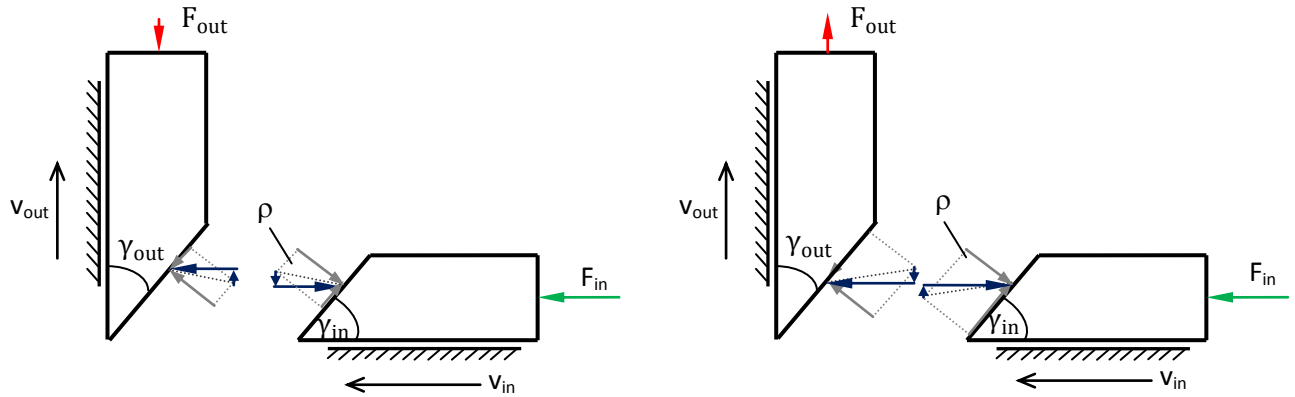


Figure 1a: Principle of the wedge sliding gear: non self-locking (left) and self-locking (left)

A more general description as in figure 1a shows the following figure. In this figure is $\gamma_{out} + \gamma_{in} \neq \pi/2$ valid.

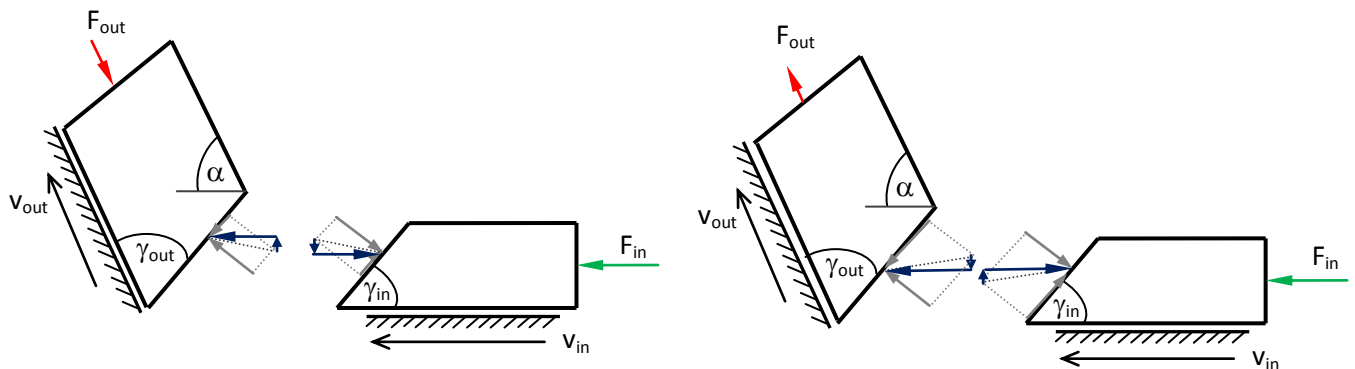


Figure 1b: General principle of wedge sliding gear: non self-locking (left) and self-locking (right)

The principle of the occurrence of the self-locking is the same in figure 1a and figure 1b; but the efficiency is different. Both principles are commonly used for self-locking. The principle in figure 1a is typically included in the worm gear and the screwed transmission. The principle of **figure 1b** is used in crossed-helical gears. From the literature (e.g. Volmer, 1978a, p.280) it is well known that the worm gear (in case of self-locking) has efficiency below 50%. Accordingly the worm gear is not a possible solution in this thesis. In contrast the self-locking crossed-helical gear can reach higher efficiencies. In the literature (Bouchè, 1988, p.61÷63) it is described that such a gear can reach efficiencies around 78% at the boarder of self-locking.

1.1.3 Problems with self-locking gears

One problem with self-locking gears is the low efficiency. Another problem is that vibrations may occur in the gear. Here, the phenomena chattering, rattling and banging must be mentioned (Hinrichsen, 2007, p.5). All these non-linear vibrations have related causes which are similar to the slip-stick effect (described in: Bhushan, 2013, p.358÷366). But they only occur under certain conditions which are not entirely clear, but their appearance must be considered in a thesis of self-locking and self-braking. Best studied is the chattering, so this is described in more detail in the following.

Disadvantages that may arise from such vibrations are increased noise and increased abrasion. They can also lead to an (unwanted) acceleration of the actuator (Hinrichsen, 2007, p.5).

The phenomenon of chattering always occurs at state transitions to self-locking gear (not to self-braking). Thereby it is observed that the contact surfaces of the force-transmitting elements continuously changes. In that process the acceleration changes from a defined state into an undefined state which leads to a blocking gear. Thus the torque ratio is increased, resulting in a renewed change of the contact surfaces. Furthermore the masses of the vibrating system must meet certain requirements (Hinrichsen, 2007, p.10÷11). In the literature there are some conditions for avoiding chattering. One relative simple, is the condition accordingly to Fügen (see equation (1-1); (Hinrichsen, 2007, p.14)).

$$m_2 - m_1 * \tan(\gamma) * \tan(\rho - \gamma) > 0 \quad (1-1)$$

Where m_1 describes the mass of that body which drives in operation mode, m_2 is the mass of that body which drives in case of power outage, γ stands for the wedge angle of the body with index one and ρ is the friction angle.

This condition is only valid for the case which is shown in figure 1a (e.g. the worm gear). Then body number 1 stands for the input body (see figure 1a) which describes the worm and body number 2 represents the output body which means the driven wheel.

1.1.4 Common solutions for self-locking gears with high efficiency

The following two options are given to get a gear, depending on the load, to a stop by using an additional device. The first option describes the typically used device, the second option stands for a wide range of creative ideas to achieve high efficiency with additional devices.

Freewheel

In the following figure a typical freewheeling arrangement is visible (left). A freewheel is commonly used in bicycles and in shiftable gears which are used in cars or aircraft gears.

The freewheel, which is shown in **figure 1c** transmits the power of the clamping rollers to the outer ring. These rollers are designed with angles (α) which are smaller than the friction

angle (ρ). Therefore the freewheel locks the retroactive power flow from the machine to the motor side. Without any argument it can be argued that such an arrangement is similar to the principle which is shown in figure 1a.

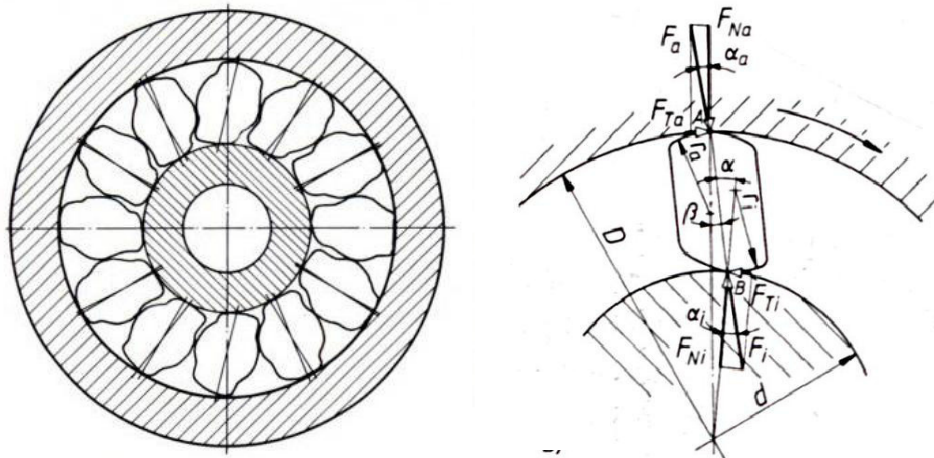


Figure 1c: Freewheel (left; Hiersig, 1995, p.399), with forces (right; Wittel, 2011, p.449)

Non self-locking worm arrangement

This solution is taken from the patent DE 3442138 A1. It is also described in (Bouch , 1988, p.64-66). The assembling is shown in **figure 1d**. It consists of a non self-locking worm gear, two freewheels and two multi-disk clutches.

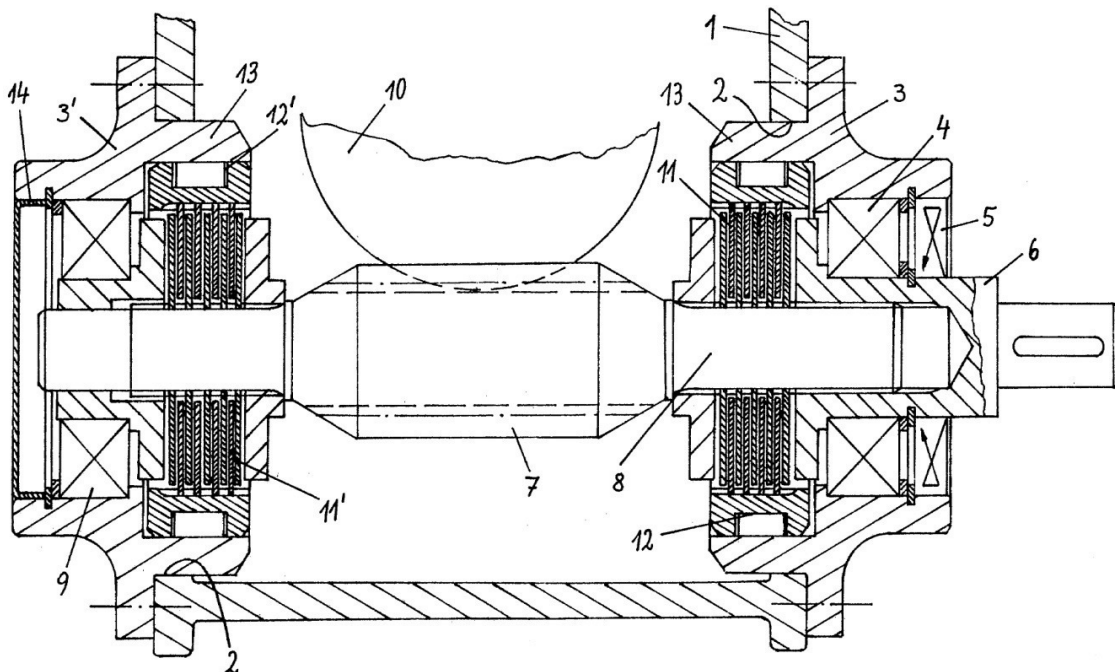


Figure 1d: Arrangement of self-locking worm gear with high efficiency (DE 3442138 A1, Fig.1)

The axial force of the worm (7) closes one clutch (11 or 11') permanently. This force is proportional to the braking torque of the clutch. Therefore this mechanism is able to perform self-locking.

In normal operation mode those freewheel (12 or 12') which is located at the blocked multi-disk clutch, deblock the closed clutch. The other freewheel has opposite locking direction; so it blocks the clutch which is open. With this combination less power losses occur by closing one clutch while normal operating.

If the motor power is reduced suddenly the application is able to create self-locking. This is because the torque of the closed clutch is supported by the locked freewheel.

1.2 Relationship between this thesis and the systematic design procedure

For innovations and designing new products there are several approaches to come to a solution. One of them, which give a focused approach to the issue, is the systematic design procedure. This systematic design procedure is well known in the literature (Pahl, 2007). Accordingly to the VDI guideline 2222 the systematic design procedure of products can be presented as it is visible in **figure 1e**.

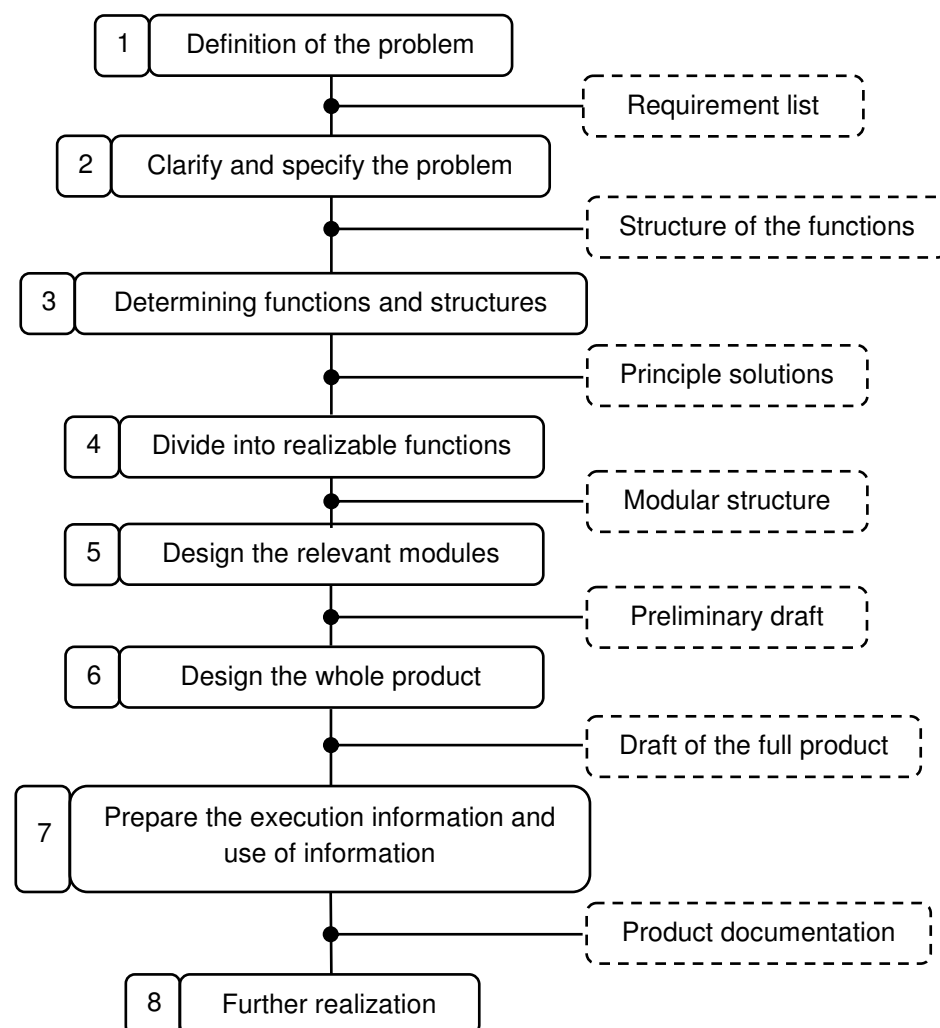


Figure 1e: Systematic design procedure accordingly to VDI guideline 2222 (according to Pahl, 2007, p.198)

In the following the general systematic design procedure is described and the relations to this thesis are mentioned.

- 1) Figure 1e shows that the systematic design procedure starts with a definition of the issue. For this thesis this is done in chapter 1.1.
- 2) By defining a requirement list this definition can be clarified in more detail. In this step is necessary to fix the requirements in quantitatively as possible. In this master thesis the requirement list is given in table 1.1.
- 3) Defining the functionalities and the principle structure of the product should lead to principle solutions for the issue. This step is the main task in this master thesis. The most important aim is to find out if there are gears which can satisfy the requirement list best.
- 4) The issue should be divided into parts which are more suitable for the designers. The modules which are the outcome of this dividing should be designed relatively independent of each other. This step is not necessary in this thesis because there are only a view parts and no modules to design.
- 5) When the problem can be divided into models. They have to be drafted in this step. This step is not necessary in this thesis.
- 6) If the drafting of the modules is finished, the modules can be assembled to one product. To design this is the next step of the systematic design procedure. This step is not possible in this master thesis.
- 7) It is necessary to compile a documentation and information which can be used by customers. This step is not needed in this thesis.

As it is mentioned above, the aim of this master thesis is not to create a new product. Hence not all steps of the procedure like it is shown in **figure 1e** have to be done.

1.3 Requirement list in more detail

The following requirements are specified for this thesis but they are also generally applicable to gears which must ensure a cheap, quiet, safe, 24-hour operation in harsh environmental conditions. Accordingly to this general pretension of this thesis, most of the following requirements are not quantified in more detail.

The most important aims were summarized at the beginning of this chapter.

Table 1.1: Requirement list in detail

Demands D or Wishes W	Requirements	Quantitative
	• Geometry:	
W	- total dimensions: cylindrical	as small as possible
W	- small bearing area	
W	- parallel or coaxial axes of shafts	
	• Kinematics:	
D	- continuous movement at output shaft	
	- driving in both directions	
	• Forces:	

W	- low weight	
D	- able to transmit high torques	above 1000 Nm
W	- high gear ratio	around 100
D	- load dispersal to multiple teeth	
	• Energy:	
D	- high efficiency while operation	overall efficiency above 90%
D	- uncomplicated self-locking	
W	- no additional cooling system	
	• Signal:	
D	- no extra sensors, controls or other mechanism which can be manipulated from outside without impact to the operation of the gear	
	• Manufacture:	
W	- with standardized methods	
W	- no extra heat treating	
	• Assembling:	
W	- easy assembling and disassembling	
	• Usage/ Operation:	
D	- silent operation	
D	- low abrasion	
	• Maintenance:	
D	- long maintenance interval	

In the following the requirements of **table 1.1** are described in more detail.

The requirements of the category 'Geometry' are very common; it is not necessary to discuss them in more detail. The demands of 'continuous movement' and 'driving in both directions' are also very common aims in gear design, special if passengers or goods are transported.

The requirements of the category 'Forces' are more customized. In this thesis the gear should be able to transmit high torques (above 1000 Nm). Due to the high torques the load shall be transmitted by multiple teeth, in order to increase the safety. Furthermore the gear ratio should be around 100. These are typical demands of conveyor gears.

In the category 'Energy' the requirement 'high efficiency while operation' is state of the art. Due to possible problems with common self-locking gears (see chapter 1.1.3), the demand 'uncomplicated self-locking' is necessary in this thesis. Due to a cheap operation, the gear design should support splash lubrication in the gearbox.

Accordingly to the introduction, one of the most important aims of this thesis it is to avoid additional devices to trigger the self-locking. This is the intention of the category 'Signal'.

Both demands of the category 'Manufacture' have the aim to create a cheap gearbox. The same reason can be presented for the requirement 'easy assembling and disassembling'.

Another important aim of this thesis is to create a gear which is as much silent as possible. This is also a typical demand in mechanical engineering. The last requirement 'long maintenance interval' is similar to the demand 'low abrasion'. The difference of the two requirements is that 'low abrasion' shall describe the influences of the mesh to the maintenance. In contrast 'low maintenance' stands for the properties of the full gearbox (bearings, sealing and oil change interval).

2 Procedure in this thesis and principle solutions

The conceptual formulation and the main aims of this thesis were given in chapter 1. In the following the process to find such a solution will be described in detail.

Based on the approach of the systematic design, **figure 2a** shows the general approach of this thesis.

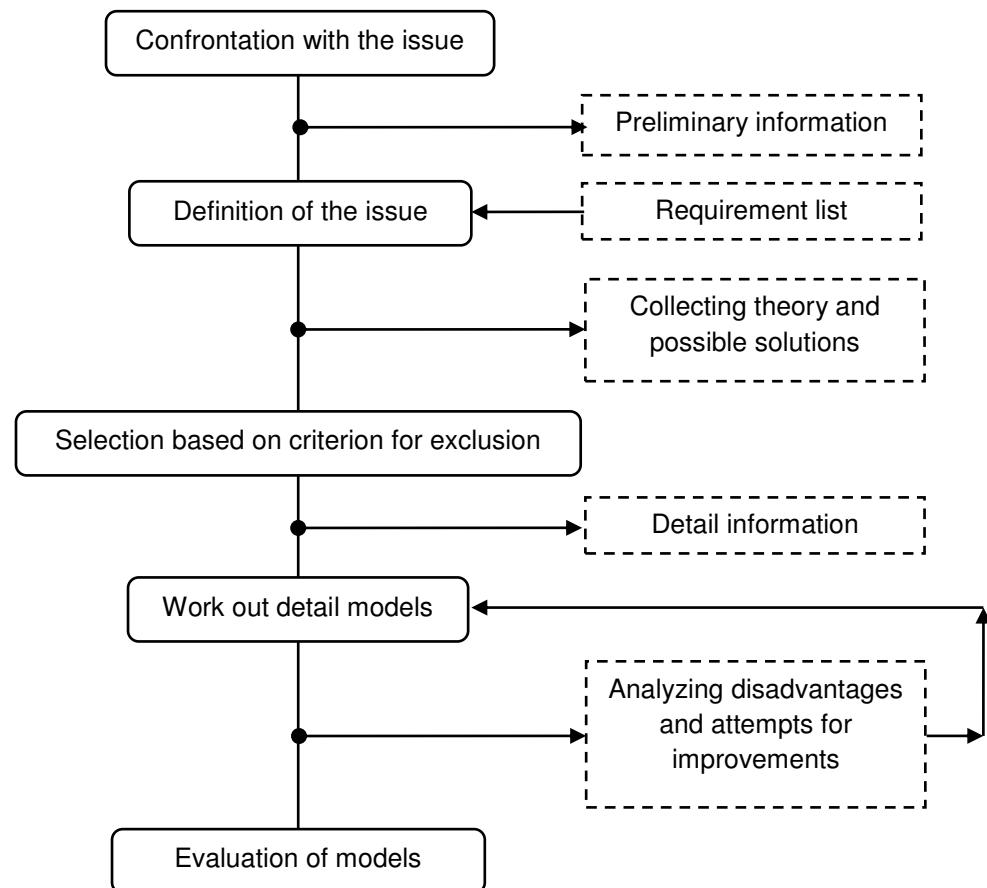


Figure 2a: General approach of this thesis

In the beginning a brainstorming and a patent research is done, to find possibilities for self-locking. In figure 2a this is represented by 'Collecting theory and possible solutions'. This search also includes gear concepts for which the literature does not explicitly mention self-locking behavior. With the requirement list (table 1.1) the issue is defined exactly.

By use of criteria for exclusion (usage of additional device or not) and by comparing the patent research, the literature as well as the requirements, three concepts are pursued (see **figure 2b**). Subsequently more information about these concepts is taken from literature to get all 'detail information' which is necessary to calculate these gears. Based on the information, different models of each concept are created and multi-body-simulated. The outcome of the simulations is used for to analyze the models. With the findings of this analysis it is attempted to correct the disadvantages of these models.

This leads to new models which are evaluated to find out which model satisfies the requirement list best (chapter 7).

As it can be seen in figure 2b, eight gear concepts are the outcome of the literature und patent search. In the following these concepts are presented briefly.

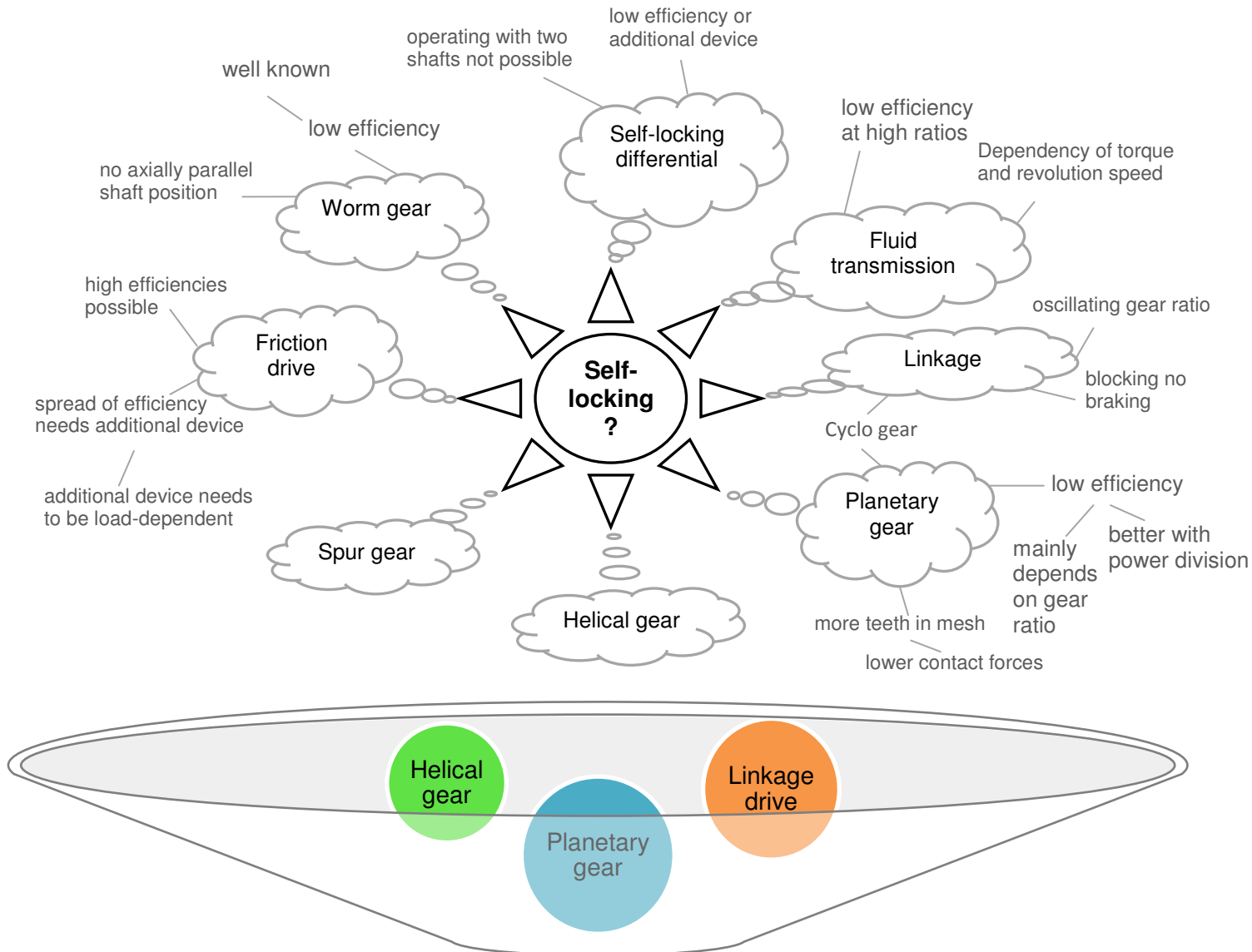


Figure 2b: Selecting procedure in this thesis

Self-locking differential

This kind of gears is well known in the literature. They are used in the automotive technology to reduce speed compensation or to apply more torque to that wheel with poor grip. Therefore they have a housing which is driving and two driven output shafts (three shaft operation). **Figure 2c** shows a common self-locking differential from literature (Looman, 2009, p.412) and below the modified idea to create self-locking in two shaft operation.

In the literature the possibility of self-locking in theses gears is described by the locking value S . It can be presented as $S = \text{braking torque} / \text{input torque}$. In case of $0 < S < 1$ one of the torques at the output shafts (T_l or T_r) is reduced if the other one increased. If S is equal to 1 then the

corresponding shaft is locked. In case of two shaft operation (see figure 2c(below)) the solution of the set of equations (2-1) is $e=1$. Therefore input and output torques are equal; that means no possibility for self-locking because $S=\text{constant}=1$. As a result the output shaft is locked permanently.

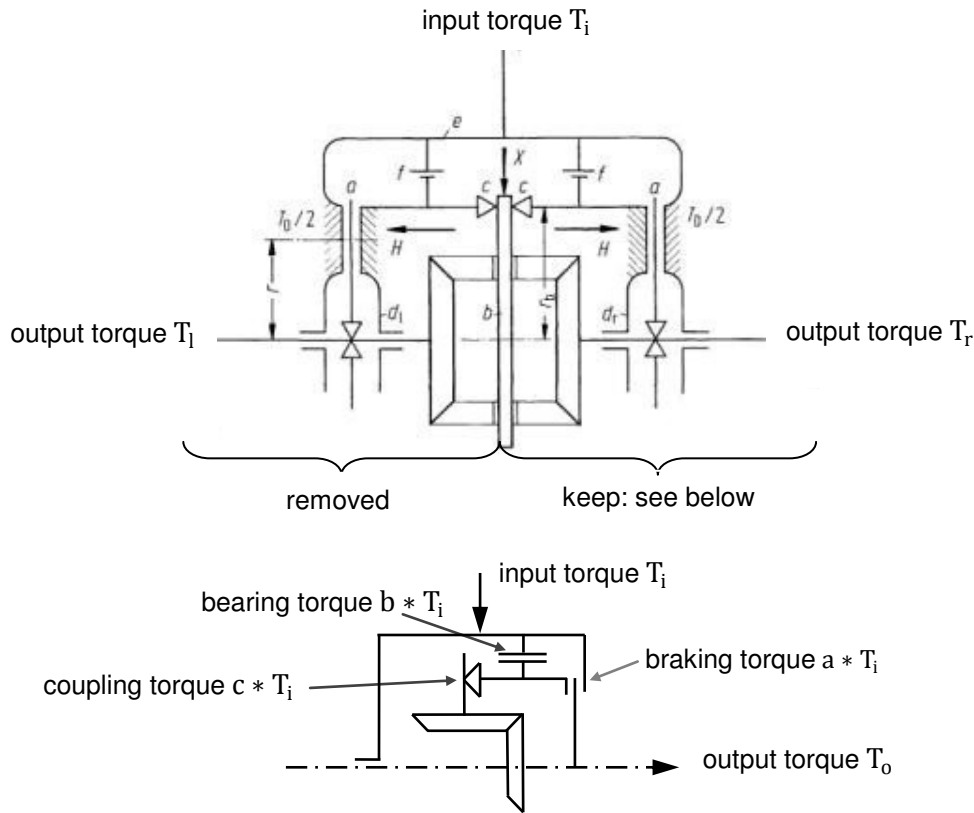


Figure 2c: Self-locking differential arrangement: above from literature (Looman, 2009, p.412), below idea in this thesis

With the input, bearing, coupling, braking and output torque follows the system of equations:

$$\left. \begin{aligned} \text{I: } T_i + b * T_i + a * T_i &= 0 \\ \text{II: } a * T_i - b * T_i - c * T_i &= 0 \\ \text{III: } c * T_i - 2 * a * T_i - e * T_i &= 0 \end{aligned} \right\} (2-1)$$

Fluid transmission

These gears are known as Föttinger converter. They consist of a pump wheel, a turbine wheel and a guide wheel (see **figure 2d**). The pump wheel is driven by the motor, the guide wheel is fixed to the housing by a freewheel and the turbine wheel is fixed to the output shaft. The pump accelerates the fluid. After that the fluid is decelerated by the guide wheel. Therefore the torque at the turbine is higher than the torque at the motor side.

One characteristic of these gears is that torque, speed and efficiency are interdependent. Furthermore these gears are not useful to perform high gear ratios. Therefore fluid transmissions are not suitable to satisfy the requirements of this thesis.

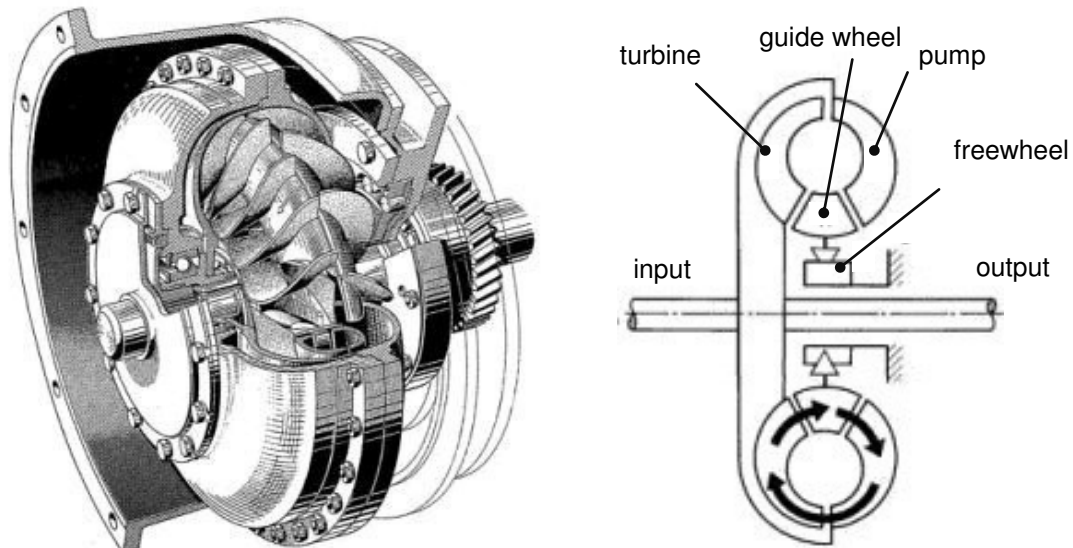


Figure 2d: Fluid transmission arrangement (left) and principle (right) (both: Looman, 2009, p.140)

Linkage drive

These gears consist of several linkages which are connected by joints. Commonly four linkages are used (see **figure 2e**). Typically these gears have positions in which no force can be transmitted. These positions are called dead-center positions (see chapter 6). Furthermore common linkage drives have no constant gear ratio (as seen in figure 2e).

During the patent research some patents are found which describes the self-locking behavior of linkage drives. In chapter 6, one of these gears and the argument for self-locking will be described in more detail.

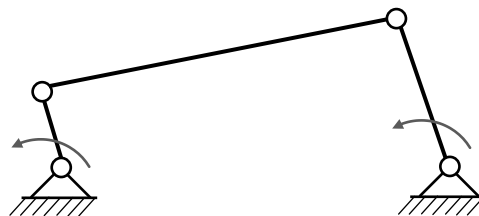


Figure 2e: Linkage drive

Planetary gears

This kind of gears consists of two central wheels, one or more planets and a planet carrier on which the planets are mounted (see figure 5b). As a result these gears have three shafts. All of them can transmit power (three shaft operation) or one shaft can be fixed with the housing (two shaft operation). Therefore it is possible to divide or summate powers with these gears. In case of self-locking these gears perform with low efficiency (<50%). By usage of more than one planet these gears have internal power division (i.e. load sharing).

In the literature it is well known that this kind of gears is able to perform self-locking by usage of standardized teeth. To reach higher efficiency they can be used in parallel connection. This possible solution is described in chapter 5.

Helical and spur gear

In the literature (Kapelevich, 2013) a design approach for self-locking spur gears is found. This procedure can lead to a self-locking helical gear. This possible solution is described in chapter 4 in detail.

Friction drive

This kind of gears transmits the power without teeth (see **figure 2f**). Thus it is possible to reach high efficiency. Self-locking cannot be performed without additional device, because these gears have a symmetry of power losses (same losses insignificant which body is driven or driving).

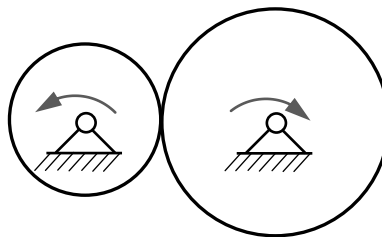


Figure 2f: Friction drive

Worm gear

This solution (see **figure 3c**) and its self-locking properties are well known in the literature. As it is mentioned in chapter 1.1.2 these gears are self-locking with low efficiency. Another disadvantage of these gears is that the axes are crossed.

Based on the literature and patent search the helical gear, the planetary gears and the linkage drives are investigated in more detail. The outcomes of this investigation are cad-models which are designed with Pro/Engineer. They are described in chapters 4 (helical gear), 5 (planetary gears) and 6 (linkage drive) in more detail.

Before the outcomes are described in detail the next chapter gives a general analysis of efficiencies of selected gears from a general point of view.

3 General examination of the efficiency of selected gears

3.1 Influences on the efficiency of gears with tooth system

In a gear (e.g. **figure 3a**) there are several zones where power losses accruing. All together they are relevant for the overall gear's efficiency. Because of that the main power losses are described in this chapter, in which the main focus is on the geometric influences.

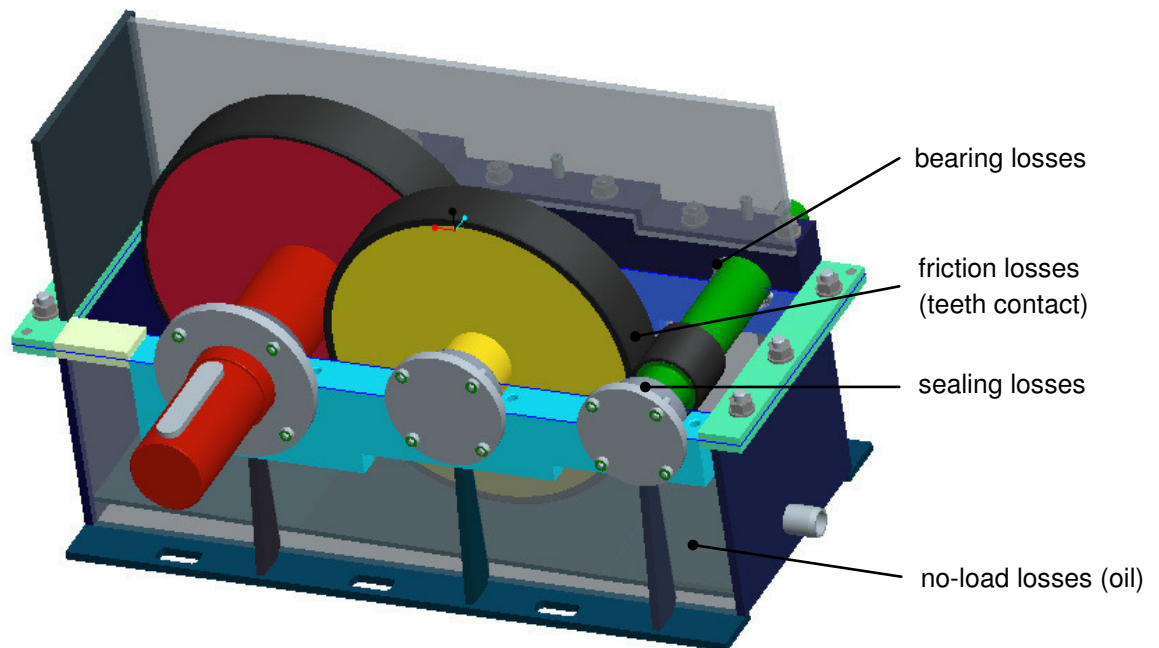


Figure 3a: Typical industrial gear

The following numerical values are given in the literature (Niemann, 2003, p.219÷228) for the power losses which are mentioned above (figure 3a).

Sealing losses

By using contact seals, these losses have to take into consideration. Their influence increases with decreasing rotational speed. Typically contact seals are used for a circumferential speed of <8 m/s (extreme case: <35 m/s).

Bearing losses

These losses depend mainly on the type of bearing which is chosen. In literature empiric values are given:

- roller bearings: 0.1% of the input power
- radial slide bearing: 0.5÷1.5% of the input power
- axial slide bearing: low efficiency

Furthermore it should be considered, that slide bearings are only useful for high rotational speeds.

No-load losses

These losses depend on the lubrication type which is chosen. There are two possibilities:

a) Splash lubrication:

These losses result because the oil volume is a resistance for the gears movement. When the teeth dive into the oil the wheel tries to take along the oil between the teeth. This results in turbulences of the oil and additional heating (additional to the friction in the mesh). Using Splash lubrication is only useful for circumference speeds less than 12 m/s.

Splash losses depends on

- Number of gears
- Immersion depth of the teeth
- Viscosity of the oil (increasing viscosity results into increasing losses)
- Shape of housing (circular shapes better to provide a rotating oil flow).

b) Injection lubrication:

These losses accrue by crimping oil between teeth, accelerating, deflecting oil and ventilation losses (friction at disks). Injection losses depends mainly on

- Injected oil volume
- Increasing helix angel decreases losses for crimping and accelerating oil
- Less rotational speed ($5 \div 10$ m/s): increasing viscosity results in higher losses.

Friction loss of the mesh

This loss accrues from friction at the tooth flank. Decisive for this kind of loss is the direction of sliding velocity and the type of contact at the tooth flank.

Gears with crossing axis (e.g. worm gear) have sliding velocities in lengthwise direction; this result in low mesh efficiencies.

Gears with parallel axis have only sliding velocities along the involutes tooth contour and as a result higher mesh efficiencies.

Another criterion is the shape of contact. Especially in worm gears there have line contact (in direction of the velocity) which additionally leads to high abrasion and generation of heat. In case of self-locking worm gears this is one effect which leads to low efficiency. Contrariwise spur gears have line contact in another direction as the sliding velocity.

The following picture gives an overview of gears from the perspective of axle positions. As it is shown in **figure 3b**, the main characteristic in that classification of the gears is the relative position of the axes together. Under that condition the efficiency of some of these gear types are listed and compared in the following.

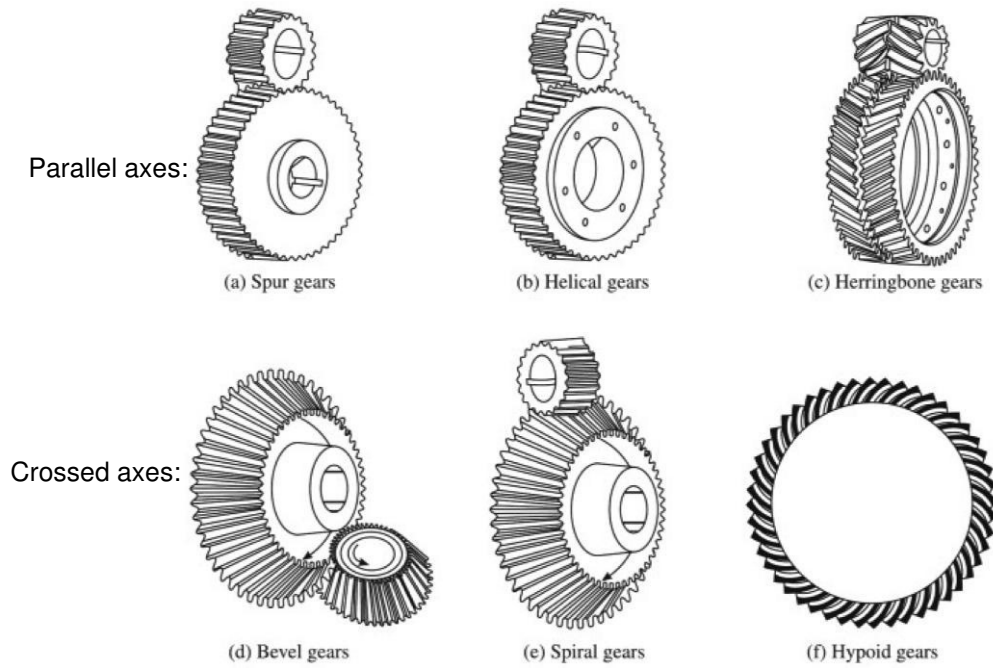


Figure 3b: Classification of gears according to position of axles (Ravi, 2011, p.187)

If all losses which mentioned above are taken into consideration, the overall efficiency of a gearbox can be presented as

$$\eta = 1 - \frac{P_{L_{\text{sealing}}} + P_{L_{\text{bearing}}} + P_{L_{\text{no-load}}} + P_{L_{\text{mesh}}}}{P_{\text{in}}} = 1 - \frac{P_{L_{\text{sealing}}}}{P_{\text{in}}} - \frac{P_{L_{\text{bearing}}}}{P_{\text{in}}} - \frac{P_{L_{\text{no-load}}}}{P_{\text{in}}} - \frac{P_{L_{\text{mesh}}}}{P_{\text{in}}}. \quad (3-1)$$

Where η represents the overall efficiency of the gearbox, $P_{L_{\text{sealing}}}$ the power losses caused by the seals, $P_{L_{\text{bearing}}}$ the power losses generate by the bearings, $P_{L_{\text{no-load}}}$ power losses mainly determined by the lubrication, $P_{L_{\text{mesh}}}$ power losses produced by the friction at the teeth.

3.2 Comparing efficiencies of selected gears

In this chapter the efficiencies of common gears are compared to find out general relations and to identify possible gears which can fulfill the requirement list.

3.2.1 Worm gear

Figure 3b is not showing the worm gear, but it can be argued that this gear is special. It is the only gear where two different bodies are in mesh (worm meshes with worm wheel). This kind of gears has asymmetric efficiency behavior i.e. different characteristics if worm or worm wheel is driven (**figure 3c**). This is understandable because the tangential component (force

or velocity) of the driving body appears in axial direction of the driven body. In the literature (Volmer, 1978a, p.281) there are common equations (in terms of angles) for the efficiencies

$$\eta_{wo \rightarrow wh} = \frac{\cos(\alpha_n) - f * \tan(\gamma)}{\cos(\alpha_n) + f * \frac{1}{\tan(\gamma)}} \quad (3-2)$$

$$\eta_{wh \rightarrow wo} = \frac{\cos(\alpha_n) - f * \frac{1}{\tan(\gamma)}}{\cos(\alpha_n) + f * \tan(\gamma)} \quad (3-3)$$

Equation (3-2) describes the efficiency when worm is driving and in case of driving wheel equation (3-3) represents the efficiency. In both equations α_n describes the profile angle in normal section, f the average friction coefficient γ the average gradient angle.

Power losses in terms of input power and angles (for the case of driving worm)

$$P_l = f * F_{th} * v_s = f * \frac{P_{in}}{\cos(\alpha_n) * \sin(\gamma) + f * \cos(\gamma)} * \frac{1}{\cos(\gamma)} = P_{in} * \xi_v \quad (3-4)$$

Power losses in terms of input power and angles (for the case of driving worm wheel)

$$P_l = f * F_{th} * v_s = P_{in} * \left(1 - \frac{\cos(\alpha_n) - f * \frac{1}{\tan(\gamma)}}{\cos(\alpha_n) + f * \tan(\gamma)} \right) = P_{in} * \xi_b \quad (3-5)$$

Where α_n describes the profile angle, γ is the average gradient angle, f the average friction coefficient, F_{th} the force which is applied on the teeth, v_s the sliding velocity, P_{in} the input power and P_l describes the power losses. Some of the symbols are shown in the following figure.

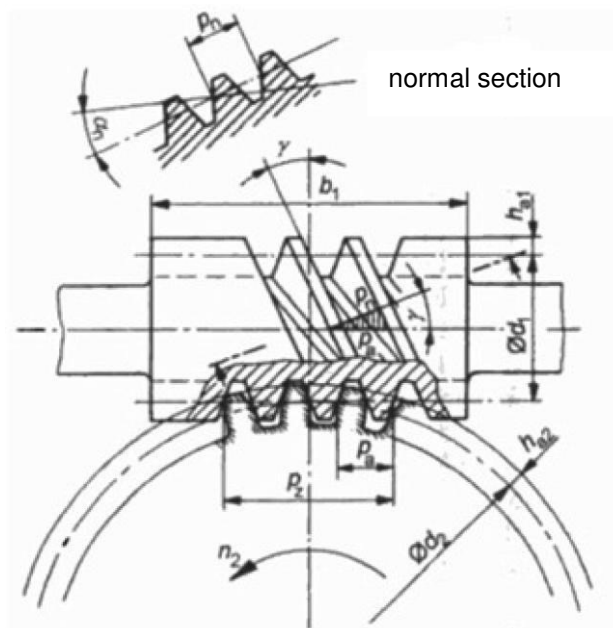


Figure 3c: Worm gear (Künne, 2001, p.282)

In equations (3-4) and (3-5) it is apparent that the input power is proportional to the power losses. This proportionality is necessary for self-locking.

Furthermore all terms in equations (3-4) and (3-5) including angles are in the denominator. This indicates that small gradient angles γ results in big power losses. The influence of the profile angle α_n is less for small gradient angles, because its term is only multiplied with $\sin(\gamma)$.

In the following **figure 3d** the ration $P_l/P_{in}=\xi_v$ in case of driving worm is presented. That means this ratio represents the power losses. Thus the efficiency can be presented as $\eta=1-\xi_v$. Parameter λ at the abscissa represents the profile angle α_n in case of blue and red lines (left ordinate) and gradient angle γ in case of green and orange dashed lines (left ordinate). With this representation, it is possible to imagine a three dimensional plot of such a relationship (not drawn).

The trend shows that the efficiency decreases with larger profile angles α_n (blue and red lines represent $\gamma_1=5^\circ$ respectively $\gamma_2=2^\circ$) and increases with larger gradient angles (green and orange dashed lines represent $\alpha_1=14.5^\circ$ respectively $\alpha_2=28^\circ$). All lines are plotted with an average friction coefficient of $f=0.1$.

Furthermore it can be argued that a change of gradient angle in smaller than about 30° has more influence on the efficiency, as a change of the same size at larger values of the gradient angle.

Another statement of this diagram is that the trend (variable gradient angle: green and orange dashed lines) over the profile angles α_n is not symmetrically to $\gamma=45^\circ$. This is understandable because a gradient angle close to $\gamma \rightarrow 90^\circ$ means that the tangential component of the worm results completely in axial component of the worm wheel.

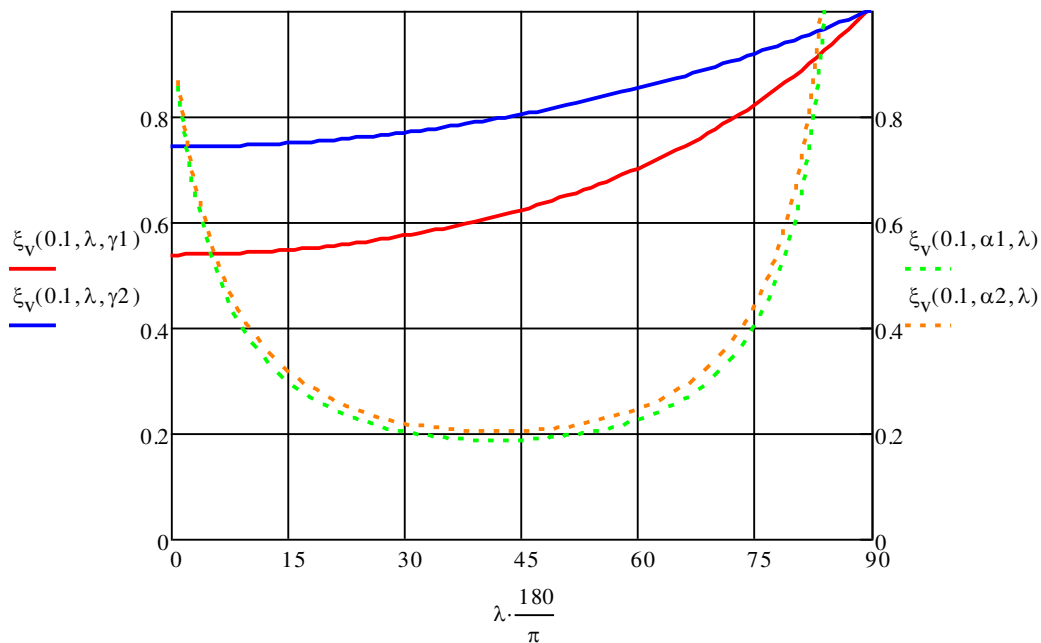


Figure 3d: Power losses of the worm gear in case of driving worm

In **figure 3e** the ratio $P_l/P_{in}=\xi_b$ in case of backdriving is plotted (driving worm wheel). Parameter λ has the same intention as in figure 3d. The drawn lines include the same information as above (blue and red lines represent $\gamma_1=5^\circ$ respectively $\gamma_2=2^\circ$; green and orange dashed lines represent $\alpha_1=14.5^\circ$ respectively $\alpha_2=28^\circ$). All lines are plotted with an average friction coefficient of $f=0.025$.

In principle the same statements as above can be made. The asymmetric behavior of the power losses to $\gamma=45^\circ$ can be seen at less gradient angles. This can be explained because γ in case of backdriving gradient angle close to $\gamma=0^\circ$, means that the tangential component of the worm wheel results in axial component of the worm. As can be seen for small angles, the power losses are large. Self-locking in this range of gradient angle is possible.

The conclusion of the two figures above is that self-locking is not possible without high power losses in driving direction.

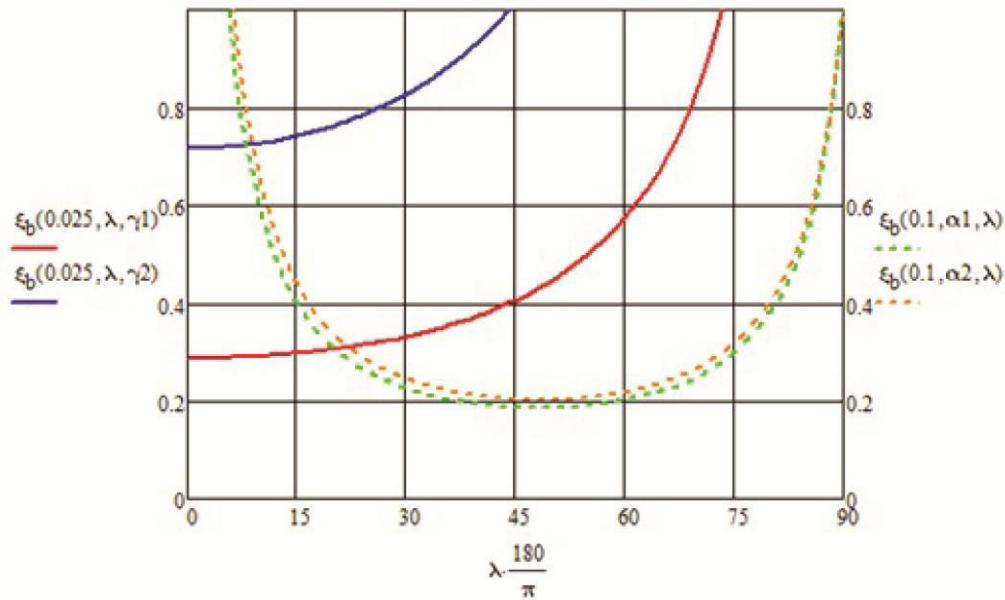


Figure 3e: Power losses of worm gear in case of driven worm wheel

3.2.2 Crossed-helical gear

As you can see in figure 3b, the crossed-helical gear is a gear with two cylindrical bodies and crossed axis. Accordingly it combines properties of helical and worm gear.

The power losses can be described as

$$P_l = f * F_{th} * v_s = f * c * \left(\sin(\beta) + \frac{\cos(\beta)}{\cos(\Sigma - \beta)} * \sin(\Sigma - \beta) \right) * P_{in} = \xi * P_{in} \quad (3-6)$$

with

$$c = \sqrt{1 + (\tan(\beta - \rho))^2 + \frac{(\tan(\alpha_n))^2 * (\cos(\rho))^2}{(\cos(\beta - \rho))^2}}. \quad (3-7)$$

Where α_n describes the profile angel in normal section, β is the helix angle of the pinion, Σ the sum of both helix angles (pinion and gear), f the average friction coefficient, ρ the friction angle ($\rho = \text{atan}(f)$), F_{th} the force which is applied on the teeth, v_s the sliding velocity, P_{in} the input power and P_l describes the power losses. Some of the symbols are shown in the following picture **figure 3f**.

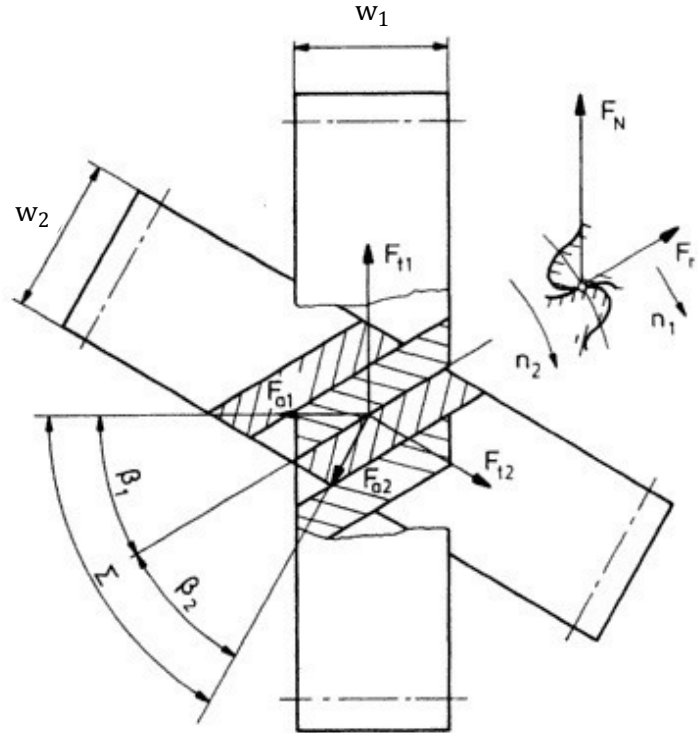


Figure 3f: Crossed-helical gear (index 1 represents the pinion and index 2 represents the wheel)
(Perović, 2002, p. 407)

In **figure 3g** the ratio $P_l/P_{in} = \xi$ is plotted. Parameter λ has the same intention as in figure 3d. The figure also shows the dimensionless power losses on two axes. The left one shows the dimensionless power losses for variable helix angels and the right axes in case of variable profile angel α_n . The drawn lines include the following information.

- Lines with variable β (left ordinate):
 - blue line: $\alpha_n = 14.5^\circ$, $\Sigma = 10^\circ$ and $f = 0.1$
 - red line: $\alpha_n = 28^\circ$, $\Sigma = 10^\circ$ and $f = 0.1$
 - green line: $\alpha_n = 14.5^\circ$, $\Sigma = 90^\circ$ and $f = 0.1$
 - brown line: $\alpha_n = 14.5^\circ$, $\Sigma = 90^\circ$ and $f = 0.2$
- Lines with variable α_n (right ordinate):
 - light blue dashed line: $\alpha_n = 15^\circ$, $\Sigma = 90^\circ$ and $f = 0.1$
 - orange dashed line: $\alpha_n = 60^\circ$, $\Sigma = 90^\circ$ and $f = 0.1$
 - pink dashed line: $\alpha_n = 60^\circ$, $\Sigma = 10^\circ$ and $f = 0.1$
 - grey dashed lines: $\alpha_n = 60^\circ$, $\Sigma = 10^\circ$ and $f = 0.2$

The diagram below (figure 3g) depicts the link between worm gear and spur gear. In case of small angles Σ the behavior of such a gear, tend to those of the helical gear (see blue, red pink and grey lines). For higher angles Σ the gear behaves more like a worm gear (see green, brown, light blue and orange lines). Accordingly, the green and brown lines in figure 3g are similar to those of the orange and green dashed lines in figure 3e (driving worm wheel).

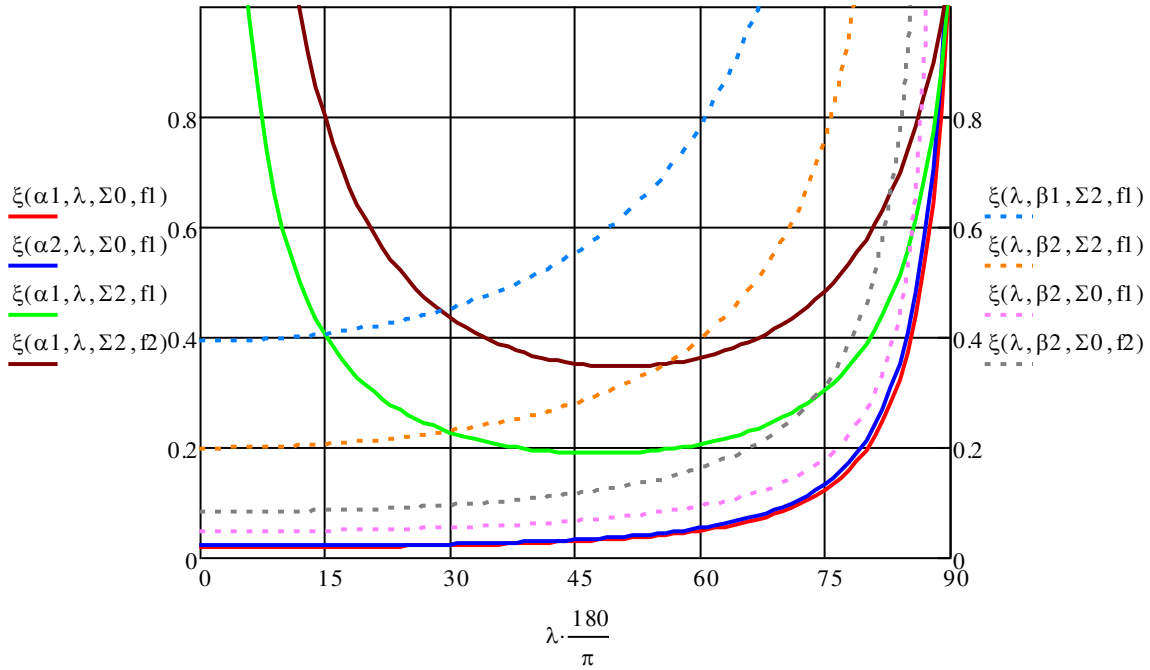


Figure 3g: Power losses of the crossed-helical gear in case of driving pinion

As a result it can be argued, that the cross helical gear gets closer to the behavior of a worm gear, if the sum of both helix angles Σ tends to 90° .

3.2.3 Spur gear, helical gear and also bevel gear

A comparison of the kinematics of these three gears shows that they are similar. One difference is that spur and helical gears have parallel axes and bevel gears have crossed axes. Hence the efficiency of the bevel gears is defined at a middle diameter. Therefore, it is allowed to define the efficiency of the bevel gears similar to those of the spur gears. In this context, the following equations are only valid for helical gears (but with $\beta = 0$ also for spur gears), but in core the statements are transferable to bevel gears.

The power losses can be described as (Niemann, 2003, p.276)

$$P_l = f * F_{th} * v_s = f * \frac{\varepsilon_{\alpha t} * \pi}{\cos(\beta) * \cos(\alpha_{wt})} * \left(\frac{1}{N_1} + \frac{1}{N_2} \right) * P_{in} \quad (3-8)$$

where $\varepsilon_{\alpha t}$ can be presented as

$$\varepsilon_{\alpha t} = \frac{N_1}{2\pi} * \left[\sqrt{\left(\frac{d_{a1}}{d_{b1}}\right)^2 - 1} + \frac{N_2}{N_1} * \sqrt{\left(\frac{d_{a2}}{d_{b2}}\right)^2 - 1} - \left(1 + \frac{N_2}{N_1}\right) * \tan(\alpha_{wt}) \right]. \quad (3-9)$$

With the following set of equations it is possible to determine $d_{a1,2}$, $d_{b1,2}$ and α_{wt}

$$\alpha_t = \text{atan}\left(\frac{\tan(\alpha_n)}{\cos(\beta)}\right) \quad (3-10)$$

$$d_{b1,2} = \frac{N_{1,2}}{\cos(\beta)} * m_n * \cos(\alpha_t) \quad (3-11)$$

$$d_{w1} = \frac{2 * a * N_1}{N_1 + N_2} \quad (3-12)$$

$$d_{w2} = \frac{N_2}{N_1} * d_{w1} \quad (3-13)$$

$$\alpha_{wt} = \arccos\left(\frac{d_{b1,2}}{d_{w1,2}}\right) \quad (3-14)$$

$$d_{1,2} = N_{1,2} * \frac{m_n}{\cos(\beta)} \quad (3-15)$$

$$c_{\min} = 0.2 * m_n \quad (3-16)$$

$$h_{fp} = 1.25 * m_n \quad (3-17)$$

$$d_{r1,2} = d_{1,2} + 2 * x_{1,2} * m_n - 2 * h_{fp} \quad (3-18)$$

$$d_{a1,2} = 2 * a - d_{f1,2} - 2 * c_{\min}. \quad (3-19)$$

Where α_n is the profile angle at the pitch diameter in the normal section, α_t is the profile angle at the pitch diameter in the transverse section, α_{wt} is the profile angel at the operating diameters ($d_{w1,2}$) in the transverse section, β the helix angel, $\varepsilon_{\alpha t}$ the transverse contact ratio, f the average friction coefficient, F_{th} the resulting force which is applied on the teeth, v_s the sliding velocity, $N_{1,2}$ the number of teeth of the pinion (index 1) and gear (index 2), P_{in} the input power, P_l the power losses, $d_{1,2}$ the pitch diameters, $d_{a1,2}$ the addendum diameters, $d_{r1,2}$ the root diameters, $d_{b1,2}$ the base diameters, c_{\min} the radial clearance, h_{fp} the foot height of the reference profile, $x_{1,2}$ the x-shift factors, m_n the module in normal section and a the center distance.

Equation (3-7) is determined under condition of constant friction coefficient. In fact the friction coefficient depends on the sliding velocity. The following figure 3h shows a typical trend of the friction coefficient.

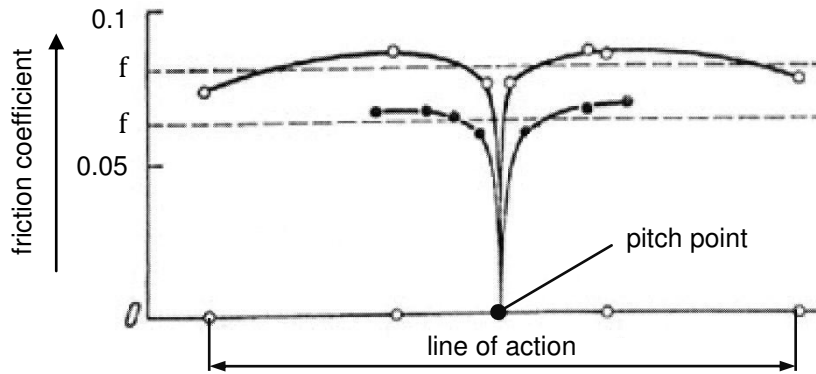


Figure 3h: Trend of the friction coefficient across the line of action (Niemann, 2003, p.223)

For two bodies 1 and 2 the sliding velocities typically look like it is shown in the following figure 3i. As is can be seen, the sliding velocity has a linear trend and changes its sign at the pitch point. At the pitch point the sliding velocity is zero itself (see chapter 4.3.1). Figure 3i also shows the directions of the sliding velocities at each body.

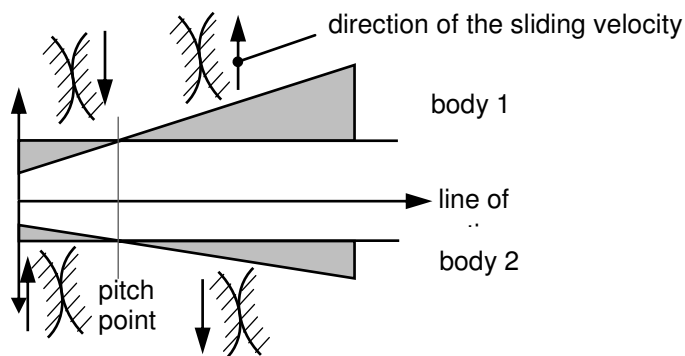


Figure 3i: Typical trend of sliding velocity across the line of action (according to: Niemann, 2003, p.38)

The trend which is shown in the following **figure 3j** presents the transverse contact ratio $\varepsilon_{\alpha t}$ at the ordinate across the profile angle in normal section α_n at the abscissa, for different pairs of teeth. The lines have the following intention

- red line: $N_1=10, N_2=11, \beta = 0^\circ$
- blue line: $N_1=100, N_2=110, \beta = 0^\circ$
- green line: $N_1=10, N_2=15, \beta = 0^\circ$
- orange line: $N_1=100, N_2=150, \beta = 0^\circ$
- brown line: $N_1=10, N_2=11, \beta = 15^\circ$.

The module in normal section m_n is chosen with 1.5 mm for all combinations. In the gear is no x-shift modification.

For less power losses the transverse contact ratio has to decrease as it can be seen in equation (3-7). For that the profile angle has to increase (compare red and brown lines). The fact that the transverse contact ratio needs to be a positive real number, is a boarder for such an increasing (see brown and blue lines).

Another statement of the figure below is that the transverse contact ratio decreases with a larger spread of number of teeth (compare blue, green and orange lines). By comparing blue and red lines it can be argued that the helix angle β has only less influence to the transverse contact ratio (the effect occurs through the influence of β to α_{wt}). This relationship is shown in the next figure 3k (compare blue and red lines in figure 3j).

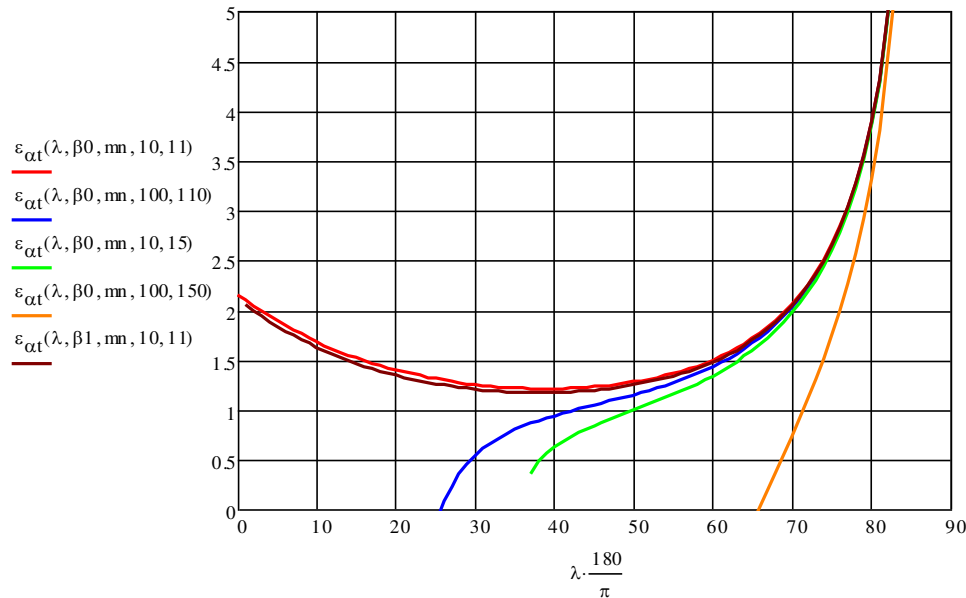


Figure 3j: Transverse contact ratio $\epsilon_{\alpha t}$ depending on the profile angle α_n in normal section

Figure 3k shows the operating profile angle (α_{wt}) in the transverse section as a function of the parameter λ . This parameter represents the profile angle in normal section α_n in case of dark blue, red and green lines (left ordinate) and represents the helix angle β in case of grey, brown and light blue dashed lines (right ordinate).

The figure is plotted for the following parameters:

- Lines with variable α_n (left ordinate):
 - red line: $\beta = 0^\circ$
 - blue line: $\beta = 15^\circ$
 - green line: $\beta = 60^\circ$
- Lines with variable β (right ordinate):
 - light blue dashed line: $\alpha_n = 14.5^\circ$
 - brown dashed line: $\alpha_n = 28^\circ$
 - grey dashed lines: $\alpha_n = 60^\circ$

For all lines, the module in normal section m_n is 1.5 mm, the numbers of teeth $N_1=10$ and $N_2=11$ are assumed. Furthermore there is no x-shift modification.

One statement of figure 3k is that, the profile angle in the transverse section (α_{wt}) increases with rising profile angle in normal section (α_n). An increasing profile angle α_n leads to higher power losses, compare figure above. It can be established that an increase of the helix angle β , with a constant profile angle α_n , results in larger profile angles α_{wt} . In which the rate of

change is not constant. For small helix angles β the relationship between α_n and α_{wt} is approximately linear (red and blue lines). Whereas at large angles β the relationship is non-linear (green line).

Another statement of figure 3k is that, the helix angle β changes also at values of constant profile angles α_n . This results in a non-linear shape, wherein the slope of the curve is larger when the profile angle α_n increases. That means a change in the profile angle α_n at higher values have more influence on the profile angle α_{wt} (and to the efficiency) than at lower values of the profile angle in normal section α_n .

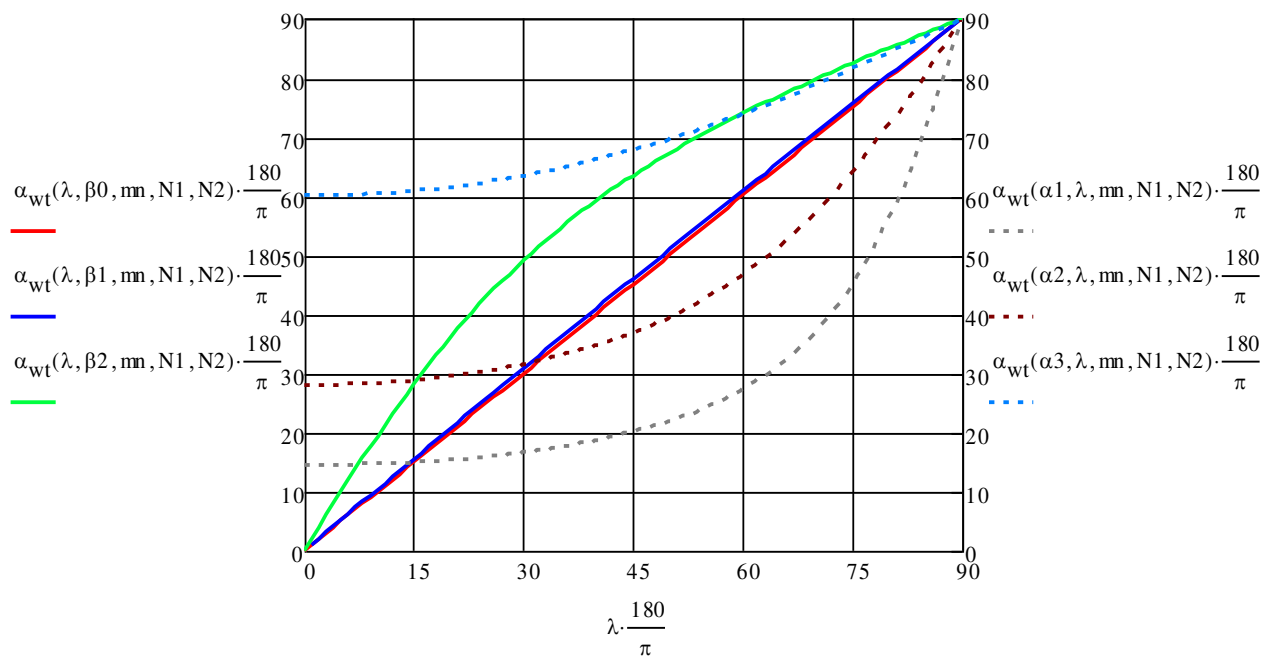


Figure 3k: Relationship of the profile angle in transverse section α_{wt} with the profile angle in normal section α_n (left ordinate) and with the helix angle β (right ordinate)

Figure 3l presents the dimensionless power losses of spur and helical gears. The plot is done for the same values as figure 3k and figure 3j. There are two ordinates (left and right). The left ordinate represents variable profile angles α_n and the right ordinate represents variable helix angles β . The lines in figure 3l are plotted for the following values:

- Lines with variable α_n (left ordinate):
 - red line: $\beta = 0^\circ$
 - blue line: $\beta = 15^\circ$
 - green line: $\beta = 60^\circ$
- Lines with variable β (right ordinate):
 - light blue dashed line: $\alpha_n = 14.5^\circ$
 - brown dashed line: $\alpha_n = 28^\circ$
 - grey dashed lines: $\alpha_n = 60^\circ$

For all lines, the module in normal section m_n is 1.5 mm, the numbers of teeth $N_1=10$ and $N_2=11$ are assumed. Furthermore there is no x-shift modification and a average friction coefficient of $f=0.1$ is chosen.

In the figure the red and light blue dashed lines represents the spur gear. Contrariwise the remaining lines represent helical gears.

As it can be seen in the figure, the standardized profile angel α_n of 20° guarantees less power losses. If the profile angel increases the power losses also increases. It can be argued that this kind of gears tend to the crossed-helical gear if the sum of both helix angels tend to 0. This can be seen by comparing the red and blue lines of figure 3l and figure 3g.

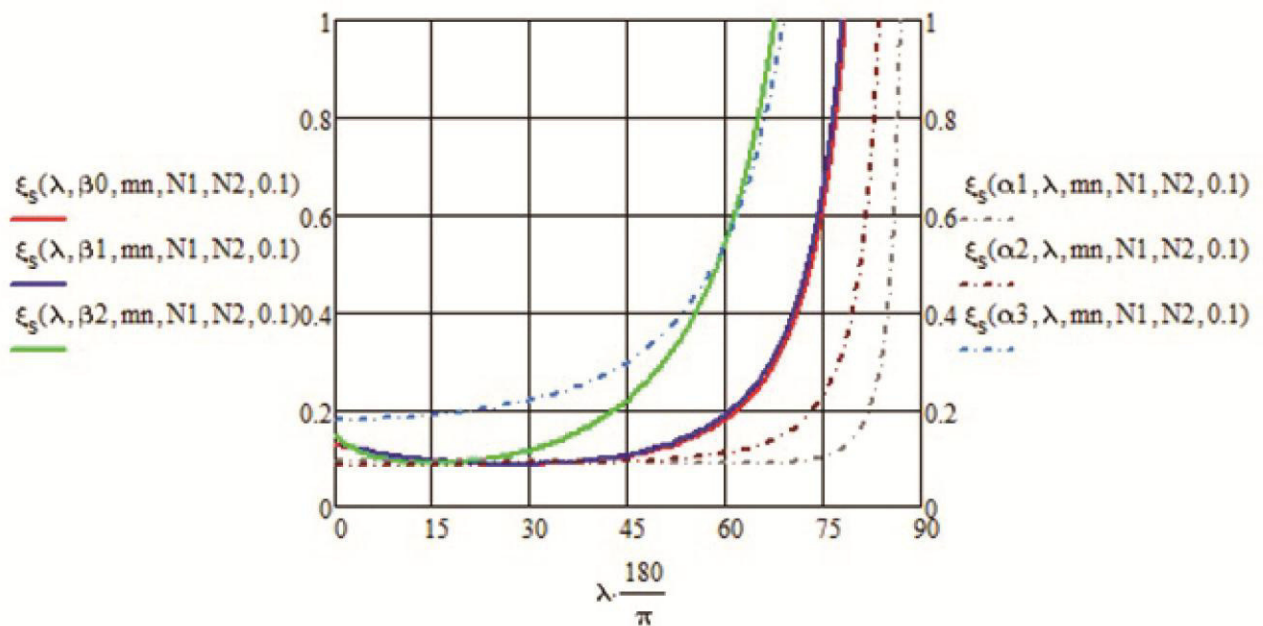


Figure 3l: Power losses of spur gear and helical gear

Furthermore it can be established that the main influence to the efficiency, raises from the profile angel in transverses section α_{wt} . This is due to the strong relationship of the angles α_n and β . In the figure this can be seen by comparing e.g. the green and the light dashed blue lines.

The general relationships of this chapter are used to analyse a gear arrangement like it is described in the next chapter.

4 Self-locking helical gear

4.1 Basic idea how the self-locking should be generated

The following **figure 4a** shows the basic idea of the self-locking helical gear with relatively high efficiencies.

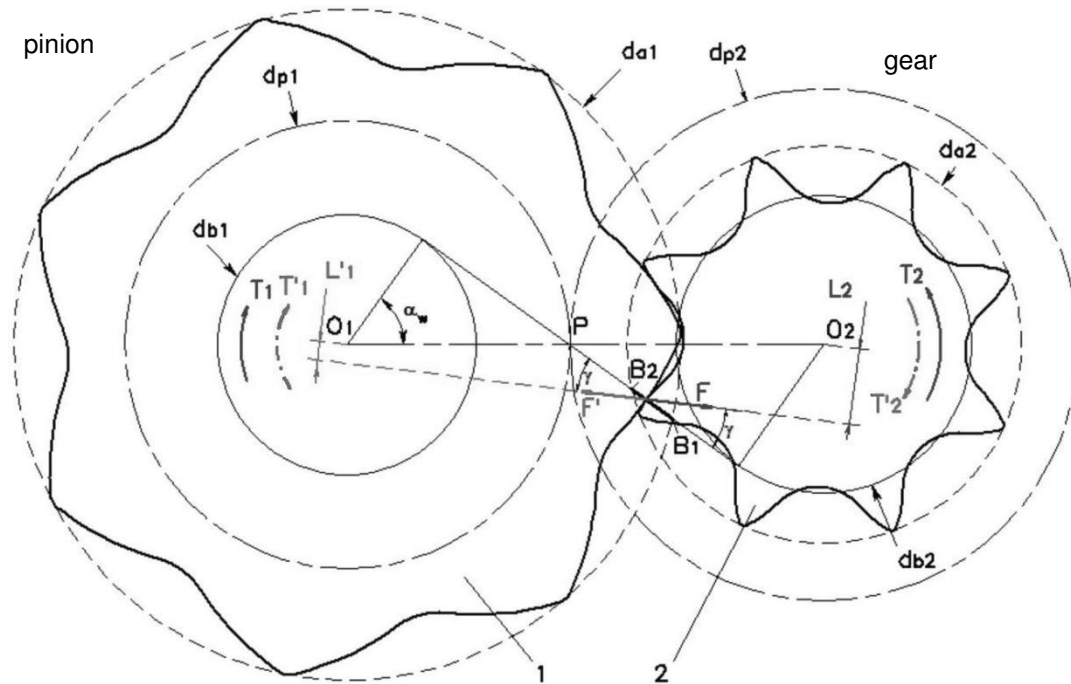


Figure 4a: Self-locking helical gear (Kapelevich, 2013, p.182)

In figure 4a there are two different bodies shown. Index 1 describes the pinion and index two the wheel. Furthermore there are two different directions of torques visible; one for the normal driving direction (T_1 and T_2 ; solid lines) and the other one (T_1' and T_2' ; dash-dotted lines) in case of power outage. In case of power outage the wheel (body 2) drives the arrangement. As it is visible, the torque at the pinion is not able to change direction. That means that T_1 and T_1' have same directions. In comparison to figure 1a that means that self-locking occur.

This constant direction of the torque T_1 (or T_1') is due to two effects:

1. Shifting the contact point (=increasing the pinion and decreasing the wheel)
2. Calculate with friction to deflect the force (=creating a lever L_1')

In the literature (Kapelevich, 2013, p.184) values for the average friction coefficient f ($=0.1 \div 0.3$) and the profile angel in transverse section α_{wt} ($=75^\circ \div 85^\circ$) are given. As it is visible in figure 4a such high profile angels are necessary to keep the deflection of the force (due to friction) as small as possible.

In the literature it is described that this self-locking approach is able to create efficiencies around 85%. Therefore it is subject of investigation in this thesis.

4.2 Procedure for realization of the self-locking geometry

In the literature (Kapelevich, 2013) a full set of equations is described to design gears beyond the commonly used design approach. Wherein must be noted that these calculation procedure do not depend on the self-locking behavior of the gear. It is a general calculation procedure. In the following the main important equation to realize the self-locking is described.

4.2.1 Self-locking condition, its background and its analysis

In the literature (Kapelevich, 2013, p.184) the self-locking condition is presented as

$$f > \frac{1}{\left(1 + \frac{N_2}{N_1}\right) * \tan(\alpha_{wt}) - \frac{N_2}{N_1} * \tan(\alpha_{a2})}. \quad (4-1)$$

Where $N_{1,2}$ represents the number of teeth at pinion (index 1) and wheel (index 2), α_{wt} describes the profile angel in transverse section, α_{a2} the profile angel at the addendum diameter of the wheel.

This equation leads to a design like it is shown in figure 4a. The remaining calculation procedure which is used to define the mesh is given in chapter 4.2.2.

The following **figure 4b** shows the background of equation (4-1).

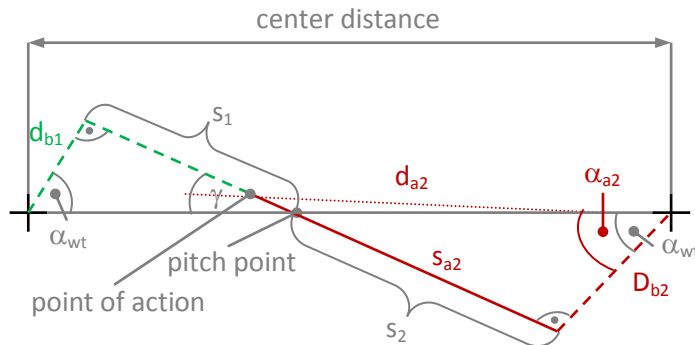


Figure 4b: Background of the self-locking condition

The identifiers in figure 4b have the same meaning as in equation (4-1). Due to figure 4b the self-locking condition can also be presented as

$$s_{a2} < s_2 \text{ or } s_1 < s_1 + s_2 - s_{a2}. \quad (4-2)$$

If the gear ratio and the relationships between base diameter and addendum diameter are considered, equation (4-2) can be written as

$$\frac{d_{b1}}{\tan \gamma} < d_{b1} * \tan(\alpha_{wt}) + u * d_{b1} * \tan(\alpha_{wt}) - u * d_{b1} * \tan(\alpha_{a2}) \quad (4-3)$$

With some rearrangements, equation (4-3) can be expressed in the same terms as equation (4-1).

The main statement of this self-locking condition is that the point of action must be located below the direct junction of the center points. As it is visible in **figure 4c**, this is only possible with a small profile angel at the addendum diameter of the wheel (α_{a2}) and (assuming similar average friction coefficient as in literature) a high profile angel α_{wt} .

Figure 4c shows the plot of the self-locking condition equation (4-1). The plot is done with a gear ratio N_2/N_1 of 1.1 and average friction coefficient f of 0.1. It can be argued that higher gear ratios and higher average friction coefficient increase the 'area of self-locking'.

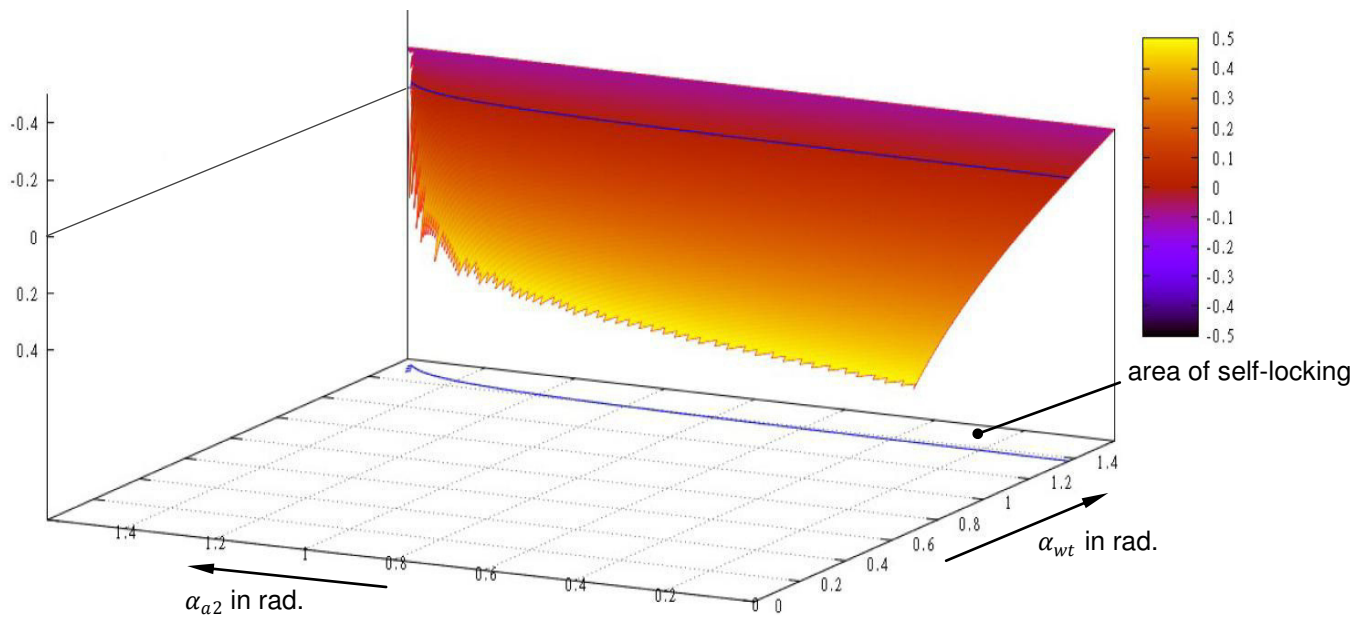


Figure 4c: Plot of the self-locking condition

The 'area of self-locking' contains all possible combinations of the profile angel in transverse section α_{wt} and the profile angel at the addendum diameter of the wheel which leads to self-locking. This area increases if the average friction coefficient and/or the gear ratio increase(s). If both angels tend to 90° ($=1.57$ rad; end of scale in figure 4c) then there is no possibility for self-locking any more.

4.2.2 Used calculation procedure in detail²

In the following the calculation procedure which is drafted to calculate the geometry before the data are implemented in a cad software is described in detail. Wherein must be mentioned that the described procedure is only one of many possibly approaches.

² All symbols which are not named in detail in this chapter are described in the nomenclature or in the text above.

As input the number of teeth of pinion (index 1) and wheel (index 2) $N_{1,2}$, the module in normal section m_n , the profile angel in normal section α_n , the helix angel β , the mesh width w , the center distance a , the back clearance A_s and the teeth width at the addendum diameter $S_{a1,2}$ are chosen.

The gear ratio is defined as

$$u = \frac{N_2}{N_1}. \quad (4-4)$$

The module in transverse section is

$$m_t = \frac{m_n}{\cos(\beta)}. \quad (4-5)$$

The involute function can be presented as

$$\text{inv}(\alpha) = \tan(\alpha) - \hat{\alpha} \quad (4-6)$$

where α represents the profile angel at angel diameter (in radians).

After the calculation of the profile angel in transverse section at the pitch diameters (equation (3.9)), pitch diameters (equation (3-14)), the base diameters (equation (3-10)), operation diameters (equation (3-11) and (3-12)) and profile angel at the operation diameters in transverse section (equation (3-13)) the sum of the x-shift factors can be calculated with

$$x_{\text{shiftSum}} = x_1 + x_2 = \frac{(\text{inv}(\alpha_{wt}) - \text{inv}(\alpha_t)) * (N_1 - N_2)}{2 * \tan(\alpha_n)}. \quad (4-7)$$

As result of the self-locking condition (4.1) the addendum diameter can be presented as

$$\alpha_{a2} = \text{atan}\left(\frac{(1 + u) * f * \tan(\alpha_{wt}) - 1}{u * f}\right) \text{ and } d_{a2} = \frac{d_{b2}}{\cos(\alpha_{a2})}. \quad (4-8)$$

The x-shift modification of the wheel is defined as

$$x_2 = \frac{\left(\frac{S_{a2} * \cos(\alpha_{a2})}{d_{b2}} - \text{inv}(\alpha_t) + \text{inv}(\alpha_{a2})\right) * d_2 - A_s - m_t * \frac{\pi}{2}}{2 * m_t * \tan(\alpha_n)}. \quad (4-9)$$

The x-shift modification of the pinion is represented by

$$x_1 = x_{\text{shiftSum}} - x_2. \quad (4-10)$$

Accordingly the gears are designed as x-tooth system. This is not necessary due to the self-locking because other possible calculation procedures work without x-shift modification. But these other procedures need additional input which do influences the geometry directly. The drafted approach of this thesis is a suitable procedure without any additional input.

By numerical solving, the following equation gives the addendum diameter of the pinion

$$S_{a1} = \frac{d_{b1}}{\cos(\alpha_{a1})} * \left(\frac{m_t * \left(\frac{\pi}{2} + 2 * x_1 * \tan(\alpha_n) \right) + A_s}{d_1} + \text{inv}(\alpha_t) - \text{inv}(\alpha_{a1}) \right) \text{ and}$$

$$d_{a1} = \frac{d_{b1}}{\cos(\alpha_{a1})}. \quad (4-11)$$

The following two equations give those diameters with the last contact point (endpoint of the line of action) of pinion (equation (4-12)) and wheel (equation (4-13)).

$$\alpha_{f1} = \text{atan}((1 + u) * \tan(\alpha_{wt}) - u * \tan(\alpha_{a2})) \text{ and } d_{f1} = \frac{d_{b1}}{\cos(\alpha_{f1})}. \quad (4-12)$$

$$\alpha_{f2} = \text{atan}\left(\frac{(1 + u)}{u} * \tan(\alpha_{wt}) - \frac{\tan(\alpha_{a2})}{u}\right) \text{ and } d_{f2} = \frac{d_{b2}}{\cos(\alpha_{f2})}. \quad (4-13)$$

Additionally the angels α_{f1} and α_{f2} must be positive to avoid interferences between the teeth in mesh.

The root diameters are defined as

$$d_{r1} = 2 * \left(a - \frac{d_{a2}}{2} - c_{\min} \right) \text{ and } d_{r2} = 2 * \left(a - \frac{d_{a1}}{2} - c_{\min} \right). \quad (4-14)$$

In equation (4-14) the radial clearance is given by equation (3-15).

The axial contact ratio ε_β can be presented as

$$\varepsilon_\beta = b * \sin(\beta) * \frac{m_n}{\cos(\beta)}. \quad (4-15)$$

The transverse contact ratio $\varepsilon_{\alpha t}$ can be calculated with equation (3-8) and the sum of both gives the total contact ratio.

The efficiency can be presented as

$$\eta = 100 - \frac{50 * f * (\cos(\beta))^2}{\cos(\alpha_{wt})} * \frac{H_s^2 + H_t^2}{H_s + H_t}. \quad (4-16)$$

Wherein H_s and H_t determines specific sliding velocity ratios; they can be given as

$$\left. \begin{aligned} H_s &= (1 + u) * \cos(\alpha_{wt}) * (\tan(\alpha_{a2}) - \tan(\alpha_{wt})) \text{ and} \\ H_t &= \frac{(1 + u)}{u} * \cos(\alpha_{wt}) * (\tan(\alpha_{a1}) - \tan(\alpha_{wt})). \end{aligned} \right\} (4-17)$$

Wherein it should be noted that this equation represents an approximate formula, because the friction coefficient cannot be determined exactly (see figure 3h).

The equations which mentioned above define all values which are relevant to design a cad-model of such a self-locking helical gear. The exact structure of the cad-model is described in the appendix.

4.2.3 General relationships in the design procedure of a self-locking helical gear

In addition to the calculation procedure it is necessary to identify the most important relationships of the parameters in the equations which are given in chapter 4.2.2. **Figure 4d** shows the general relationships of the self-locking gear design approach.

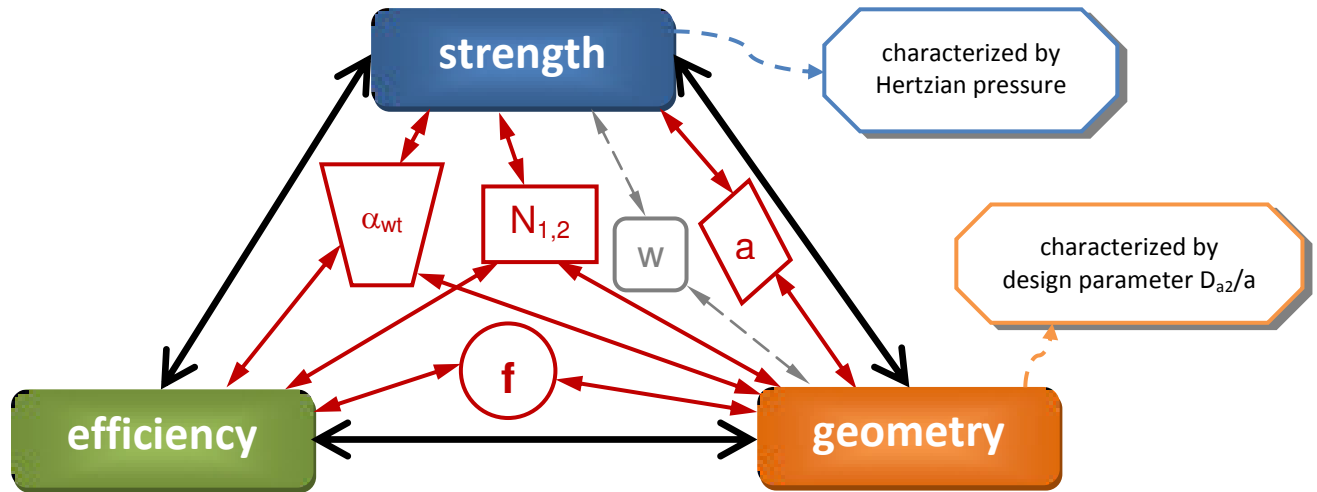


Figure 4d: Parameter study of the design approach of the self-locking helical gear

In figure 4d the triangle consisting of strength, efficiency and geometry includes the general relationships between these three influences. In this thesis the parameters which determines the strength (chosen criteria is the Hertzian pressure) are not calculated, but accordingly to literature (Niemann, 2003, p.140) it can be argued that a higher profile angel (e.g. α_{wt}) provides higher Hertzian pressure at the tooth flank. Therefore the geometry influences the strength and thus indirectly the efficiency.

To evaluate the quality of a calculated geometry, in this thesis it is recommended to use the design parameter D_{a2}/a (addendum diameter of the wheel/center distance) as criteria for quick evaluation. To create self-locking with high efficiencies, it can be argued that the design parameter should reach values in a range of 0.15÷0.5. This is the result of many tests with the calculation procedure given in chapter 4.2.2. But it is not task of this thesis to investigate such limits in detail. Thus it is possible that there are also solutions for self-locking outside this range.

With figure 4d it can be argued that the main influences are caused by

- average friction coefficient f
- profile angel at the operation diameter α_{wt}
- number of teeth $N_{1,2}$ (respectively gear ratio u)
- center distance a

The influence of the mesh width is less and therefore it is not considered.

The knowledge of these relationships is important to create self-locking helical gears and to identify the limits of such an approach (see chapter 4.4).

4.3 Comparison of the geometry with the fundamental law of gearing and with conventional procedure

4.3.1 Comparison of the geometry with the fundamental law of gearing

Due to the design which is shown in figure 4a, it has to be verified if this approach fulfills the fundamental law of gearing. Regardless if the mechanism acts two-dimensional or three-dimensional, the fundamental law of gearing can be expressed as

„For constant angular velocity ratio in gears, the contact normal must at all stages of the meshing be located in such a way that $q \tan \Phi$ remains a constant namely p .“ (Phillips, 2003, p.42)

The parameters q and Φ describe the shortest distance and the shortest angle between the contact normal and the pitch line. The parameter p is called the pitch and the point P is called the pitch point (instantaneous center of rotation). They are visible in the next figure.

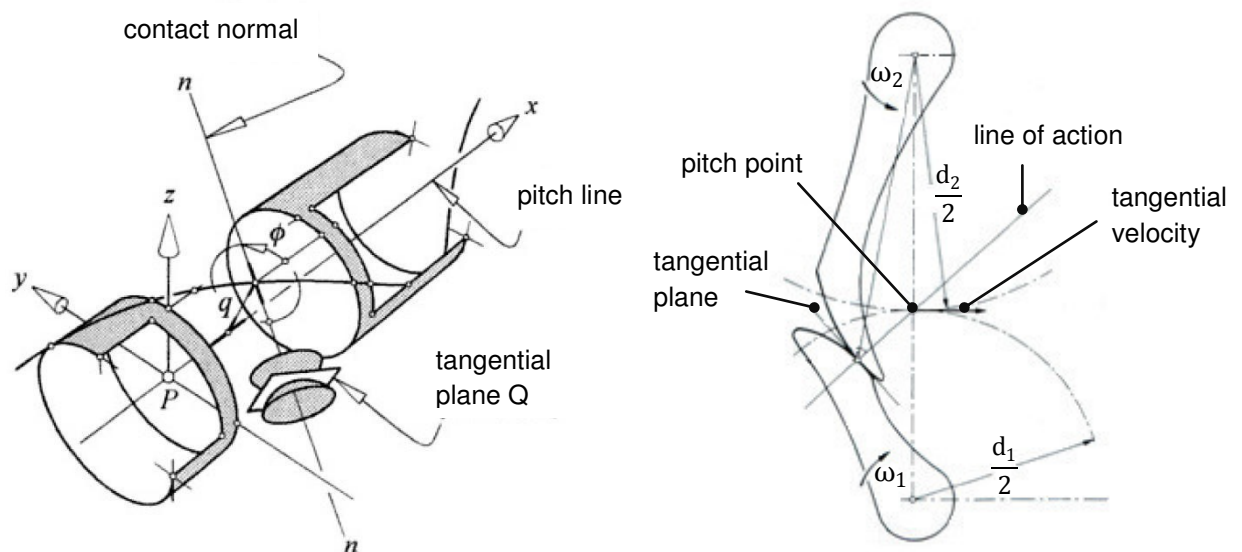


Figure 4e: General Fundamental law of gearing (Phillips, 2003, p.42, left) and two dimensional gearing (Niemann, 2003, p.33, right)

This law guarantees the movement of such a gear, in two-dimensional as well as in three-dimensional mechanism. It is also independent of the type of tooth profile which is used.

For the self-locking helical gear the general fundamental law of gearing can be specified to

“The contact normal intersects the center distance in the pitch point which divides the center distance in the inverse ratio of the angular velocities.” (Niemann, 2003, p.34)³

³ Translation by the author of this thesis

For the special two dimensional gearing there are consequences of the fundamental law of gearing are:

- zero velocity in the pitch point (therefore no friction coefficient see figure 3h and figure 3i)
- sliding velocity in all other contact points
- constant gear ratio
- in the point of action those line which is perpendicular to the teeth surfaces is the same for the engaged flanks
- the radii of curvature cannot have the same size if the centers of curvature are on the same side of the engagement point
- the pitch line of the three dimensional case (figure 4e(left)) gets a single point in case of two dimensional gearing

By comparing these consequences, it can be argued that the design of the self-locking helical gear satisfy all of them. Taking the two effects, mentioned in chapter 4.1, into account it can be argued that the design of such a self-locking helical gear is no violation of the fundamental law of gearing.

4.3.2 Comparison with conventional calculation procedure

The equations (3-9) up to (3-19) give the main important diameters of the pinion and wheel. To prove that there are no interferences between the teeth equations (4-18) and (4-19) determine the minimum number of teeth and limit of x-shift.

$$z_L = \frac{2 * \cos(\beta)}{m_n * (\sin(\alpha_t))^2} * [h_{a0} - \rho_{a0}(1 - \sin(\alpha_n)) - x_{1,2} * m_n] \quad (4-18)$$

$$x_L = 1 - \frac{z * (\sin(\alpha_t))^2}{2 * \cos(\beta)} \quad (4-19)$$

Where z_L represents the minimum number of teeth, h_{a0} the addendum height of the tool, ρ_{a0} the radius of the tool at the addendum and x_L the limit of x-shift.

There are other tests to prove interferences, but the two criteria mentioned in equations (4-18) and (4-19) are the main important ones.

Especially equations (3-17), (3-18), (3-19), (4-18) and (4-19) show the differences between the calculation approach of the self-locking helical gear and the common procedure. With equation (3-17) a tool is defined and with this chosen tool the main diameters are defined (see equations (3-18) and (3-19)). Furthermore this procedure needs an x-shift to lift the operation diameter from the pitch diameter. Wherein the x-shift is limited by interferences between teeth and tool (see equation (4-19)).

Due to the chosen tool and x-shift modification the designer restrict the area of possible solutions for the specific problem (see **figure 4f**). In the literature (e.g. Kapelevich, 2013) there are calculation procedures which do not need such chosen inputs. Instead of x-shift or

tooling parameters this approaches need dimensions of the gear (e.g. teeth width at the operation diameter) as input.

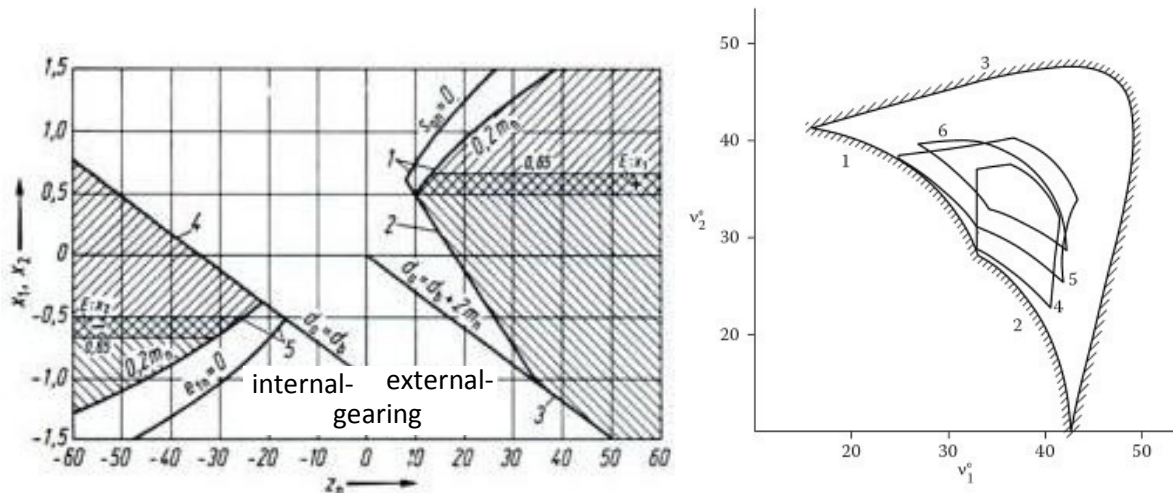


Figure 4f: Restricted area of possible solutions (Niemann, 2003, p.67, left) and more possible solutions (Kapelevich, 2013, p.9, right)

As it is visible in figure 4f(left), the common calculation approach restricts the area of possible solutions. The figure shows the minimum number of teeth of the gear. The abscissa represents the x-shifts of pinion and wheel. The gear geometry is limited by the tooth thickness at the addendum diameter (lines 1 and 5), the minimum addendum diameter (lines 3 and 4) and by interferences of tool and tooth (undercut; line 2).

Figure 4f(right) shows the profile angel $v_{1,2}$ (index 1 pinion; index 2 wheel) at the intersecting of drive and coast flank. That means the profile angel $v_{1,2}$ describes the tip diameter of the bodies. The figure should show that it is possible to realize much more gears as with the limited design approach which is represented by the common calculation procedure (figure 4f(left)). Line 1 stands for the interferences of root diameter and pinion and line 2 for those of wheel and root diameter. Line 3 is the isogram of the transverse contact ratio $\varepsilon_{\alpha t}=1$. The lines 4, 5 and 6 marks the areas with gears of profile angels $\alpha_n = 20^\circ, 25^\circ$ and 28° . Kapelevich argued that this description (right) represent more gears than the common procedure (left) (Kapelevich, 2013, p.9).

But there are still several advantages of the common calculation approach. The procedure is well known and available in the common literature. There are many experimental data of such gears, the tools are standardized and the possible manufacture processes are well reputed. One disadvantage of the common calculation approach is that the (standardized) tooling parameters influence the calculation process and thus the geometry of the teeth. However for the most gear designs the usage of this approach should lead to a well designed application.

In contrast calculation procedures which do not need any standardized input parameters (e.g. tool parameters) lead to a difficult design, because the equations are not well known, there are less experiences and in some cases the tools (e.g. cutters) have to be defined. This leads to more expensive gears and to a more sensitive supply chain.

4.4 Limits of this approach and attempts to change them

After a theoretical confronting with the self-locking helical gear and the drafting of the calculation procedure, mentioned above (chapter 4.2.2), a first model is created and tested (see **figure 4g**).

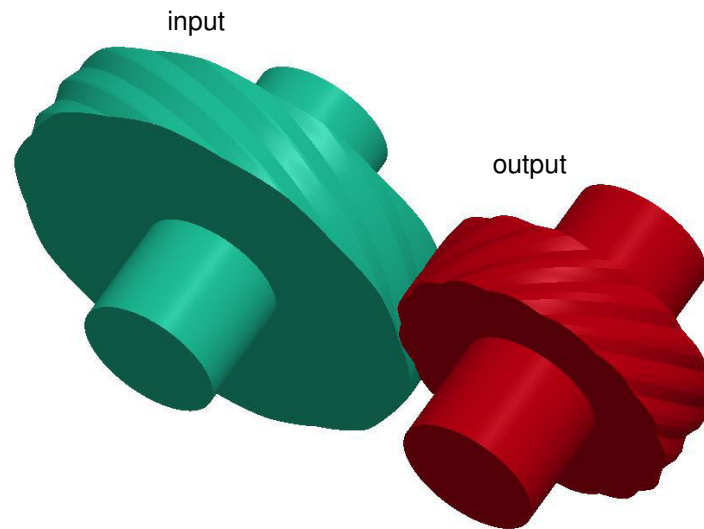


Figure 4g: First self-locking helical gear

This model is created with the following input parameters

- center distance $a=64.131$
- profile angel in normal section $\alpha_n=63^\circ$
- helix angel $\beta=73^\circ$
- module in normal section $m_n=1.5$ mm
- number of teeth $N_1=10$ (pinion) and $N_2=15$ (wheel)
- mesh width $w=15$
- back clearance $A_s=0.1$
- average friction coefficient $f=0.1$
- teeth width at the addendum diameter $S_{a1}=2$ (pinion) and $S_{a2}=2.66$ (wheel).

In **figure 4g** the green part is the input part for operation. In case of power outage the arrangement is driven at the output part (red). The multi body simulation shows that this model performs self-locking. The calculation which is done gives a mesh efficiency slightly above 94%.

4.4.1 Limitations of the approach

Bearing load

One disadvantage of the self-locking helical gear is the large bearing load. This issue is also due to the large profile angel. In this thesis no research about bearings is done, but there are well known solutions for highly loaded bearings in the literature (e.g. Harnoy, 2005).

Axial force

Another disadvantage of this design is the large axial force. For this issue several solutions are available in the literature. **Figure 4h** gives an overview of these solutions.

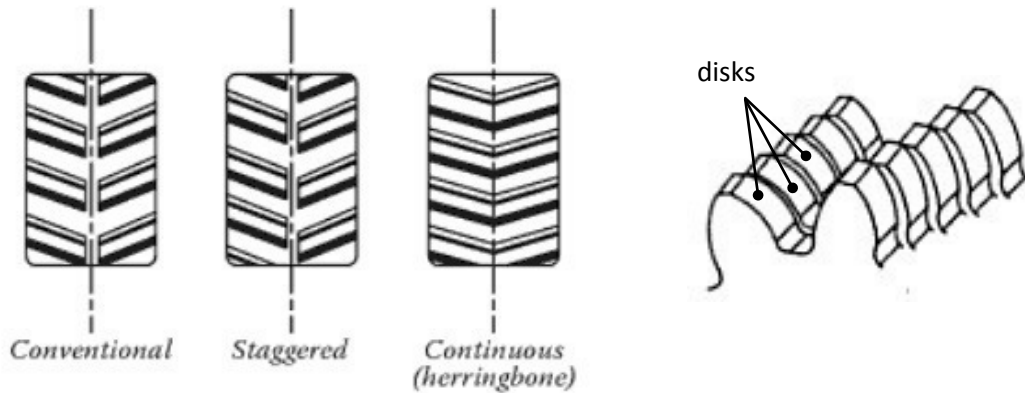


Figure 4h: Overview of possible solutions to handle high axial forces (left: Dudley, 2012, p.12, right: Künne, 2001, p.271)

Figure 4h(left) shows conventional ideas to eliminate the axial forces. In contrast figure 4h(right) shows a helical gear consisting of laminated disks. This idea performs without axial forces.

The issue of axial forces is due to the large helix angel. Figure 3j and figure 3k makes clear that the transverse contact ratio $\epsilon_{\alpha t}$ for such a self-locking helical gear is low. It can be argued that the transverse contact ratio for such a gear is typically in a range of 0.075 up to 0.2. Therefore a helical gear must be used to guarantee a total contact ratio above 1.

Pressure at the tooth flank

Another issue of such a design is that the pressure at the tooth flank. Due to the large profile angel, it will be high. This pressure is not calculated in this thesis but due to the literature (Niemann, 2003, p.140) this statement can be done.

Relationship of average friction coefficient, geometry and lubrication

Such gear arrangement cannot be calculated with average friction coefficients significant smaller than 0.1. Therefore the question arises if a well lubricated gear can support such high friction coefficient of around 0.1. The following **figure 4i** shows the relationship of materials, average friction coefficient and used lubricant (Tabor, 1966, p.II.36).

In this investigation two different kinds of lubricants are used. Both lubricants have a dynamic viscosity around 12 Pa*s. As it can be seen, the researchers show that materials with high Vickers hardness are able to support average friction coefficients around 0.1. Steels which are typically used in gears have these high harnesses. Therefore it is possible to support well lubricated gears with average friction coefficients around 0.1.

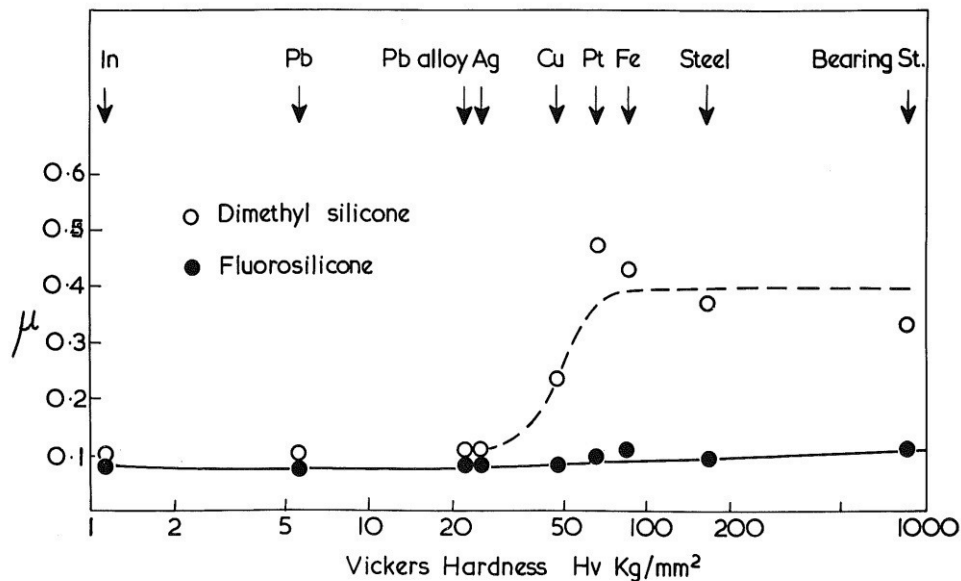


Figure 4i: Relationship of lubricant, material and average friction coefficient (Tabor, 1966, p.11.36)

Extreme x-shift

Another disadvantage is the large x-shift which is necessary for the self-locking. Due to that the wheel (transmits more torque proportional to the gear ratio) has to transmit disproportionately more load compared to non x-shifted gears.

Flat teeth

An analysis of the model which is shown in figure 4g makes clear, that the teeth of such a self-locking helical gear are very flat (around 1.5 mm). This is a result of the profile angel at the operating diameter. To transmit high torques larger teeth are needed. But increasing the tooth height is only possible by increasing the full gear. This is because of the relationship between profile angel and tooth geometry. The mentioned relation cannot be changed by using involute teeth (compare figure 4b). Therefore the idea arises to use other tooth profiles with the same basic idea as seen in figure 4a. The approach and the outcome of these ideas are described in the following chapter.

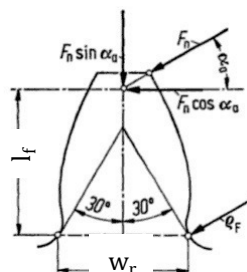


Figure 4j: Basic idea of calculation the strength at the root

In contrast it has to be noted that flat teeth, also have advantages. Figure 4j shows the basic idea of the standardized calculation procedure. Crucial for the tooth breakage are the

stresses at the root diameter; especially the bending stress. This bending stress mainly depends on the lever of the contact force (l_f in figure 4j). In case of flat teeth the lever is reduced. Combining a large tooth with at the root (w_r), these profiles provides less bending stresses.

4.4.2 Attempts to change the limits

As it is mentioned above there are some ideas to fix the issues mentioned in chapter 4.4.1. The following **figure 4k** shows the approach of these ideas.

Figure 4k shows all ideas in this thesis to fix the issues of the involute self-locking helical gear. The ideas which are pigmented green represent those models for which the self-locking behavior can be proved in the multi body simulation. Those ideas which are framed in red (or orange), marks ideas which are not suitable for this thesis or which are not performing self-locking.

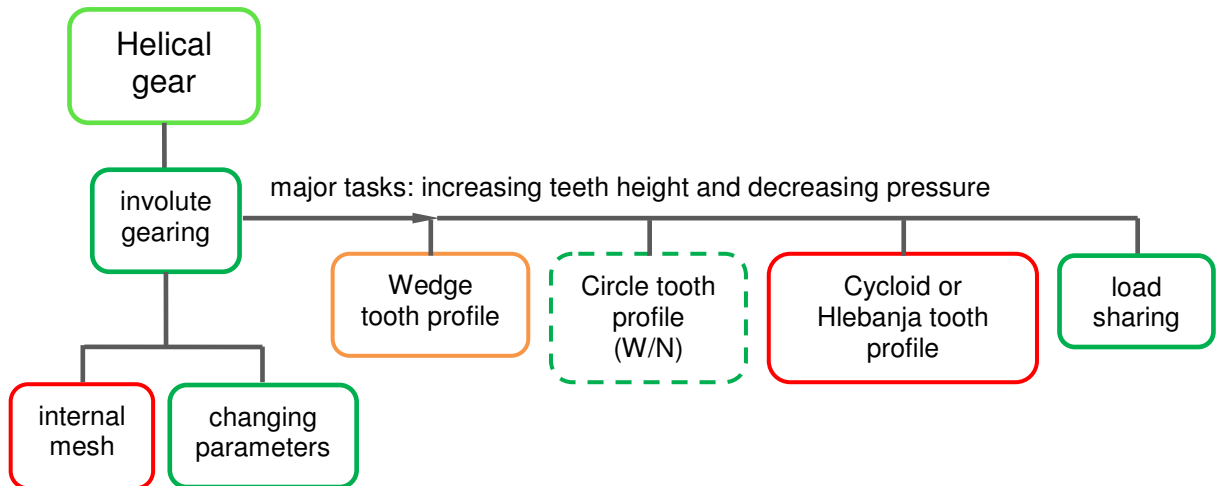


Figure 4k: Ideas to fix the issues of the self-locking helical gear

Idea: internal mesh

This idea arises because: internal meshes have less Hertzian pressure at the tooth flank. This is due to the contact of convex-concave surfaces.

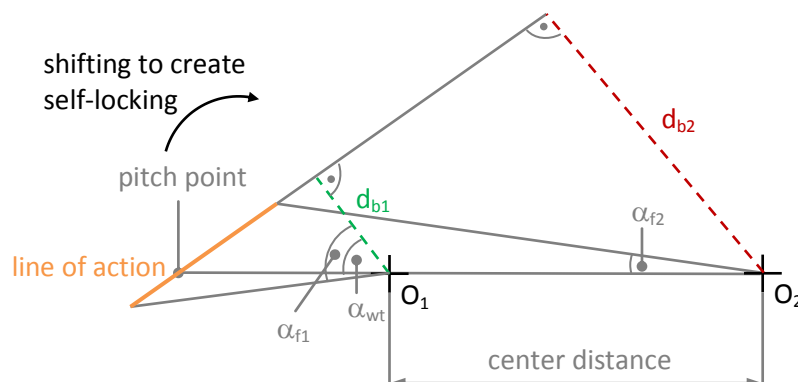


Figure 4l: Sketch of a conventional internal gear

Therefore the analysis of the self-locking condition is useful (see figure 4b) to see if it is possible to prescind the ideas of the external to the internal mesh. **Figure 4l** shows the result.

Due to the two effects which creates self-locking (see chapter 4.1) it is necessary to shift the active portion of the line of action (orange line in figure 4l) behind the dashed green line (D_{b1}) in the figure. This is not possible because the angel α_{f1} gets negative and that means interferences between the teeth. Therefore this idea is not possible.

Idea: changing parameters

This is the most obvious of all ideas (see figure 4k). By changing the input parameter it is possible to reach insignificant higher teeth. To evaluate the quality of such a scheme, in this thesis it is recommended to use the design parameter D_{a2}/a (see figure 4d) as criteria for evaluation. To reach more teeth height test with the calculation software shows that this design parameter should be close to 0.5. In **figure 4m** a model with

- center distance $a=155$
- profile angel in normal section $\alpha_n=65.33^\circ$
- helix angel $\beta=75^\circ$
- module in normal section $m_n=4$ mm
- number of teeth $N_1=6$ (pinion) and $N_2=14$ (wheel)
- mesh width $w=40$
- back clearance $A_s=0.1$
- average friction coefficient $f=0.075$
- teeth width at the addendum diameter $S_{a1}=1.85$ (pinion) and $S_{a2}=1.69$ (wheel)

is shown. The pinion is the input part in operation mode. In case of power outage the gear is driven at the wheel. This model (figure 4m) has a teeth height of around 10 mm at the input and 5 mm at the output; but an efficiency of only 75%.

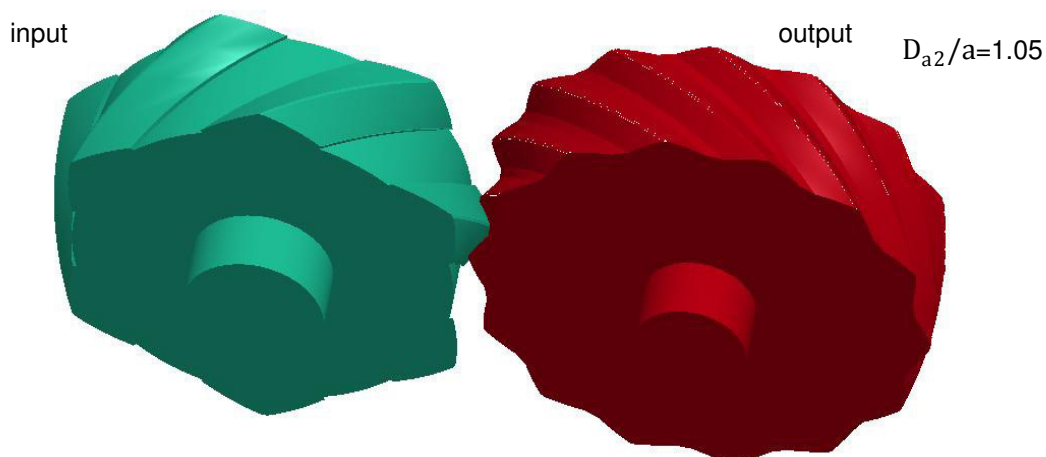


Figure 4m: Model with increased teeth height

Another model which is visible in **figure 4n** shows that it is possible to increase the teeth height of the wheel by decreasing the teeth height of the pinion. The basic idea of this

procedure is a mesh which is defined by the involute function and the input parameters. Therefore it is possible to different teeth with different teeth height in this mesh.

The **figure 4n** shows the model (right) and the basic idea (left). This gear is created with a model with

- center distance $a=45$
- profile angel in normal section $\alpha_n=70.894^\circ$
- helix angel $\beta=73.861^\circ$
- module in normal section $m_n=1.668$ mm
- number of teeth $N_1=7$ (pinion) and $N_2=8$ (wheel)
- mesh width $w=10$
- back clearance $A_s=0.1$
- average friction coefficient $f=0.03$
- teeth width at the addendum diameter $S_{a1}=1$ (pinion) and $S_{a2}=0.25$ (wheel).

By an analyzing these models it can be argued that a substantial increase in tooth height (of both bodies) cannot be achieved without decreasing the efficiency. Although the tooth height of the wheel can be increased this idea seems to be not suitable, since the outer diameter of the wheel must also be reduced in size and higher torques act at this body.

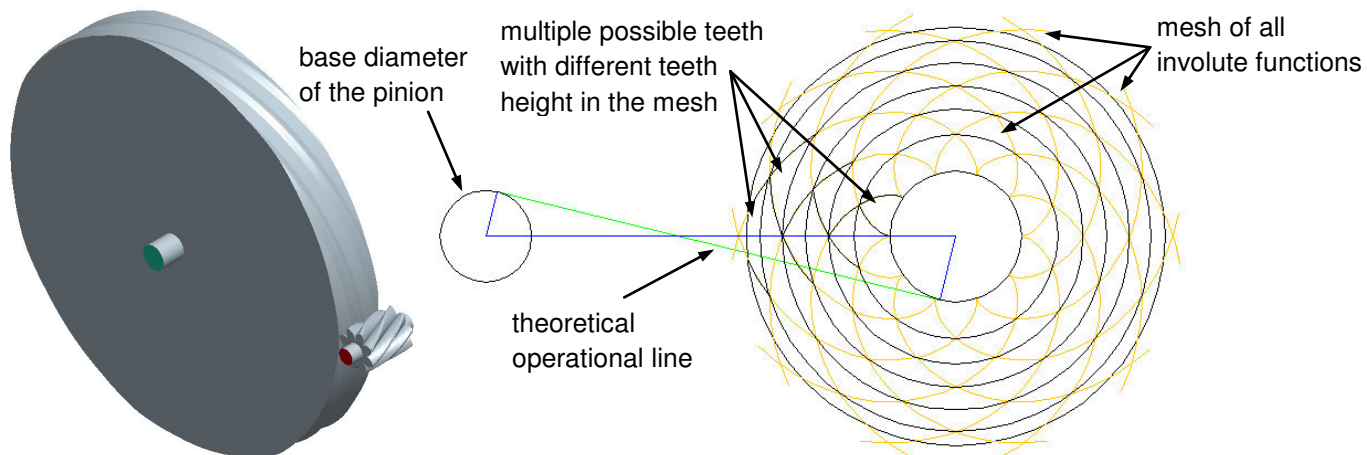


Figure 4n: Model (right) and basic idea to increase teeth height at the wheel (left)

Idea: wedge edge tooth profile

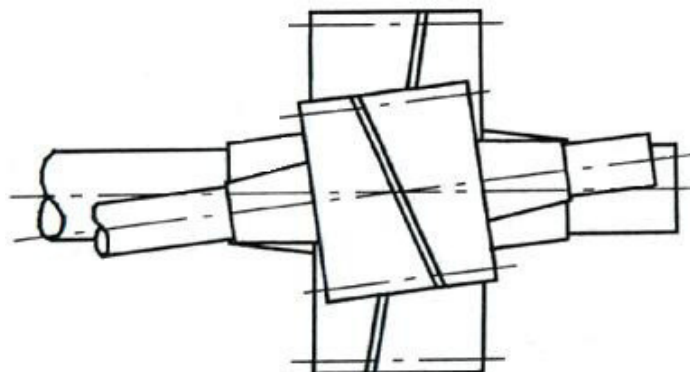


Figure 4o: Wedge edge gear with crossed axis (Bouchè, 1995, p.63)

This idea is out of literature (Bouch , 1995, p.63). In this publication, a wedge edge gear with crossed axis (compare chapter 1.1.2) and efficiencies of around 78% are described. This design has not necessarily involute teeth. **Figure 4o** shows the design.

As it is described in the literature this design leads to similar issues as the self-locking design in figure 4g. Therefore this approach seems to be possible but without advantages compared to the self-locking helical gear.

Idea: circle tooth profile (Wildhaber/Novikov profiles)

In principle Wildhaber/Novikov tooth shapes are known in the literature (e.g. Niemann, 2003, p.46). Similar to the self-locking helical gear these profiles have a very less transverse contact ratio (theoretically only point contact) and high axial contact ratio (and helix angel). Disadvantageous of these gears is that they are sensitive to variations of the center distance. They are used to transmit high powers (e.g. helicopter gears). **Figure 4p** real design from the first patent of Ernest Wildhaber.

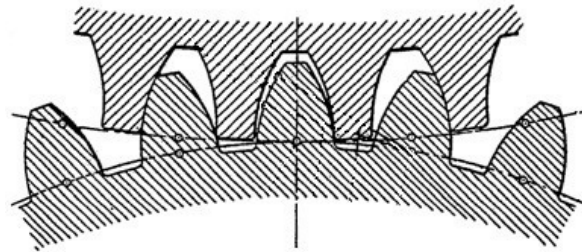


Figure 4p: Wildhaber/Novikov tooth profiles (GB 266163 A, Fig.1)

For this thesis, no equations to calculate Wildhaber/Novikov profiles are available. Therefore one model with similar geometry and approach, like in **figure 4g**, is drawn but the exact tooth shape is not calculated. Special the position of the radii of curvature is critical. Hence the efficiency of these concepts is not known. But it can be assumed that in its core equation (3-8) is also valid for this kind of gear. Hence it can be expected that this concept has also high efficiency, because there is a low transverse contact ratio.

In principal this circle tooth profiles leads to similar issues like flat teeth and high bearing loads. But in contrast the consequences of these issues seem to be more suitable as those of the self-locking helical gear. That means in comparison to the involute gearing the teeth are higher.

Figure 4q shows the model which is created. It is created with

- center distance $a=150$
- profile angel in transverse section $\alpha_{wt}=85^\circ$
- helix angel $\beta=45^\circ$
- module in normal section $m_n=7.071$ mm
- number of teeth $N_1=15$ (pinion) and $N_2=15$ (wheel)
- mesh width $w=50$
- average friction coefficient $f=0.07$
- teeth width at the addendum diameter $S_{a1}=6.11$ (pinion) and $S_{a2}=1.77$ (wheel).

The green part is the input while operation mode. In case of power outage the output part drives the arrangement (red).

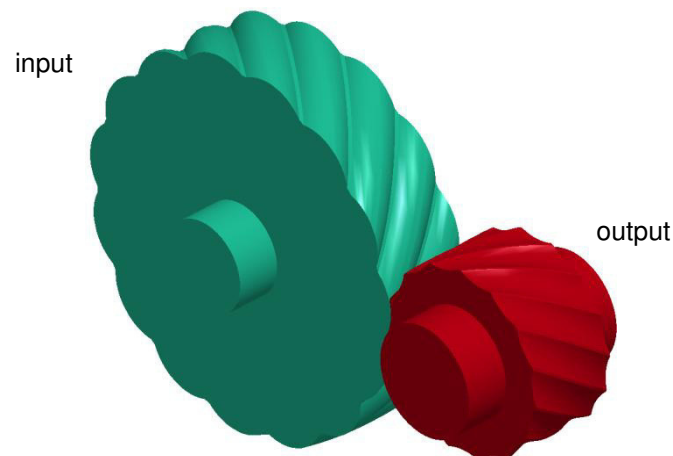


Figure 4q: Model with Wildhaber/Novikov mesh

In the multi body simulation no self-locking behavior can be proved. It is expected that this is due to the low level of information. Because of the advantages of this concept, it is still part of evaluation; however out of competition. This is done to find out if it is advantageous to investigate this idea in more detail.

Idea: cycloid or Hlebanja tooth profile

- Cyclone shape

The cyclone shape is one possible tooth profile. Therefore it is subject of investigation to clear if it is possible to prescind the same two effects as described in chapter 4.1 to this kind of tooth profile.

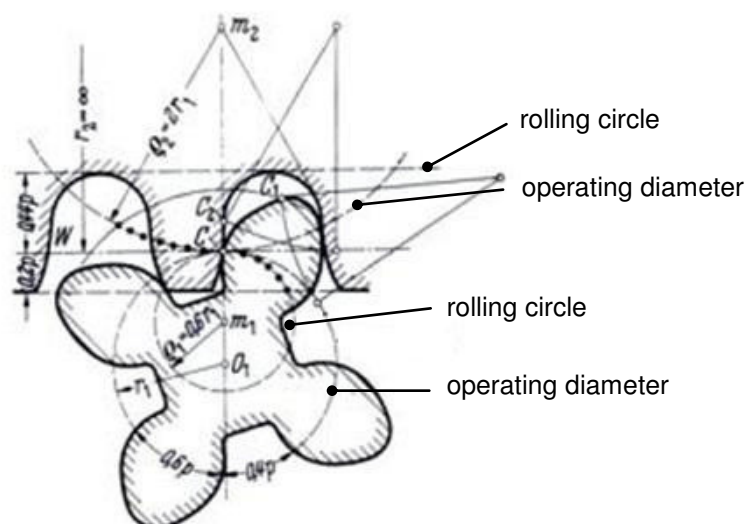


Figure 4r: Cyclone tooth profiles (Niemann, 2003, p.42)

Figure 4r shows such a cyclone shape in mesh with a rack. The identifiers which are shown in the figure are not needed in this thesis. The shape results from the unwinding of a circle on another circle. Therefore the pitch point of such a gear moves on a circle. Due to that it is not possible to prescind the self-locking idea of the self-locking helical gear to this kind of shape because a straight line is needed.

- Hlebanja tooth profile

Figure 4s shows a mesh of teeth with Hlebanja tooth profiles. The identifiers which are visible in this figure are not needed in this thesis. The shape results from a special cyclone shape; thus these two shapes are similar. Therefore this shape is not investigated in more detail because the pitch point also moves along a circle.

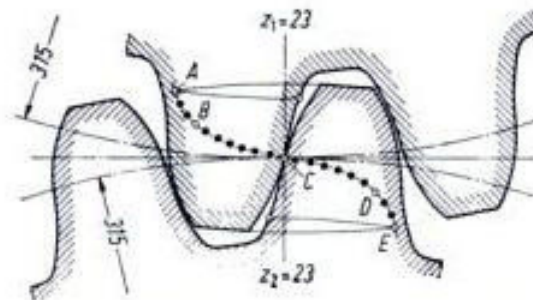


Figure 4s: Hlebanja tooth profile (Niemann, 2003: p.43)

Idea: Load sharing

All of the models which are mentioned above can be used in arrangements that support load sharing. **Figure 4t** shows one possible design which is able to manage most of the issues of the self-locking helical gear. It is based on the principle of load sharing. There is more than one wheel in contact with the driving pinion. Therefore the consequences of the high Hertzian pressure and the flat tooth shape are less in comparison to a mesh of two bodies.

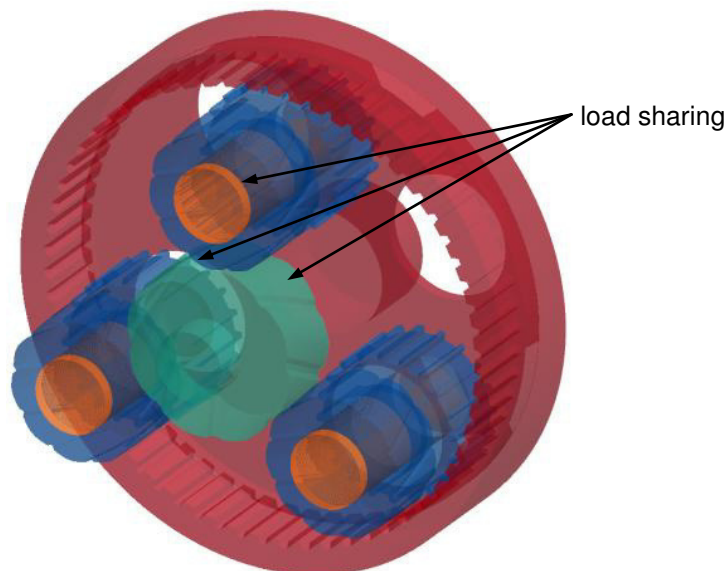


Figure 4t: Self-locking helical gear with load sharing

4.5 Conclusion of the self-locking helical gear

The approach which is chosen to design the self-locking helical gear has some disadvantages. They are described in chapter 4.4.1. As it is mentioned in the text above most of the disadvantages are manageable:

- The high bearing loads and the high axial forces handled by the design.
- The average friction coefficients which are needed to design the geometry can be supported which correct chosen oil.
- Forces can be reduced by using load sharing
- It can be expected that the high Hertzian pressures at the tooth flank can be reduced by choosing Wildhaber/Novikov tooth profiles. But due to a low level of information, the self-locking behavior cannot be proved in the multi body simulation.

In contrast the self-locking helical gear provides higher efficiencies than those gears which are mentioned in chapter 1.1.2 (e.g. worm gear).

Those disadvantages which cannot be managed are those which lead to flat teeth shapes and to disproportional distribution of the load between pinion and wheel (due to extreme x-shift; see figure 4n). Due to the two effects which lead to self-locking (see chapter 4.1) and accordingly to the parameter study of figure 4d, it can be argued that there are two different procedures to design the self-locking helical gear:

- a geometry with less x-shift and more friction (characterized by average friction coefficient) leads to less profile angel at the operation diameter and therefore to larger tooth height and less efficiency (compared with approach described below; see figure 4m) or
- a geometry with less average friction coefficient and more x-shift leads to larger profile angel at the operation diameter and due to that to flat teeth shapes and higher efficiency (see figure 4g).

Finally it can be argued that the self-locking helical gear from literature cannot fully satisfy the requirement list best because it is not possible to transmit high torques in small dimensions. Thus there are other models which can eliminate the main disadvantages. This fact will be part of the evaluation process (see chapter 7).

Furthermore, a proposal for a new model can be made. If the Wildhaber/Novikov mesh from figure 4q is combined with the load sharing idea (figure 4t) more disadvantages can be eliminated. Due to the simplicity of this idea no model for this is created in this master thesis.

5 Planetary gears in parallel connection

In the requirement list it is defined that the gear should have an overall gear ratio around 100 and the outer diameter should be as small as possible. The resulting high power density (ratio of transmitted power to gearbox volume) is a typical advantage of planetary gears. Together with the possibility of self-locking these gears seems to be useful for this thesis.

Table 5.1 shows a comparison of advantages and disadvantages of planetary gears.

Table 5.1: Comparison of advantages and disadvantages of planetary gears

advantages	disadvantages
coaxial mount	high construction costs
compact design	expensive
high gear ratios in one stage	more expensive by usage of many planets (load balancing is more complicated)
internal power division	
load balancing	sensitive to interferences
multiple degrees of freedom	lower efficiency in some cases
silent operation	high load at the planet mountings (as higher as the rotational speed)
small rotating masses	
symmetrical structure	

In the following some basics of planetary gearing, which are relevant for this thesis, are given.

5.1 Short theory of planetary gears

5.1.1 Differentiation of planetary gears and conventional gears

The following **figure 5a** shows the idea which is used to create a planetary gear out of a conventional gear. In the conventional gearbox (in figure 5a(left) a coaxial gear is drawn) all rotational axes of the wheels have zero velocity. That means they are fixed in the housing which represents the inertial system.

At a planetary gear not all the rotational axis are fixed to the housing. Therefore the center points of the wheels which are not at the same axis as the input and output parts, has a second relative velocity. These parts are called the planets. They are located at the planet carrier, which substitutes the housing fixed rotational axis of the planets in the conventional gear. The wheels which have the same rotational axis as the in- and output are called the central gears. The axes of the central gears are the only axes which are mounted in the inertial fixed housing.

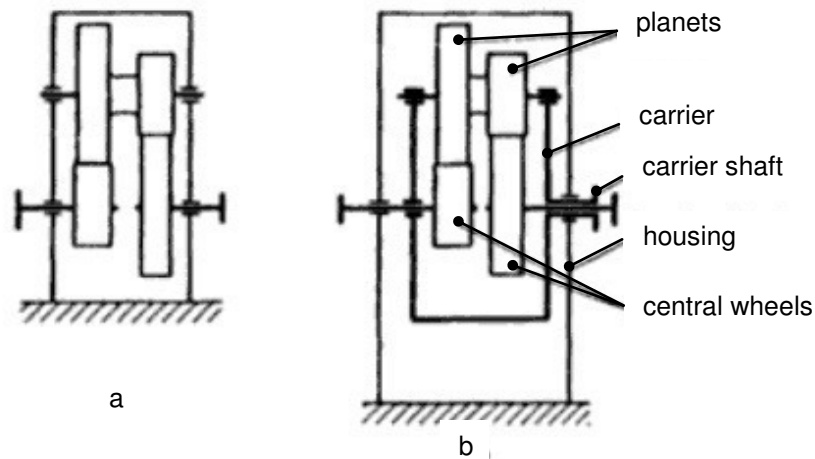


Figure 5a: Conventional (a) and planetary gearbox (b) (Müller, 1982, p.8)

Figure 5b shows the structure of a typical planetary gear. It consists of two central wheels, three planets and their carrier (not visible).

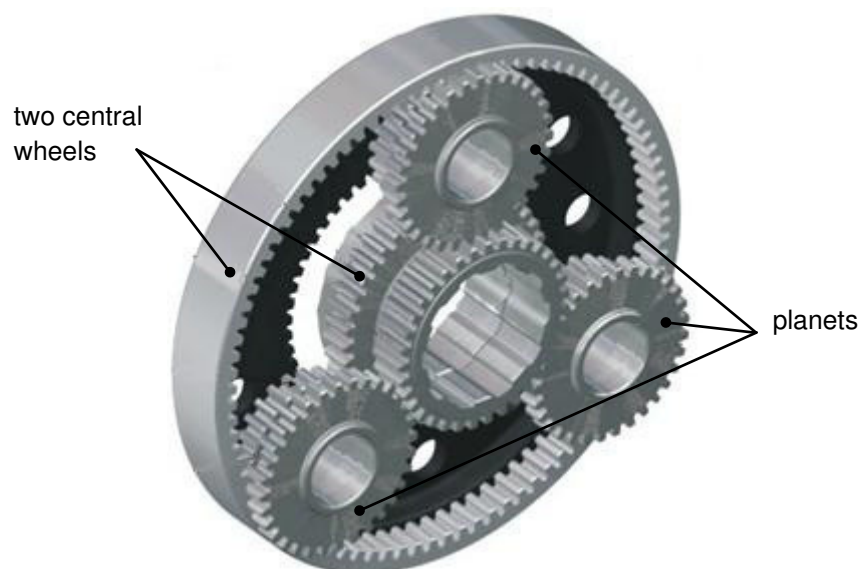


Figure 5b: Typical planetary gear (Rohloff AG)

More generally as in figure 5a planetary gears can be drawn as symbols. **Figure 5c** shows the symbol for a conventional gear (left) and a planetary gear (right), including the indices of the bodies which are used in this thesis.

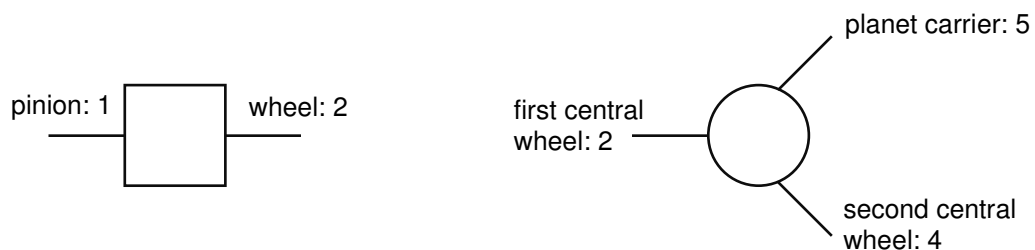


Figure 5c: Symbols of conventional gears (left) and planetary gears (right)

Accordingly to the design (figure 5b), in a planetary gear it is possible to realize internal power division. This can be done by usage of more than one planet.

5.1.2 Possible operational modes, gear ratios, rotational speeds and torques

In figure 5c the general symbols of the conventional and the planetary gears are shown. Accordingly it is clear that input and output of the conventional gearbox are at pinion and wheel. There are only two possibilities to drive the gear. Therefore this gearbox has only two gear ratios and only two directions of power flow (from pinion to wheel and vice versa).

In contrast the planetary gearbox has three possible output shafts. If one of this shafts is fixed to the housing (zero velocity), the planetary gear acts in two shaft operation. If all there shafts are able to transmit powers then the gearbox acts in three shaft operation mode. In three shaft operation it is possible to have two input shafts (power summation or summation gear) or two output shafts (power division or division gear).

Accordingly to these multiple shafts, the planetary gears have more than two gear ratios. In sum they have six so called relative ratios between the shafts. The main important relative ratio is the basic ratio. This is the ratio of the two central wheels in case of a planet carrier which is fixed to the housing. This basic ratio depends only on the number of teeth and the gear design. For the most common gear designs the basic ratio can be found in the literature (Müller, 1998, p.49; Volmer, 1978b, p.18÷19).

The remaining five relative ratios i_{ab} (a and b represent the indices of figure 5c) can be presented as,

$$\left. \begin{aligned} i_{24} &= \text{basic ratio from literature and } i_{42} = \frac{1}{i_{24}} \\ i_{25} &= 1 - i_{24} \text{ and } i_{52} = \frac{1}{i_{25}} \\ i_{45} &= 1 - \frac{1}{i_{24}} \text{ and } i_{54} = \frac{1}{i_{45}}. \end{aligned} \right\} (5-1)$$

Where i_{ab} is the relative ratio between the shafts a and b (e.g. i_{25} is the ratio from central wheel 2 to carrier 5).

These relative ratios are valid in three shaft operation as well as in two shaft operation. They are needed to calculate the rotational speeds as well as the torques.

For both operation modes the rotational speeds can be calculated by the Willis equation. It can be presented as

$$n_a - n_b * i_{ab} - n_c * (1 - i_{ab}) = 0 \quad (5-2)$$

Where n_a , n_b and n_c represents the rotational speeds of the free chosen shafts a, b and c and i_{ab} is the relative ratio between the shafts a and b.

For three shaft operation the Willis equation can be used well as in two shaft operation. In two shaft operation it has to be taken into account that one of the rotational speeds is zero.

Accordingly to the theory mentioned above it can be argued that the rotational speeds only depends on the number of teeth and the gear design.

5.1.3 Powers, power flow and efficiency of the planetary gears

Compared to the conventional gears, planetary gears have additional powers inside. Due to the additional movement of the planet carrier, there are two kinds of powers. One is the so-called rolling power; the other one is called the coupling power. The rolling power has the same intention as in the conventional gears (see chapter 3). This is the power which is transmitted by the teeth. In contrast the coupling power is that power which is needed to rotate the axes of the planets. The sum of booth powers gives the total power which can be used at the shafts.

Accordingly to the two powers in a planetary gear it must be distinguished between basic efficiency and efficiency. The power losses that caused by the friction of the mesh, can be characterized by the basic efficiency η_0 . This parameter has the same intention as the mesh efficiency at a conventional gear. It represents the possibility how much of the rolling power can be transmitted.

In contrast the efficiency is determined by taking the coupling power into account. Therefore the torques of the planetary gear, have to be calculated by considering the efficiency and the direction of the power flow. This direction of the power flow depends on which parts are driven and which are driving. It can be determined by the sign of the basic ratio (see **table 5.2**).

In these considerations it has to be noticed, that the efficiency of the planetary gear is not the same as the overall efficiency of the gearbox. The additional power losses as described in chapter 3.1 have to be taken into account to calculate the overall gear's efficiency.

If the torques are calculated under consideration of the power losses they can be written as

$$\left. \begin{aligned} \frac{M_4}{M_2} &= -i_{24} * \eta_0^{\text{sign}}, \\ \frac{M_5}{M_2} &= i_{24} * \eta_0^{\text{sign}} - 1 \text{ and} \\ \frac{M_5}{M_4} &= \frac{1}{i_{24} * \eta_0^{\text{sign}}} - 1. \end{aligned} \right\} (5-3)$$

With M_2 the torque at the first central wheel, M_5 the torque applied to the carrier, M_4 the torque at the second central wheel, i_{24} the base ratio, sign the direction of the power flow and η_0 the base efficiency.

These equations (5-3) are valid for two shaft operation as well as for three shaft operation. If the power losses are not taken into account, the torques of all shafts can be also expressed in terms of the relative ratios. That means the torques can be calculated independently of the

rotational speeds. Both only depend on the number of teeth and the gear design. This is one of the main important information for designing planetary gears.

Table 5.2: Determination of the direction of the power flow (Bouchè, 1988, p.148)

	$i_{24} > 1$	$i_{24} < 1$
forward driving (normal operation)	-1	+1
backward driving	+1	-1

According to the two different powers inside the gearbox, planetary gears can have low efficiency even if the power losses at the teeth are less. This is possible because the rolling and the coupling power can have opposite effects.

It is easy to understand that the efficiency of the whole gear is only influenced by the basic efficiency, the basic ratio and the sign of the power flow. This is clear because the rotational speeds and torques can be calculated independent. Thus the equations to calculate the efficiency of a planetary gear has the form $\eta = f(\eta_0, i_{24}, \text{sign})$. Where η_0 describes the basic efficiency, i_{24} is the basic ratio and sign represents the direction of the power flow.

In the literature (Müller, 1998, p.49; Volmer, 1978b, p.33) there are tables in which equations for efficiencies, in terms of the basic ratio, are listed. In fact these tables are not necessary to calculate such gears if rotational speeds and torques are calculated correct. Then the efficiency can be calculated by equation (5-4).

$$\eta = - \frac{\sum M_{\text{out}} * n_{\text{out}}}{\sum M_{\text{in}} * n_{\text{in}}} \quad (5-4)$$

Where η_0 describes the efficiency of the gear, M_{out} the torque(s) at the output shaft(s), n_{out} the rotational speed(s) of the output shaft(s), M_{in} the torque(s) at the input shaft(s) and n_{in} the rotational speed(s) at the input shaft(s).

The overall efficiency of the planetary gearbox (including bearings, seals and lubrication) can be calculated with equation (3-1). There the efficiency of the planetary gear (equation (5-4)) must be used instead of the term $\frac{P_{L_{\text{mesh}}}}{P_{\text{in}}}$.

5.1.4 Compound planetary gears

Such gearboxes consist of more than one planetary gear which is described above. One or more shaft(s) can be bounded to another gear (not necessarily a planetary gear). Therefore this is a special kind of planetary gearing, which follows in its basic considerations the same approach as the planetary gears above. Hence the equations (5-1) up to (5-4) can be taken to calculate these gears. But it has to be taken into account that bonds of torque(s) ($\sum T = 0$) and rotational speed(s) at the bounded shaft(s) have to be satisfied. Thus these bonds change the properties of the full gearbox.

With such compound planetary gears it is possible to create serial- and parallel connections like shown in the next figure.

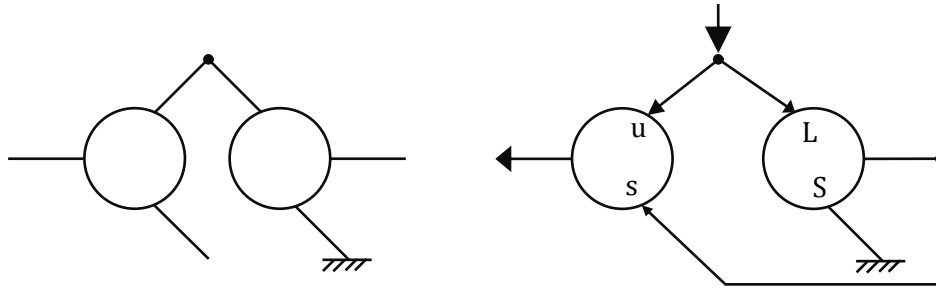


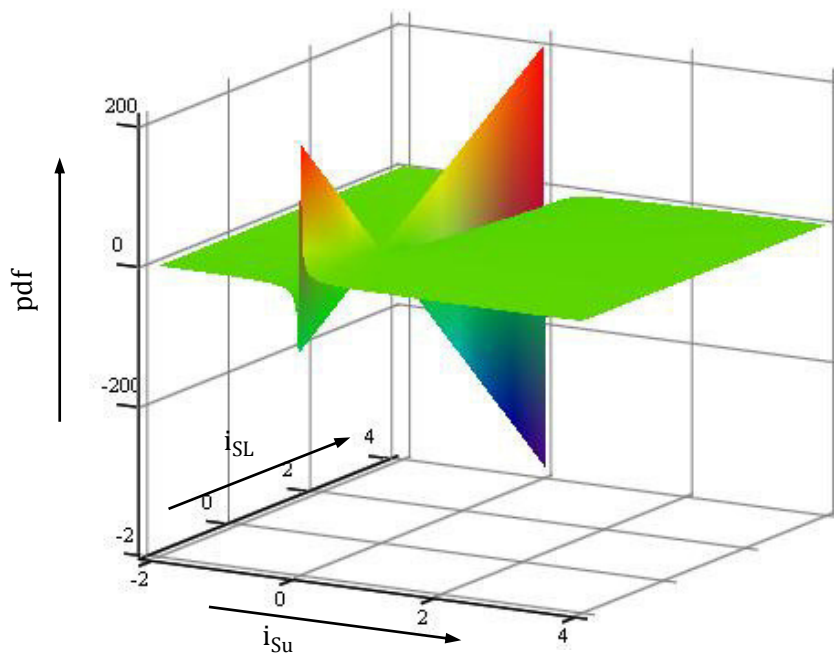
Figure 5d: Serial connection (left) and parallel connection (right) of planetary gears

In this thesis parallel connections are most important. The main parameter of a parallel connection, as it is shown in **figure 5d**, is the power division factor (pdf). This factor can be presented as

$$\text{pdf} = 1 - \frac{i_{SL}}{i_{Su}}. \quad (5-5)$$

Wherein i_{Su} describes the relative ratio of the self-locking gear from shaft s to shaft u and i_{SL} represents the relative ratio of the summation gear between shaft S and shaft L .

In this thesis the intention of a parallel connection is that most of the power is transmitted with less power losses to the output. If the power division factor is larger than 1 in the literature (Volmer, 1978b, p.58÷59) it is described that the power flow occurs as shown in figure 5d(right). This flow seems to be useful for this thesis. To find out the general behavior of the pdf, equation (5-5) is plotted over a $i_{SL} - i_{Su}$ plane (**figure 5e**).

Figure 5e: pdf plotted over a $i_{SL} - i_{Su}$ plane

As it can be seen in figure 5e, the pdf becomes largest in case of small ratio i_{Su} and high ratio i_{SL} .

5.1.5 Self-locking Planetary gears

In the literature (Müller, 1998, p.50÷51; Volmer, 1978b, p.50÷52) it is described that planetary gears can perform with self-locking in two shaft operation as well as in three shaft operation. The cause of self-locking is that the coupling power and the rolling power can have opposite effects (as mentioned above). If these two powers sufficiently counteract each other, self-locking occurs. In principle, the following **figure 5f** makes this visible.

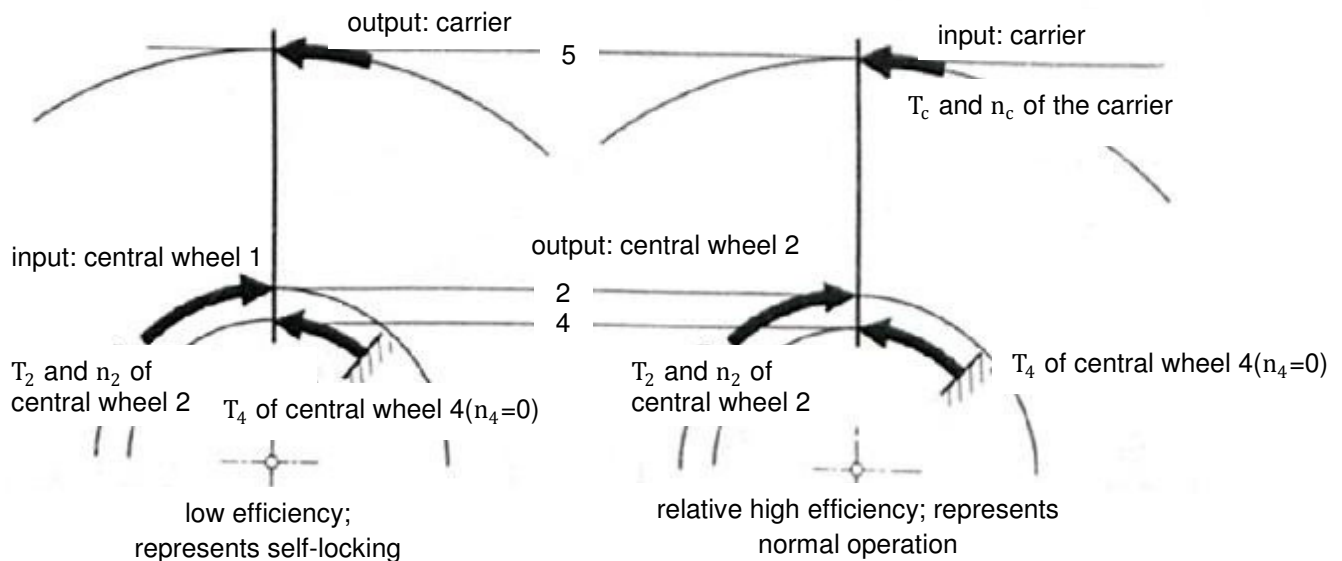


Figure 5f: Basic idea of self-locking planetary gears: normal operation (left) and self-locking (right) (Müller, 1998, p.51)

As it is visible in figure 5f the efficiency is much lower in case of driving central wheel (right) as in case of driving carrier (left). Highly simplified this can be explained as follows.

The arrows mark the direction of the torques and rotational speeds of each shaft. In the case which is drawn, the two powers (rolling and coupling) have different effects. This is due to the small difference of the diameters of the two central wheels. If the input is close to the fixed central wheel the self-locking of the planetary gear performs like driving against a fixed wall. Thus the efficiency is low.

As mentioned above self-locking planetary gears have low efficiency (<50%). If they are used in parallel connection higher efficiency can be provided. The basic idea is described in the literature (Bouché, 1988, p.154), wherein most of the input power should flow directly to the output of the transmission.

The self-locking condition and some general statements follow from the following examination:

If the equilibrium condition for torques is written as

$$M_2 + M_4 + M_5 = 0. \quad (5-6)$$

With M_2 the torque at the central wheel number 2, M_5 the torque applied to the planet carrier and M_4 the torque at the central wheel number 4. All torques can be calculated with equation (5-3).

In the following the self-locking condition is derived only for the case of two shaft operation. While this operation mode, the equations above ((5-3) and (5-6)) show that in case of self-locking only the torque at the carrier can satisfy the equilibrium torque condition ($T_5 = 0$). That means that in two shaft operation, only planetary gears with driven planetary carrier can create self-locking (i.e. the planet carrier has to be input part in operation mode). With the equations (5-3) and (5-6) this leads to the following condition of self-locking for planetary gears

$$\eta_0 < i_{24} < \frac{1}{\eta_0}. \quad (5-7)$$

Where i_{24} describes the base ratio and η_0 the base efficiency.

This self-locking condition is in two shaft operation as valid as in three shaft operation (Volmer, 1978b, p.51), but the examination is more difficult. Thus it is only derived for two shaft operation in this thesis. In the following some general statements are given.

As it is visible in equation (5-7), the self-locking behavior is mainly influenced by the base efficiency and therefore by the friction coefficient. But in comparison to the self-locking helical gear, the average friction coefficient does not determine the gear's geometry.

Another result of equation (5-7) is that only gears with positive base ratios are self-locking.

Gears with high base efficiencies (close to 1) can also realize self-locking if the basic ratio is close to one. But these gears need high numbers of teeth and thus large outer diameters.

Additionally it has to be noted that self-locking in three shaft operation requires a summation gear (Volmer, 1978b, p.50). As mentioned above the main aim of this thesis is to find a gear with self-locking and high efficiency in operation mode. Therefore a self-locking summation gear in three shaft operation makes no sense, because these gears have only efficiencies below 50%.

Figure 5g shows five gears which can achieve all of the conditions for self-locking which are mentioned above. The central wheels (2 and 4) are drawn thick; the planets (3a and 3b) are represented by thin lines and the planet carrier (5) with dashed thin ones. Furthermore the equations for the base ratio are given below in the figure.

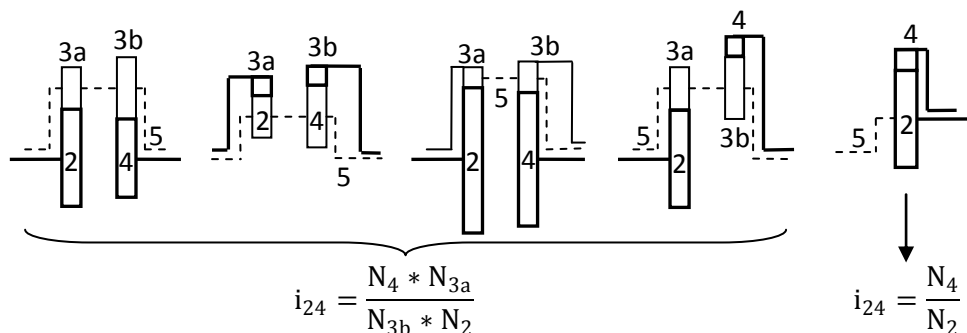


Figure 5g: Possible gear principles and there basic ratios (accordingly to Volmer, 1978b, p.18÷19)

Where N_x described the number of teeth of those body which is marked by the index and i_{24} represents the base ratio.

With the theory which is mentioned above all basics are known to calculate compounded planetary gears in parallel connection. To find solutions which perform best efficiency and self-locking the self-locking condition is investigated in more detail. The outcomes are given in the following.

Figure 5h shows the efficiency in operation mode across a plane of basic ratio and basic efficiency, including the self-locking condition. The colored plane which is shown, represents all possible self-locking gears (for a range of $i_{24}=0\div2$). This figure is plotted with Matlab. In the appendix the exact source code is presented.

As it is visible at $i_{24}=1$ there is a discontinuity. This is due to the self-locking condition. Gears which base ratios exactly one cannot be built. Also visible is that gears which base ratios less smaller than 1 have higher efficiencies than those with base ratios less above one (see also figure 5i).

Another statement is that, planetary gears with very low base ratios can also satisfy the self-locking condition (5-6) with high efficiency. But therefore low base efficiencies are needed and accordingly to that very high average friction coefficients. Thus these are only theoretical solutions.

In the literature (Müller, 1998, Volmer, 1978b) it is described that only gears around $i_{24}=1$ can satisfy the self-locking condition. In the figure below it is shown that this is false. This can be argued because the figure shows self-locking solutions with acceptable efficiency, far away from the $i_{24}=1$ discontinuity.

Furthermore it can be seen that, there is an asymptotic solution at $i_{24}=1$ and $\eta_0=1$. It seems to be advantageous to choose the design nearby this point. But it is not possible to design a gear exactly at this discontinuity.

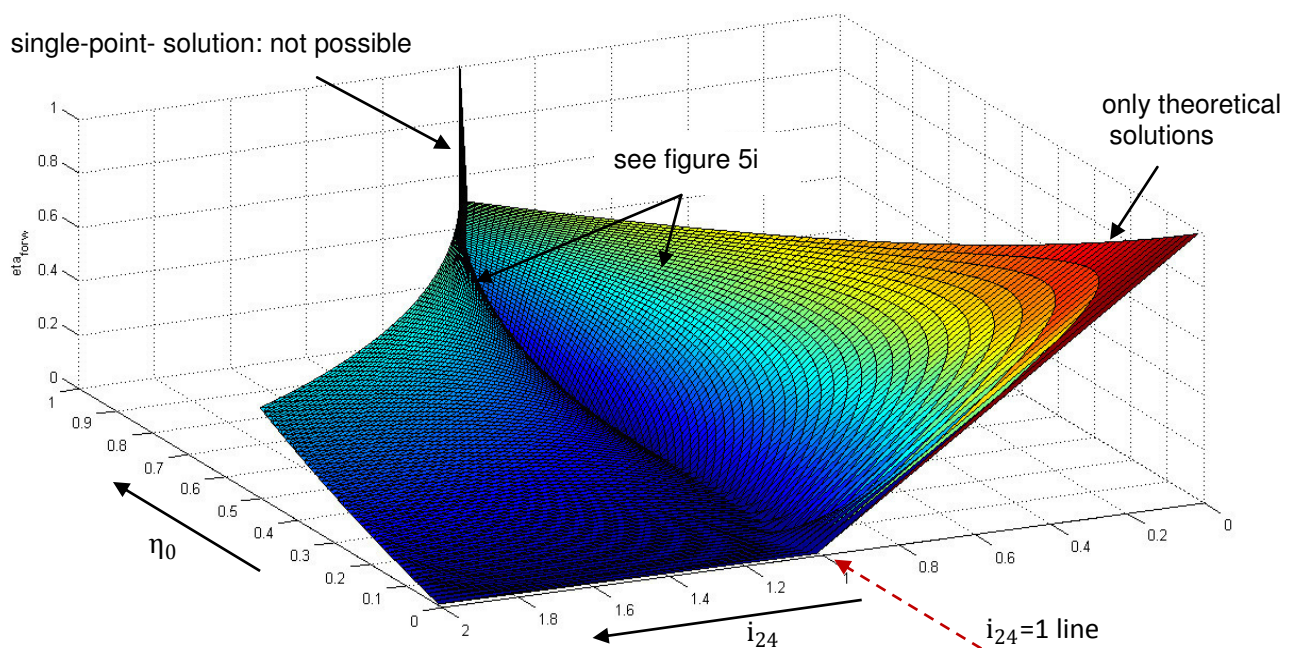


Figure 5h: 3-dimensional plot of the self-locking condition

The contour plots of figure 5h are shown in the next **figure 5i**. The figure shows the efficiency of the planetary gear at the ordinate across the base ratio at the abscissa (above) and the base ratio at the ordinate over the base efficiency at the abscissa (below).

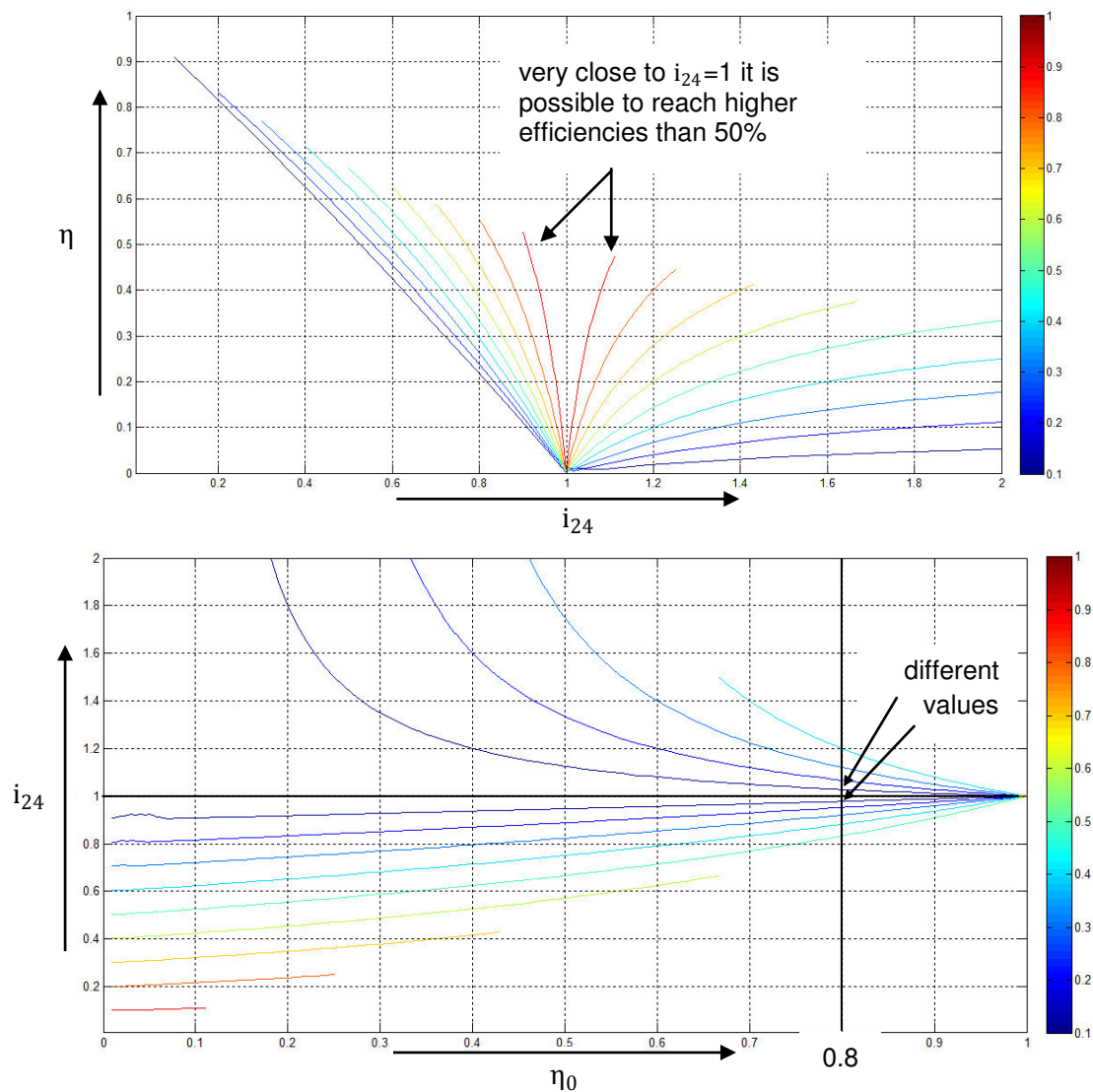


Figure 5i: Contour plot in the i_0 -efficiency plane

As it is shown in figure 5i(above) self-locking planetary gears can reach efficiencies higher as 50%, with acceptable base efficiencies and with a base ratio very close to $i_{24}=1$.

Figure 5i(below) shows that planetary gears with $i_{24}<1$ have slightly higher efficiencies than planetary gears with $i_{24}>1$ (compared at the same base efficiency e.g.: 0.8).

Finally, it must be noted that gears with relatively high efficiencies perform self-locking, but they should not be designed. This is because they are operating at the border of self-locking. That means self-locking can be calculated, but to be sure that self-locking works in the application as well, lower efficiency should be accepted in the design process (Müller, 1998, p.51).

5.1.6 Limitations in design

Assembling condition

Creating a planetary gear with one planet is relatively easy. If the power should be divided to more than one planet an assembling condition has to be satisfied. It arises by installing one planet in the mesh between the two central gears. Then the relative position of the two central gears is fixed. To avoid interferences or crashes of the teeth in the meshes the planet has to be in the same relative position after a rotation through an angle of $2\pi/(\text{number of planets})$. This is shown in the following **figure 5j**.

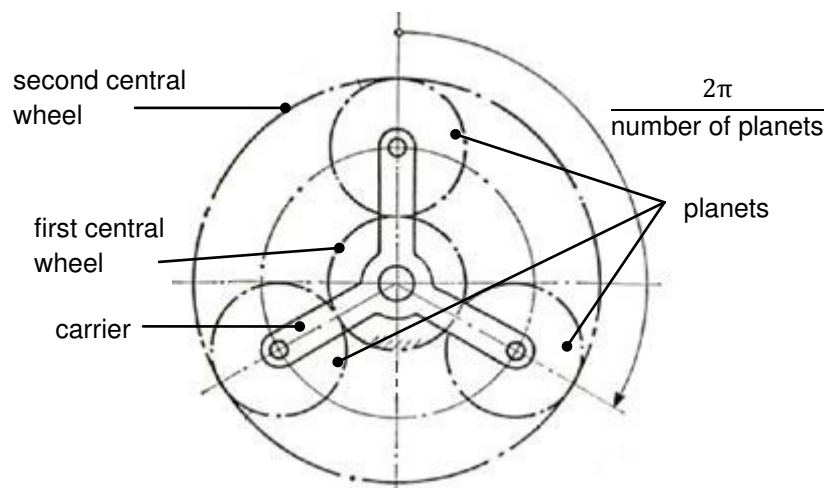


Figure 5j: Assembling condition (Volmer, 1978b, p.52)

For different structures of planetary gears this assembling conditions are available in the literature (Müller, 1998, p.49).

Limitations of the gear ratio

Another limitation is given by the number of planets which can be used. As it is visible in **figure 5k**, the planets should not touch each other. Thus the number of planets in the mesh is limited.

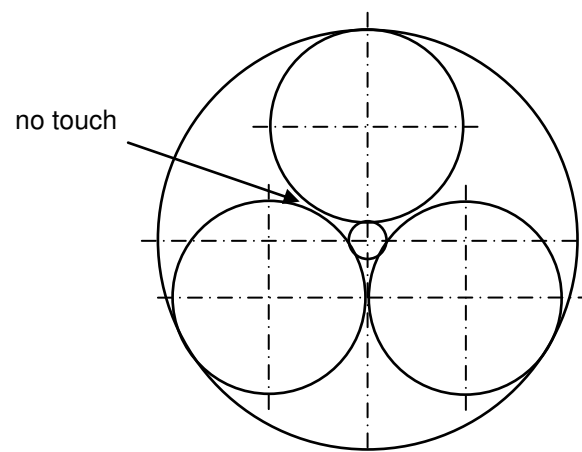


Figure 5k: Limitation of the gear ratio

Principles of load balancing

If multiple planets are used, the gear is statically overdetermined. To guarantee that all planets transmit an equal force, the principles of load balancing have to be taken into account. There are several solutions to realize that:

- non mounted inner central wheel (only possible with three planets),
- non mounted outer central wheel,
- inner and outer central wheels are not mounted and
- elastic mounted planets.

All these solutions are described in detail in the literature (Müller, 1998, p.240÷244). Hence they are not described in more detail in this master thesis.

5.2 Models of self-locking planetary gears in parallel connection

As it is mentioned above, self-locking planetary gears perform with efficiency below 50%. Thus they can be used in parallel connection to provide higher efficiency. The following **figure 5l** shows the approach of ideas as they arise in this thesis. In which green pigmented boxes mark ideas which are able to fulfill the requirement list and red ones those ideas which are not able to fulfill the requirement list. Below the figure the ideas are described in more detail.

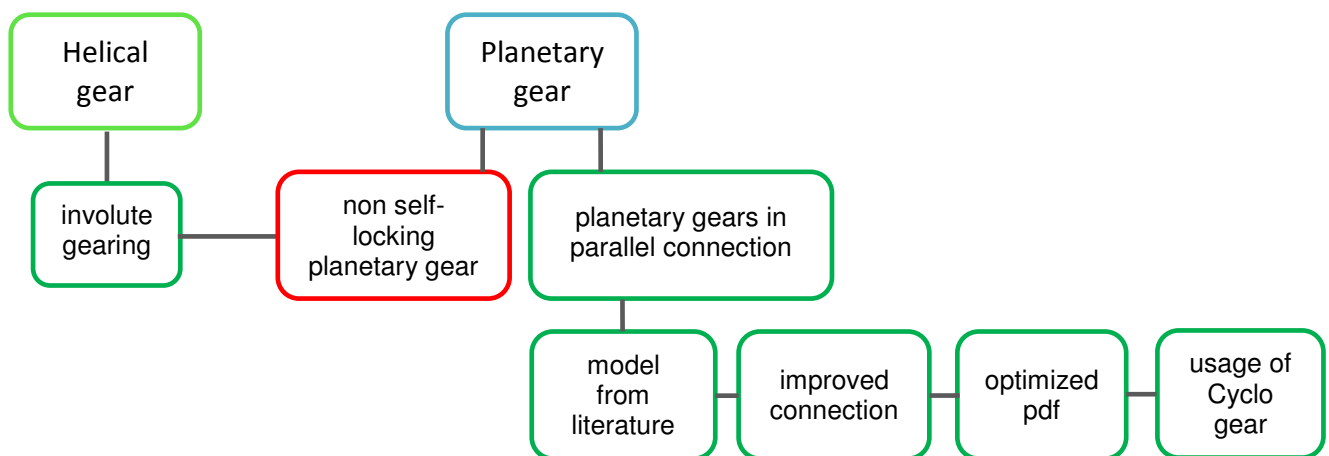


Figure 5l: Approach of self-locking planetary gears in parallel connection

Idea: Non self-locking planetary gear

The first idea is to implement the self-locking helical gear in a planetary gear in parallel connection. The intention of this is to use a self-locking helical with lower efficiency but favorable geometry (as shown in figure 4m). **Figure 5m** shows the model. It consists of three gears. The first gear divides the input power between the self-locking gear and a additional gear.

In a multi body simulation it is shown that the characteristics of the self-locking helical gear only locks the relative movement of the bodies. Thus in case of power outage, the full gear rotates with one rotational speed. Hence this model cannot be used without additional device (for example a bracket at the outer diameter). Because additional devices should not be used in this thesis, this idea is not pursued.

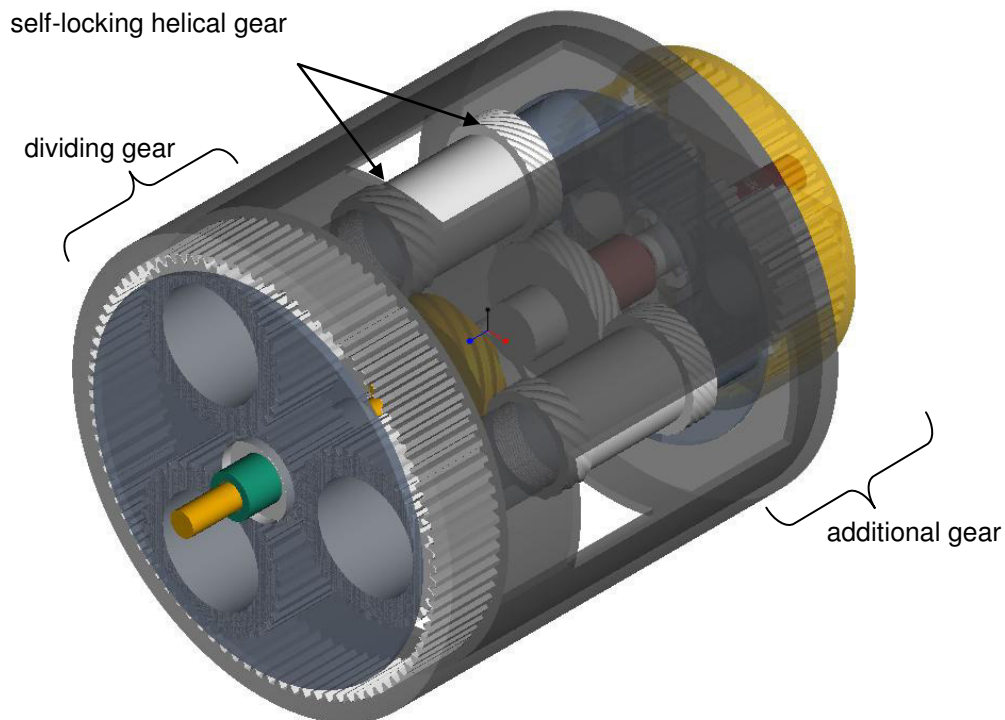


Figure 5m: Self-locking helical gear and planetary gear parallel connection

Idea: Model from literature

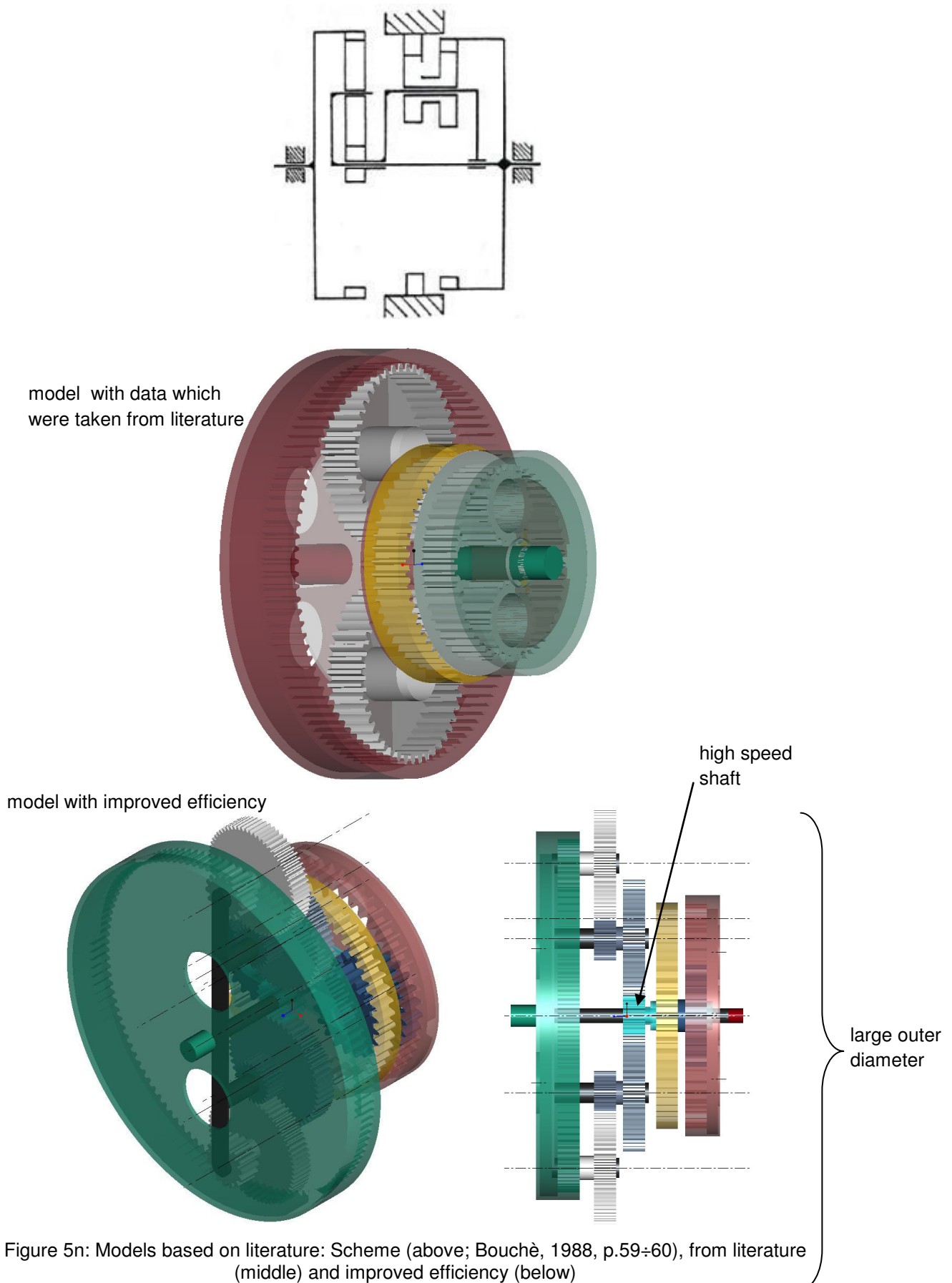
This model is implemented based on the data (numbers of teeth) which are given in the literature (Bouch , 1995, p.59-60). As it is described there, this gear performs with an overall ratio around 2 and an overall efficiency around 70%. The model is shown in **figure 5n (middle)**. It consists of two gears; one divides the input power between the self-locking gear and the output shaft, the other gear is a conventional self-locking planetary gear.

Idea: Improved efficiency

The intention of this model is to improve the overall efficiency of the idea 'Model from literature'. The model is shown in **figure 5n(below)**. In **figure 5n(above)** the scheme of these concepts is visible. This has the same structure as the model above ('Model from literature'), but due to the improved efficiency there are some detriments. The disadvantages of these models are

- relative large diameters ($>>500$ mm),
- low gear ratios (around 1.1) and
- speed increasing stages to divide the power.

If the lifetime of this gear is taken into account the last fact seems to be unfavorable. Thus other solutions are searched.



Idea: Self-locking gear in three shaft operation mode

The intention of this idea is to avoid gears with two shaft operation mode. Another reason for this investigation is the need to find another connectivity of the gear arrangement, because these connections of the shafts, seems to be unfavorable for this thesis. Figure 5o shows the general description of such an arrangement which is used in this thesis.

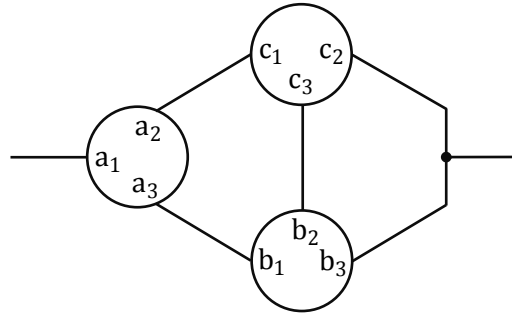


Figure 5o: General description of the arrangement in three shaft operation mode

Figure 5o shows that three gears should be used. All shafts of these gears should be connected to another gearbox. For this configuration a set of Willis equations and corresponding bonds of rotational speeds (5-8) is calculated. The meaning of the shafts varies from calculation to calculation. That means e.g. shaft a_1 could represent the first central wheel as well as the second central wheel or the carrier. In the next calculation the meaning is changed. This only influences the bonds in the set of equations (5-8). Because each gear has three shafts, it can be argued that in principle there are 27 possible combinations of bonds. Some possibilities can be excluded, because the self-locking gear has to be driven to the carrier. Furthermore it should be taken into consideration that none of the gears shall operate as a high speed gear. This also eliminates some possibilities. Therefore only six possible combinations of bonds are remaining. All of these possibilities are calculated with the following set of equations (5-8).

$$\begin{array}{lcl}
 n_{a_1} - n_{a_2} * i_{a_1 a_2} - n_{a_3} * (1 - i_{a_1 a_2}) = 0 & & \\
 n_{b_1} - n_{b_2} * i_{b_1 b_2} - n_{b_3} * (1 - i_{b_1 b_2}) = 0 & \left. \begin{array}{l} \text{Willis} \\ \text{equations} \end{array} \right\} & \\
 n_{c_1} - n_{c_2} * i_{c_1 c_2} - n_{c_3} * (1 - i_{c_1 c_2}) = 0 & & \\
 n_{a_3} = n_{b_1} & \left. \begin{array}{l} \text{bonds of} \\ \text{rotational} \\ \text{speeds} \end{array} \right\} & \\
 n_{a_2} = n_{c_1} & & \\
 n_{b_2} = n_{c_3} & &
 \end{array} \quad (5-8)$$

As a result of the equations (5-8) it can be argued that each calculation yields to a result in which one of the six rotational speeds (n_{a_1} , n_{a_2} , n_{a_3} , n_{b_1} , n_{b_2} , n_{b_3} , n_{c_1} , n_{c_2} or n_{c_3}) is zero. Hence there is no possibility for a self-locking planetary gear in three operation mode in such an arrangement as shown in figure 5o.

Idea: Improved connection

Figure 5p shows the next model with higher efficiency because of improved connection. In this gear a similar connection as in the first idea ('Non self-locking planetary gear') is used. That means this model consists of a gear which divides the power. One part of the power can be used in the self-locking gear and the other one is utilized at the two additional gear boxes. These additional gear boxes are only used to increase the overall gear ratio. Apart from the large outer diameter (around 700 mm), this concept eliminates most of the disadvantages of the model above.

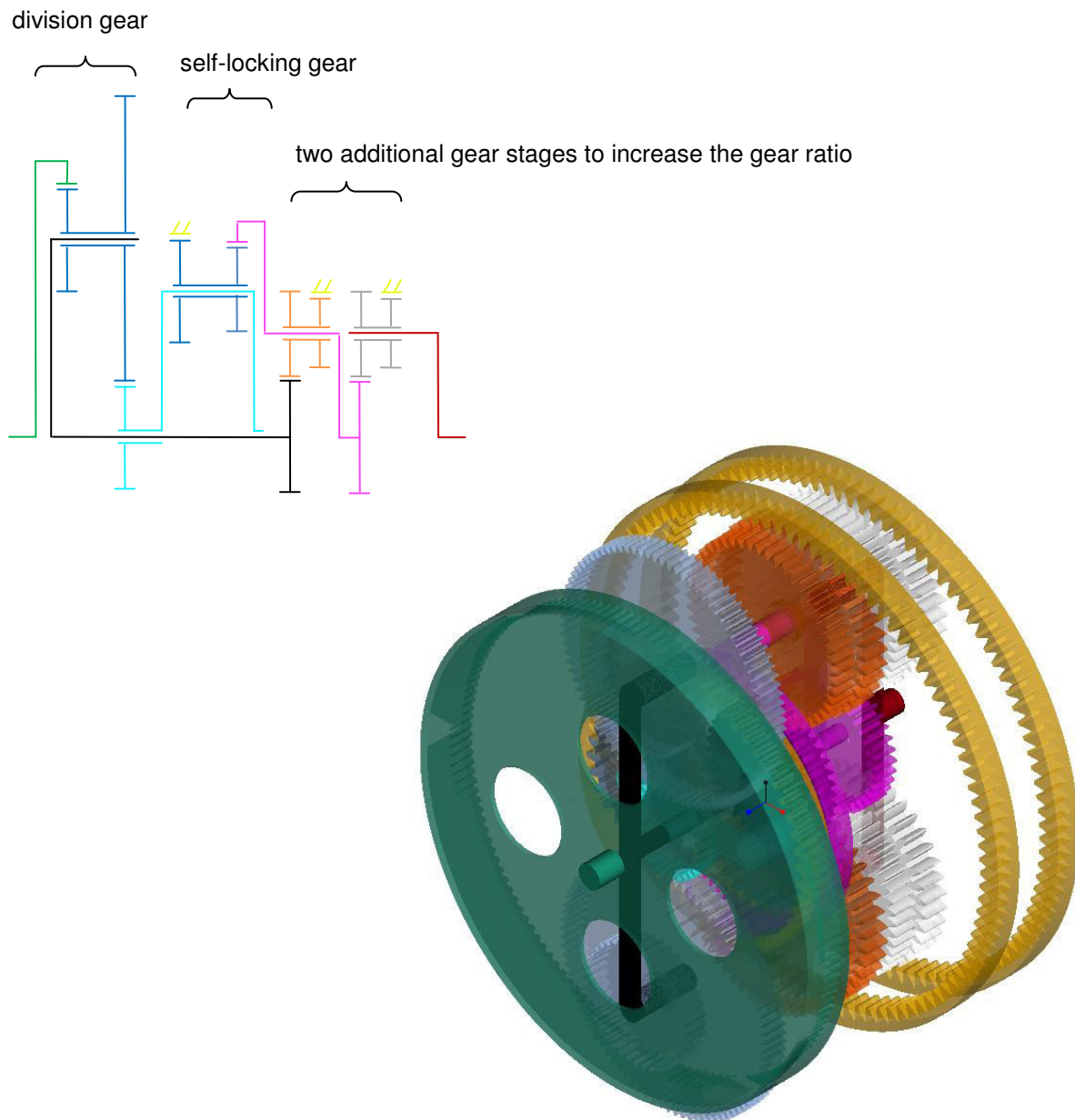


Figure 5p: Model with improved connection: Scheme (above) and model (below)

This gearbox performs with a mesh efficiency of around 93% and due to the two additional gear stages an overall gear ratio of around 21. Due to this mesh efficiency, overall efficiencies larger than 90% can be expected.

Idea: Optimized power division factor (pdf)

In order to eliminate the disadvantages of the ideas above, an optimization is started to find the best combinations of i_{Su} and i_{SL} (see figure 5d). The main condition is to take a suitable pdf into account. Other conditions for the optimization are:

- overall gear ratio around 100 and
- rotational speed of the shafts (all speeds less than input speed).

There are multiple solutions of this optimization procedure. Two of them can be presented as

$$\begin{pmatrix} i_{Su} \\ i_{SL} \end{pmatrix} = \begin{pmatrix} -2.22 \\ +19.99 \end{pmatrix} \vee \begin{pmatrix} -0.33 \\ +11 \end{pmatrix}. \quad (5-8)$$

The models which are shown in figure 5q and figure 5r are the outcome of this optimization. Because of design reasons the optima cannot be satisfied exactly, but these models are close to it.

The concept which is visible in the following **figure 5q** represents the first optimum of solution (5-8). Instead of the optimum given above in equation (5-8), this concept performs with a combination of $i_{Su} = -2.2$ and $i_{SL} = +22$. In figure 5q(above) the scheme and in figure 5q(below) the model is shown. The model consists of a self-locking gear, a summation gear and two additional gear stages to increase the overall gear ratio. One difference to the models above is that the gear arrangement is driven at the shaft which connects the self-locking and the summation gear.

This gear performs with a mesh efficiency of around 91% and an overall gear ratio around 34. Without additional stages the gear ratio is only around 3. Compared to the models above the main advantage of this concept is the relative small outer diameter (around 400mm). Due to this low mesh efficiency it seems to be difficult to design such a gear with an overall efficiency larger than 90%. But it can be expected to reach higher mesh efficiency if the design is closer to the optimum.

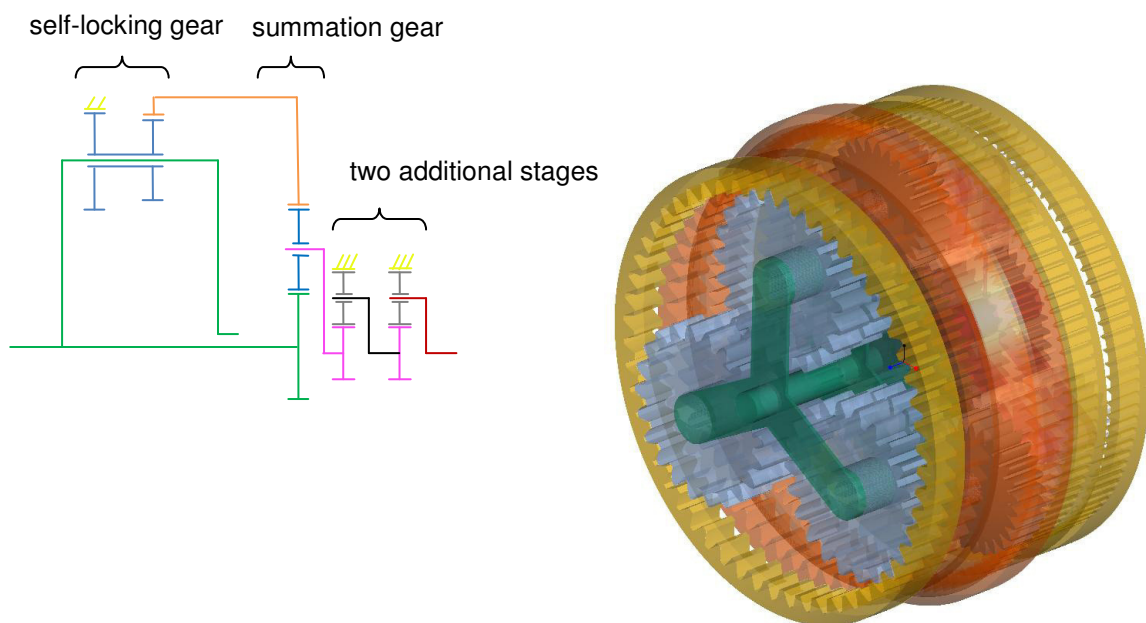


Figure 5q: Optimized planetary gear in parallel connection: Scheme (above) and model (below)

Idea: Usage of Cyclo gear

The Cyclo gear is a gear which is suitable for rough operation. It is well known in the literature (Lehmann, 1976). If the application needs to perform in such an operational mode, the following concept seems to be suitable (**figure 5r**). It represents the second optimum in solution (5-8), in which it must be noted that a combination of $i_{Su} = -0.333$ and $i_{SL} = +11$ is realized.

This concept consists of only two gears. The Cyclo gear includes the input shaft (green), as well as the output shaft (red). Thus it divides the input power into two parts. One part is used at the output shaft, the other part is utilized in a self-locking gear.

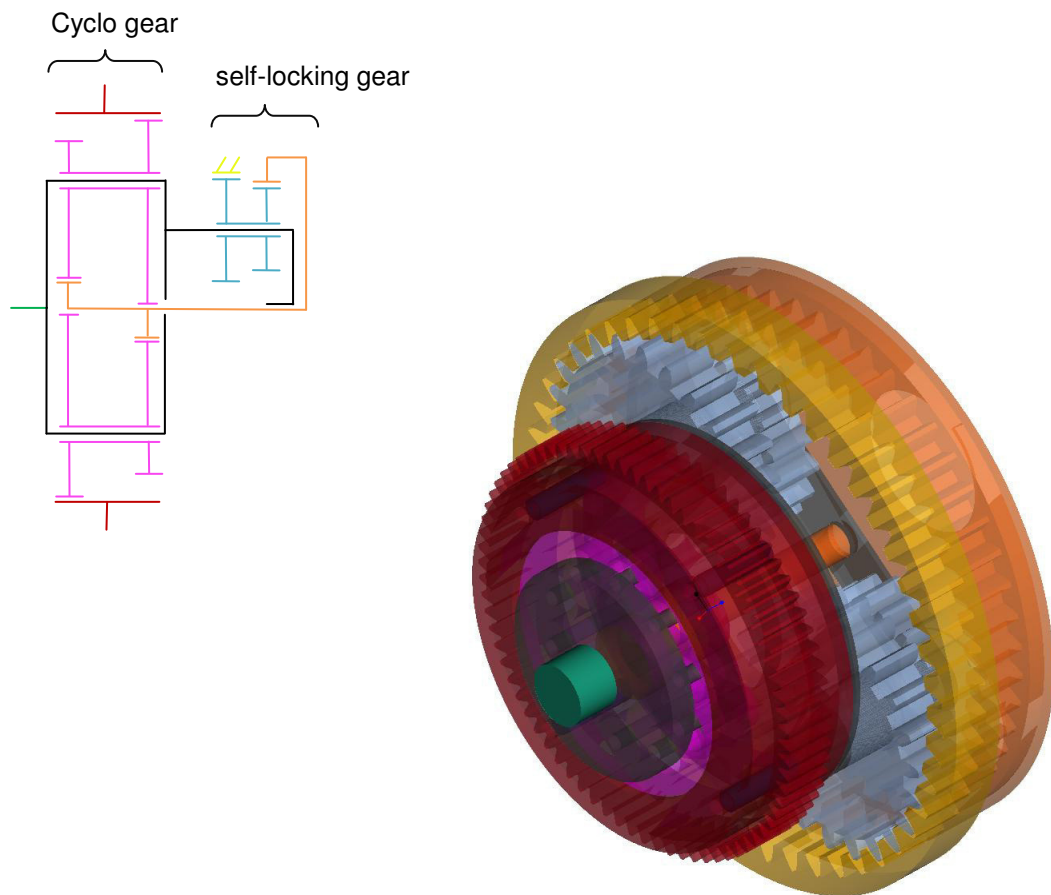


Figure 5r: Model which includes the Cyclo gear

This model performs with mesh efficiency around 97%. Due to missing additional stages the gear ratio is only around 1.2. The main advantage of this concept is a significant smaller outer diameter as in the idea 'Optimized power division factor' (around 350mm). Due to this high mesh efficiency, an overall efficiency above 90% can be expected.

5.3 Conclusion of the self-locking planetary gears in parallel connection

The models which are described in chapter 5.2, shows that it is possible to satisfy the requirement list.

The first model which is done (figure 5m), shows that it is not possible to combine the self-locking helical gear and such an arrangement of parallel connection. It can be argued that with such an arrangement there is no sense to use other self-locking gears (e.g. worm gear) instead of the self-locking helical gear. The reason for that is due to the rotating center points of the self-locking arrangement.

The main problem which cannot be solved is the relationship between well lubricated gears (high base efficiency) and outer diameter. This requires high basic efficiency and due to the self-locking condition (5-7) basic ratios very close to one. As it is mentioned above, that fact leads to large outer diameters.

Furthermore it can be argued that reaching high overall efficiency, small dimensions and high gear ratios (without additional stages) is a technical contradiction in this concept. This is due to the high power division factors (pdf) which are needed to reach high overall efficiency. Accordingly to equation (5-5), high pdf requires high gear ratios. As a result the outer diameters of the models are large. Therefore the cyclone shape is useful because with this shape many teeth at small circumferences can be realized (figure 5r). By comparing the models above this can be confirmed.

Because of the different characteristics the models which are shown in the figures 5p, 5q and 5r are part of evaluation (see chapter 7).

6 Linkage drive

6.1 Short treatise of the theory of linkage drives

This kind of gears (figure 2e) is characterized in that their bodies are connected by swivel joints or prismatic joints. In this thesis the focus is only on linkage drives with four bodies and swivel joints. Most of these gears are used to transfer nonuniform movements. Accordingly to literature (Volmer, 1978a, p.135), the advantages of these gears are

- relative easy manufacturing,
- favorable contact in the joints and
- various applications.

A possible distinction of these gears is to sort them by their numbers of bodies and degrees of freedom. The number of degrees of freedom can be expressed by the relation of Grübler (Lehmann, 1976, p.11). It can be presented as

$$F = T * (n - g - 1) + \sum_{i=1}^g b_i . \quad (6-1)$$

Where T describes the kind of the gear (T=6 for spatial movement, T=3 for plane movement), n number of bodies, g number of joints and b_i degrees of freedom of each joint with number i.

Especially linkage drives which consist of an even number of bodies (e.g. 4, 6, 8,...) perform with one degree of freedom. If the application has an uneven number of bodies (e.g. 3,5,7,...) then this gear performs with more degrees of freedom. These gears are typically used as adjustment gears.

A classification of the gears which consist of four bodies is possible according to the following aspects (Volmer, 1978a, p.135).

- Characteristics of the structure: numbers of joints and their relative arrangement
- Relations of length and the resulting movement
- Functions of the bodies (e.g. which bodies are fixed which ones are flexible).

The possibility of movement can be characterized by the relation of Grashof. If the length of the bodies is designated by l, the relation of Grashof can be presented as

$$l_{\max} + l_{\min} \leq l' + l'' . \quad (6-2)$$

Wherein l_{\max} represents the length of the longest body, l_{\min} the length of the shortest body and l' respectively l'' the length of the two remaining bodies.

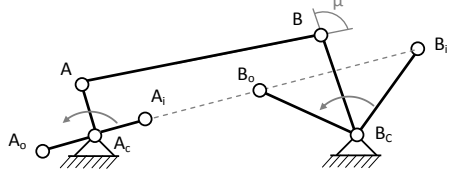
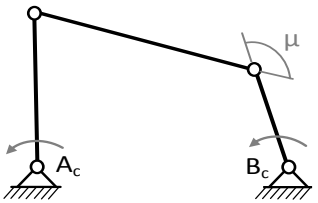
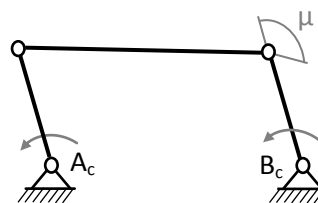
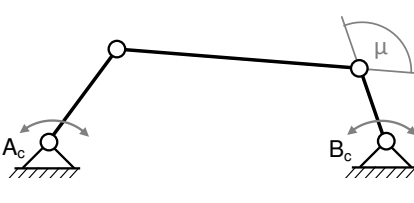
In relation (6-2), two cases can be distinguished.

- If the inequality sign in relation (6-2) is valid, the gear is performs without any problems.
- If the equality sign in relation (6-2) is valid, then the gear has positions in which the bodies form a straight line. These positions are the so-called branching positions. In such a position the shortest body normally performs with an oscillating movement

relative to its adjacent bodies. Such positions are undesirable therefore they are bypassed by the design. If the relation of Grashof (6-2) is not valid, all bodies are oscillating. Therefore there is no constant movement (Volmer, 1978a, 1978, p.136).

Table 6.1 gives a short overview of possible gear design and the relations of Grashof.

Table 6.1: Possible designs of linkage drives (according to Volmer, 1978a, p.137)

relation of Grashof	name	scheme
$l_{\max} + l_{\min} < l' + l''$	pivot linkage	
$l_{\max} + l_{\min} < l' + l''$	drag-link mechanism	
$l_{\max} + l_{\min} = l' + l''$	parallel crank shaft gear	
$l_{\max} + l_{\min} > l' + l''$	double rocker	

Another important position of a linkage drive is the so called dead-center position. There are two different dead-center positions A_c and A_i (see dashed line in table 6.1 row 1, column 3). These positions are characterized by

$$\overline{B_i A_c} = \overline{AB} - \overline{A_c A} \text{ and } \overline{B_a A_c} = \overline{AB} + \overline{A_c A}. \quad (6-3)$$

In these positions no forces from the shaft to the output shaft can be transmitted.

Another important parameter of linkage drives is the angel which is called Altsche protractor μ . This angel is variable while the movement. It represents the relative velocity of two bodies. If it is very small, the forces in the swivel joints increase. At the limit ($\mu = 0$) the forces at the joints are going to infinite. This special position ($\mu = 0$) is the dead-center position. Due to the relationship between protractor and forces, this angel describes the quality of the movement.

6.2 Possibility for self-locking

In the literature it is not described that these gears are able to perform self-locking, but there are several patents which describes the self-locking possibility at this gears (e.g. DE 10261588 A1, DE 19515132 A1). Although patents do not represent databases for knowledge, this is the reason why these gears are investigated in this thesis. The following **figure 6a(below)** shows a figure from patent DE 10127676 A1, which explains the self-locking behavior. In which it must be noted that the orange and blue lines are added by the author of this thesis. This arrangement is due to the literature (Volmer, 1978a, p.60). There is an arrangement as it is shown in **figure 6a(above)** given. Therefore the dashed grey lines from figure 6a(above) have the same meaning as the lines orange lines in figure 6a(below). Furthermore the black lines in figure 6a(above) have the same intention as the blue lines in figure 6a(below).

In figure 6a(below) the body with number 1 represents an internal gear (commonly the output part), body 2 a disk with an external gear, bodies 3, 5a and 5b are eccentrics. Wherein the body number 3 is connected to the input shaft (commonly the input part) and bodies 5a respectively 5b are able to rotate free in the housing but they have no connection with parts outside the gearbox. As it is described in the patent the force F which comes from the internal gear (1), is not able to drive the input eccentric (3). These gears have only one degree of freedom if the distances a , b and c are the same. Furthermore, the triangles $\triangle A_1B_1C_1$ and $\triangle A_2B_2C_2$ have to be congruent for this (see figure 6a(above)).

As it can be seen, these gears are equal from a kinematic point of view. One difference is that the power leaves the linkage drive at the disk (2) (as shown in figure 6a(below)). In contrast in figure 6a(above) the power leaves the linkage drive at one of the shafts A_1 , B_1 or C_1 . Due to that the linkage drive of figure 6a(above) has no constant movement and therefore no constant gear ratio. Whereas the linkage drive in figure 6a(above) have a constant gear ratio.

These gears are locked by reaching a dead-center position. If the gear is locked any forces can be applied at the output part (number 2 in figure 6a(below)). That means the state of locking cannot be overcome because it is proportional to the force F (unless the gear is destroyed). This position is shown in figure 6a(below) with the lines $R1$ and $R2$.

Additionally in the patent (DE 10127676 A1) figure 5f is given as argument for self-locking. In this thesis this argument cannot be traced because in the literature (Müller, 1998, p.51) this figure is given in content with planetary gears. Instead of that, another argument is given in the following.

In chapter 1.1.1 the self-locking and self-braking definitions accordingly to VDI guideline 2158 are given. Thus to the definition of self-locking it can be argued that self-locking needs friction forces. In the linkage drives which are shown in figure 6a, these friction forces arise in the swivel joints. As it is described in chapter 6.2 an infinitesimal Altscher protector μ leads to infinite forces in the swivel joints. Based on the friction law of Coulomb it can be argued that these forces lead to infinite friction forces in the swivel joints. Therefore it can be argued that the linkage drives are able to perform self-locking.

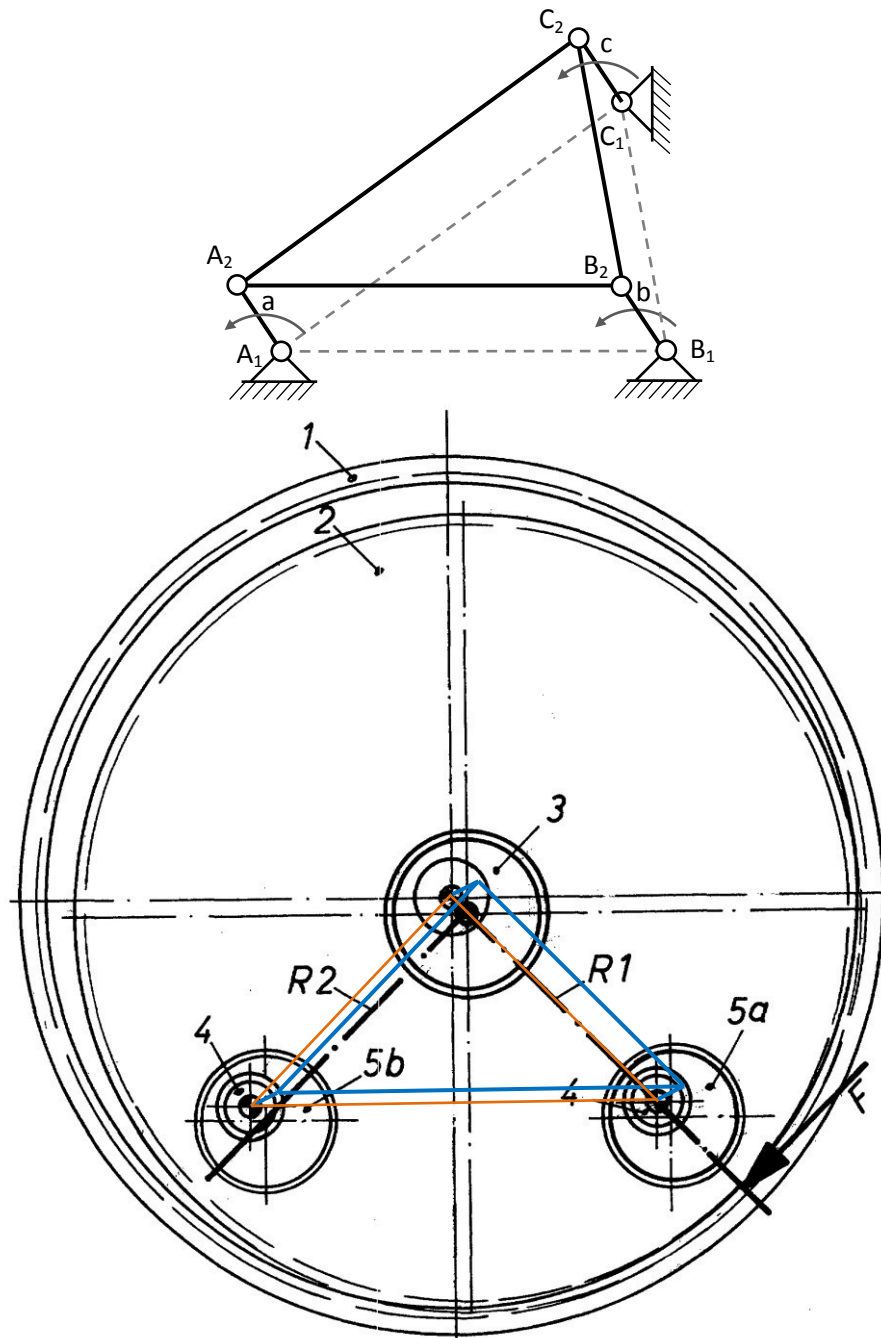


Figure 6a: Comparison of the patent (below: modified from DE 10127676 A1, Fig. 1) with literature (above: accordingly to Volmer, 1978a, p.60)

6.3 Created models

Based on the model which is found in the literature and the patent (compare figure 6a) the following models are created.

The first model is an easy model from literature (DE 10127676 A1) to test the principle of such a linkage drive like it is shown in figure 6a. **Figure 6b** shows the created model. As it is visible the gear would also work if one of the eccentrics is removed. Therefore this linkage drive cannot satisfy the main requirement of this thesis (no usage of an additional device).

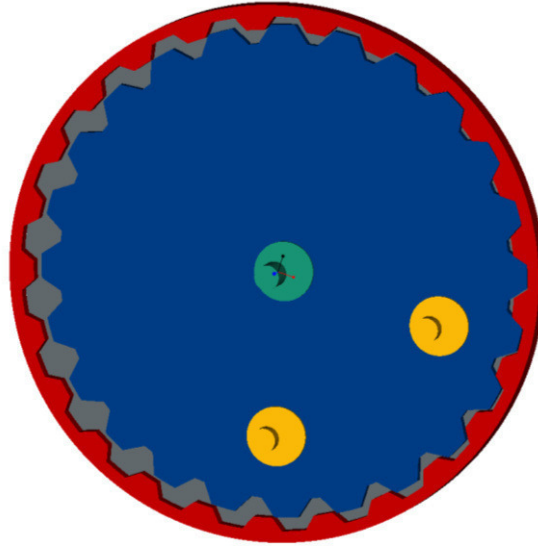


Figure 6b: First model of the linkage drive

This disadvantage is eliminated by the next model which is shown in **figure 6c**. Similar to the model above it consists of two meshes. The first one is a standardized mesh of involute teeth, the second one a mesh of rack and pinion gearing (disk with cyclone shape and rollers). Thus less friction in the mesh can be expected (and hence high overall efficiency). The following set of equations (6-4) is necessary to determine the cyclone shape (Lehmann, 1976, p.20÷23).

$$\left. \begin{aligned} x &= \frac{1}{2} (d_{b2} + d_2) * \cos \left(\frac{d_2}{d_{rol}} * \vartheta \right) + e * \cos \left(\frac{d_2}{d_{rol}} * \vartheta + \vartheta \right) \\ y &= \frac{1}{2} (d_{b2} + d_2) * \sin \left(\frac{d_2}{d_{rol}} * \vartheta \right) + e * \sin \left(\frac{d_2}{d_{rol}} * \vartheta + \vartheta \right) \end{aligned} \right\} (6-4)$$

Wherein d_2 described the pitch diameter of the disk, d_{rol} the pitch diameter of the output part, e the eccentricity and ϑ the variable parameter.

Due to the usage of the Cyclo disk it is possible to realize smallest diameters because the cyclone shape needs less space. The smallest outer diameter of the gear which can be realized is mainly determined by the required bearings at the eccentrics. This is a typical task for the design procedure. Furthermore it has to be considered that the bearing load is not constant. This is due to the relative position of two bodies, which is described by the Altsche protractor μ .

In addition to the small outer diameter there is another advantage: relatively high gear ratio. This gear ratio is determined by the number of the teeth as presented in equation (6-5).

$$u = \frac{N_{ec}}{N_{inp}} * \frac{N_{rol}}{N_{rol} - N_{disk}} \quad (6-5)$$

Where N_{inp} describes the number of teeth of the input shaft, N_{ec} the number of teeth of the eccentrics, N_{rol} the number of rollers and N_{disk} the number of teeth at the disk.

Due to the usage of the cyclone shape it is possible to realize a difference of number of teeth of one (i.e.: $N_{rol} - N_{disk} = 1$). This leads to a high overall gear ratio (around 30). Whereas the cyclone mesh has a gear ratio of 22.

Furthermore the eccentricity of the gear can be determined by

$$e = \frac{d_2}{2} * \frac{N_{rol} - N_{disk}}{N_{rol}}. \quad (6-6)$$

Where e represents the eccentricity, d_2 the pitch diameter of the disk, N_{rol} the number of rollers and N_{disk} the number of teeth at the disk.

The model which is shown in **figure 6c** satisfies the requirement list fully, because all eccentrics are driven. Thus there is load sharing in the mesh of involute teeth. If one of the eccentrics is removed the design should guarantee that the load at the remaining eccentrics is as high as it is needed to destroy the teeth. Therefore in this model no additional device is used.

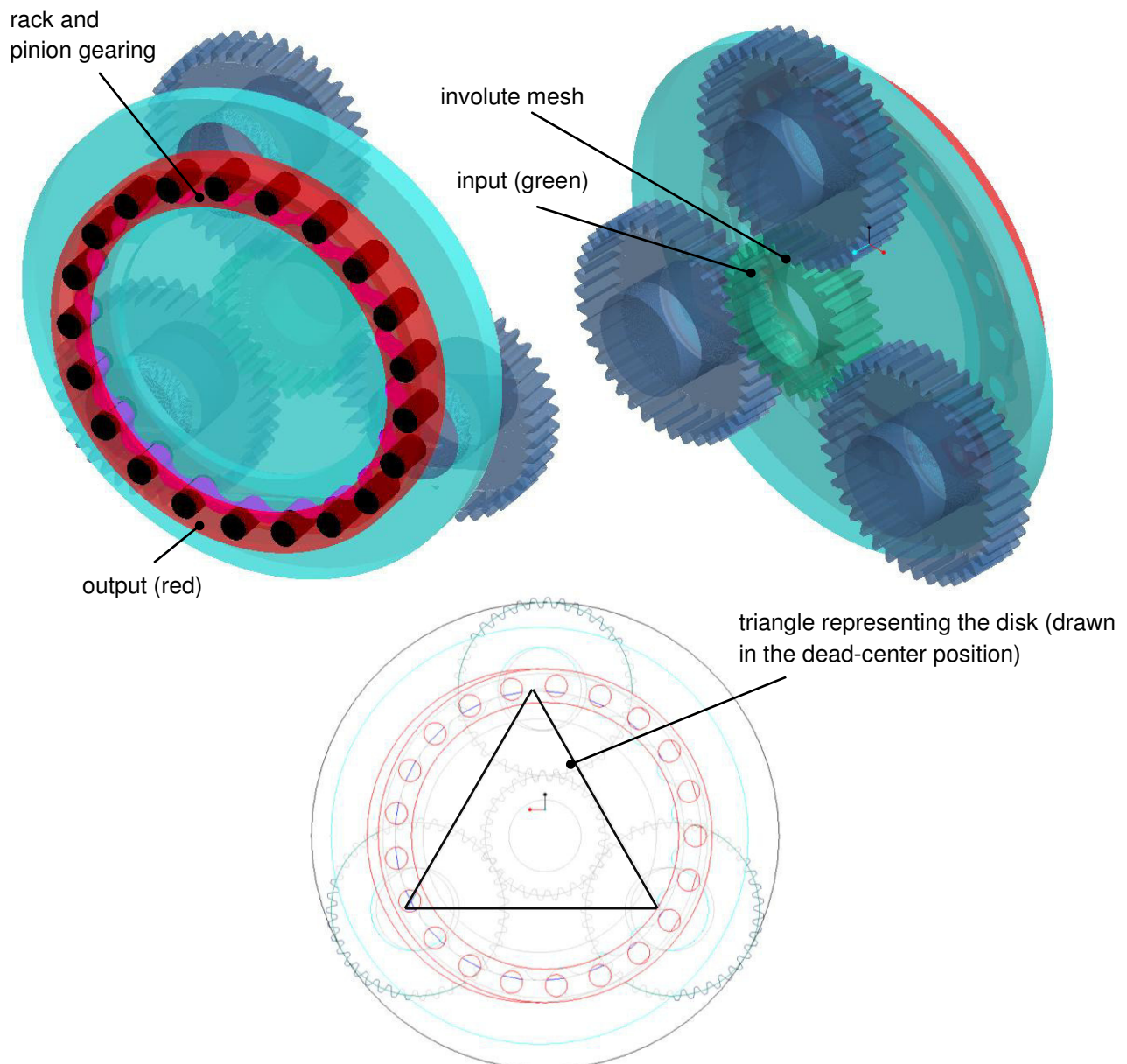


Figure 6c: Second model of the linkage drive

6.4 Conclusion of the linkage drive concept

As it is shown in chapter 6.2, it is possible to create self-locking linkage drives. In chapter 6.3 two models are presented. The last model satisfies the requirement list fully.

It must be noted that the efficiency of this model is not calculated in any way. But due to the rack and pinion gearing high efficiency can be expected, because in the contact between rollers and disk is very less friction. **Figure 6d** shows the scheme and the power flow of the linkage drive. As it can be seen the overall efficiency of this concept is determined by multiplying the mesh efficiencies of the involute mesh and those of the cyclone mesh.

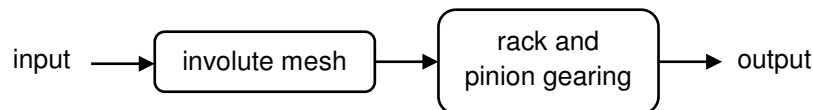


Figure 6d: Scheme of the linkage drive model

Thus it is expected to create a high overall efficiency with this concept. The premise for that is that the mesh efficiencies of both meshes are high.

A disadvantage of this concept is that the eccentrics typically act like additional devices. Only by the use of the involute mesh and through the design task, they should be indispensable necessary for the gear's performance as well as for the self-locking.

In contrast to the other concepts of chapter 4 and 5, the advantage of this concept is the possibility to realize smallest outer diameter. This diameter is mainly influenced by the size of the bearings which are used. Therefore this is also a task for the design procedure.

7 Evaluation

During the course of this thesis, several models are created, of which it can be expected that they are able to satisfy the requirement list. To clarify the extent how far these models fulfill the requirements, it is necessary to evaluate these models. Further aims of the evaluation are the objective and verifiable documentation of the decision process. It should be noted that in this evaluation procedure, models (e.g. concepts) with a corresponding level of information are assessed. This results in the problem that 'hard facts' (e.g. stresses) cannot be assessed. But this is not the essential aim of this thesis. Another problem is the selection of the criteria for evaluation because the models have very different properties. In this thesis a list criteria accordingly to the requirement list is chosen. As well as the requirement list (table 1.1) this list of criteria is also transferable to other applications which must ensure a cheap, quiet, safe and rough 24-hour operation.

In the literature (Pahl, 2007) many procedures for such an evaluation are given. In this thesis the approach accordingly to VDI guideline 2225 is chosen because this is a useful approach to evaluate concepts. That means arrangements with a low level of information.

7.1 Procedure of the evaluation accordingly to VDI 2225

This procedure is based on the fact that the total utility of any system increases if more partial benefit values with higher amount can be created in the system of evaluation. Accordingly the partial benefit values are summed up to the total utility.

In its core the evaluation procedure accordingly to VDI 2225 follows the following steps:

1) *Imagination of the aims and selection of the evaluation criteria*

In general the first step is to imagine the aims of the problem and to derive criteria for evaluation out of this aims.

2) *Weighting of the evaluation criteria*

If the properties of the evaluation criteria are very different, it is suitable to determine weighting factors. These weighting factors can be obtained by e.g. customer survey or paired comparison. In this master thesis the paired comparison is chosen. For this, the evaluation criteria are arranged in a square matrix as shown in **table 7.2**. Each criterion is evaluated against each other. The scale which is used in this thesis is shown in **table 7.1**. After evaluation against each other, the sum for each criterion is determined. With these sums a total sum is obtained. By dividing the sum of each criterion by the total sum, the weighting factors are calculated.

3) *Collecting properties of the solution*

The properties of all subjects of evaluation have to be collected and listed. In general this step is part of information and confrontation with the subject of evaluation.

Table 7.1: Scale which is typical be used for paired comparison (Pahl, 2007, p.178)

rating	meaning
0	less important
0.5	equal important
1	more important

Table 7.2: Example of a paired comparison

	criterion 1	criterion 2	criterion 3	
criterion 1		1	0.5	
criterion 2	0		0	
criterion 3	0.5	1		
sum	0.5	2	0.5	3
weighting factor	16.66%	66.66%	16.66%	

4) *Choosing general scale of values*

These values are needed to assess the subjects of evaluation. The scale is given by the VDI guideline and is shown in **table 7.3**.

Table 7.3: Scale of VDI 2225 guideline (Pahl, 2007, p.172)

rating	meaning
0	insufficient
1	just acceptable
2	adequate
3	well
4	very well

As it can be seen in table 7.1, the steps of assessment are large. Thus to that, this procedure is useful to evaluate concepts.

5) *Work out special scale of values*

In this step of the procedure it is possible to assign a problem-specific scale of values to the general scale of values. Therefore detail information about the subjects of evaluation is necessary.

6) *Evaluation of the subjects*

Each evaluation criterion of each subject of evaluation has to be assessed. These values are determined by the subjective value proposition of the author of the evaluation.

7) *Calculation of the total utility*

The sum of all assessed evaluation criteria gives the total utility of each subject. Those which gives the largest total utility fulfills the requirement list better than the other subjects of evaluation.

7.2 Evaluation procedure in detail

1) Imagination of the aims and selection of the evaluation criteria

As mentioned in chapter 7.1, the first step is to find out the criteria for evaluation. In this thesis the aims and requirements are given by the job definition. Thus the criteria for evaluation are mainly given by the requirement list (chapter 1.3).

2) Weighting of the evaluation criteria

The following **table 7.4** presents the paired comparison in detail. The assessments are a direct result of the importance of the aims of this thesis. As example the first row of **table 7.4** will be explained in the following. Reaching small diameters is a main aim in this thesis. In row one this can be seen as the follows.

The importance of the aim 'outer diameter as small as possible' is higher than most of the other aims e.g. parallel or coaxial axes. Thus it is assed with 1. Those aims which are equal important as the aim 'outer diameter as small as possible', are evaluated with 0.5 (e.g. continuous movement). The aims which are less important are evaluated with 0 (e.g. small bearing area).

As it can be seen in **table 7.4**, the main important influence is continuous movement, followed by the criteria 'driving in both directions', 'high efficiency while operation' and 'uncomplicated self-locking'. **Figure 7a** gives a compact overview of the results of the paired comparison.

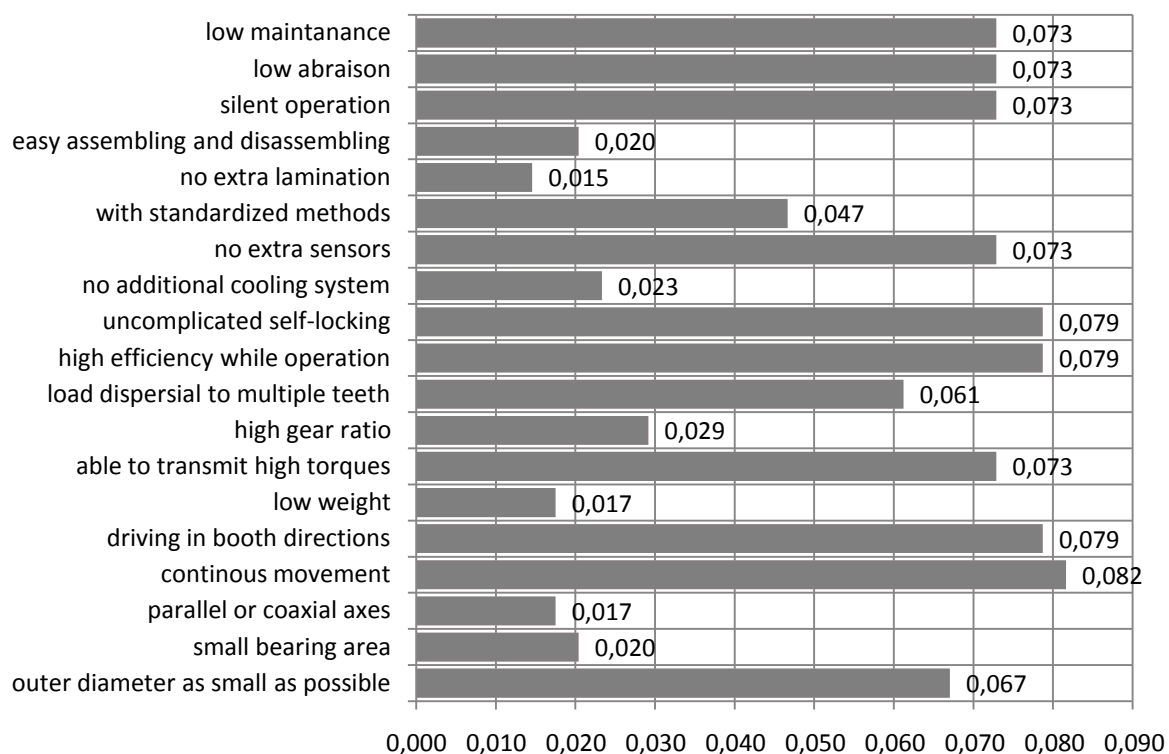


Figure 7a: Overview of the paired comparison

Table 7.4: Paired comparison in detail

	outer diameter as small as possible	small bearing area	parallel or coaxial axes	continuous movement	driving in both directions	low weight	able to transmit high torques	high gear ratio	load dispersal to multiple teeth	high efficiency while operation	uncomplicated self-locking	no additional cooling system	no extra sensors	with standardized methods	no extra lamination	easy assembling and disassembling	silent operation	low abrasion	low maintenance
outer diameter as small as possible		1	0	0.5	0.5	0	0.5	0	0.5	0.5	0.5	0	0.5	0.5	0	0	0,5	0,5	0,5
small bearing area	0		0.5	1	1	0.5	1	1	1	1	1	0.5	1	1	0.5	0.5	1	1	1
parallel or coaxial axes	1	0.5		1	1	0.5	1	0.5	1	1	1	0.5	1	1	0.5	0.5	1	1	1
continuous movement	0.5	0	0		0.5	0	0.5	0	0	0.5	0.5	0	0	0	0	0	0,5	0,5	0,5
driving in both directions	0.5	0	0	0.5		0	0.5	0	0	0.5	0.5	0	1	0	0	0	0,5	0,5	0,5
low weight	1	0.5	0.5	1	1		1	1	1	1	1	0.5	1	0.5	0.5	0.5	1	1	1
able to transmit high torques	0.5	0	0	0.5	0.5	0		0.5	0.5	0.5	0.5	0	0.5	0	0	0	0,5	0,5	0,5
high gear ratio	1	0	0.5	1	1	0	0.5		1	1	1	0.5	1	0.5	0.5	0.5	1	1	1
load dispersal to multiple teeth	0.5	0	0	1	1	0	0.5	0		1	1	0.5	0.5	0	0	0	0,5	0,5	0,5
high efficiency while operation	0.5	0	0	0.5	0.5	0	0.5	0	0		0.5	0	0.5	0	0	0	0,5	0,5	0,5
uncomplicated self-locking	0.5	0	0	0.5	0.5	0	0.5	0	0	0.5		0	0.5	0	0	0	0,5	0,5	0,5
no additional cooling system	1	0.5	0.5	1	1	0.5	1	0.5	0.5	1	1		1	0.5	0.5	0.5	1	1	1
no extra sensors	0.5	0	0	1	0.5	0	0.5	0	0.5	0.5	0.5	0		0.5	0	0	0,5	0,5	0,5
with standardized methods	0.5	0	0	1	1	0.5	1	0.5	1	1	1	0.5	0.5		0	0	0,5	0,5	0,5
no extra lamination	1	0.5	0.5	1	1	0.5	1	0.5	1	1	1	0.5	1	1		1	1	1	1
easy assembling and disassembling	1	0.5	0.5	1	1	0.5	1	0.5	1	1	1	0.5	1	1	0		1	1	1
silent operation	0.5	0	0	0.5	0.5	0	0.5	0	0.5	0.5	0.5	0	0.5	0.5	0	0		0,5	0,5
low abrasion	0.5	0	0	0.5	0.5	0	0.5	0	0.5	0.5	0.5	0	0.5	0.5	0	0	0,5		0,5
low maintenance	0.5	0	0	0.5	0.5	0	0.5	0	0.5	0.5	0.5	0	0.5	0.5	0	0	0,5	0,5	
171.500	11.50	3.50	3.00	14.00	13.50	3.00	12.50	5.00	10.50	13.50	13.50	4.00	12.50	8.00	2.50	3.50	12.50	12.50	12.50
weighting factors	0.067	0.020	0.017	0.082	0.079	0.017	0.073	0.029	0.061	0.079	0.079	0.023	0.079	0.047	0.015	0.020	0.073	0.073	0.073

3) Collecting properties of the solution

As it is mentioned above the main properties of the models are collected in the chapters 4, 5 and 6. The following tables 7.5 up to 7.9 give a short overview.

4) Choosing general scale of values

For evaluation the approach accordingly to VDI guideline 2225 is chosen in this thesis. Therefore the scale for assessing the concepts is given by the guideline (table 7.3).

5) Work out special scale of values

In this thesis the subjects of evaluation are models (i.e. concepts) with low state of information. Thus there is no detail information about the models (e.g. stresses, Hertzian pressure). Due to this issue, the efficiencies and gear ratios which are given in chapter 4, 5 and 6 do not represent the only values which can be reached with these models. They are only reference values, for evaluation and comparison. Hence it is not necessary to develop individual scales in this thesis.

6) Evaluation of the subjects

Subject 1: Involute self-locking helical gear

This model is shown in figure 4g. **Table 7.5** shows the assessment and the motivation for the values which are assigned.

Table 7.5: Evaluation of the self-locking helical gear

criteria	assessment	motivation
outer diameter as small as possible	0	Spur gears need large outer diameters
small bearing area	3	Only two but large bearings are needed
parallel or coaxial axes	4	No problems
continuous movement	4	No problems
driving in both directions	4	No problems
low weight	1	Due to the large diameters much mass is needed
able to transmit high torques	1	Due to the large profile angel high Hertzian pressures are expected
high gear ratio	1	With small diameters this is not possible
load dispersal to multiple teeth	2	If more axial load is accepted, this is possible
high efficiency while operation	4	As it was shown it is possible to perform with efficiency higher as 90%
uncomplicated self-locking	4	Self-locking behavior works well
no additional cooling system	4	As it was shown lubrication is splash lubrication is possible
no extra sensors	4	Self-locking works without additional signal
with standardized methods	2	Either rack cutters are defined or CNC machines are needed
no extra lamination	1	Due to the high torques it seems to be not possible
easy assembling and disassembling	4	Due to an easy arrangement
silent operation	4	No problems
low abrasion	2	High Hertzian pressure leads to pitting
low maintenance	2	Due to pitting

Subject 2: Wildhaber/Novikov self-locking helical gear

This model is shown in figure 4p. **Table 7.6** shows the assessment and the motivation for the values which are assigned. As mentioned above this model has no self-locking behavior. This is due to a low level of information. Thus the assessment is out of competition. If the evaluation shows that this concept is advantageous then it can be investigated in more detail. Hence the assessment is done by assuming high efficiency and uncomplicated self-locking.

Table 7.6: Evaluation of the Wildhaber/Novikov self-locking gear

criteria	assessment	motivation
outer diameter as small as possible	0	Spur gears need large outer diameters
small bearing area	3	Only two but large bearings are needed
axially parallel axis	4	No problems
continuous movement	4	No problems
driving in both directions	4	No problems
low weight	1	Due to the large diameters much mass is needed
able to transmit high torques	3	Due to the favorable contact: lower Hertzian pressure
high gear ratio	1	Due to the small diameters which are needed it is not possible
load dispersal to multiple teeth	2	If more axial load is accepted, this is possible
high efficiency while operation	4	As it was shown it is possible to perform with efficiency higher as 90%
uncomplicated self-locking	4	Self-locking behavior works well
no additional cooling system	4	As it was shown lubrication is splash lubrication is possible
no extra sensors	4	Self-locking works without additional signal
with standardized methods	2	Either rack cutters are defined or CNC machines are needed
no extra lamination	1	Due to the high torques it seems to be not possible
easy assembling and disassembling	4	Due to an easy arrangement
silent operation	4	No problems
low abrasion	3	Lower Hertzian pressure leads to reduced pitting
low maintenance	3	Due to pitting

Subject 3: Self-locking helical gear with load sharing

This model is shown in figure 4t. **Table 7.8** shows the assessment and the motivation for the values which are assigned.

Table 7.7: Evaluation of the load sharing self-locking gear

criteria	assessment	motivation
outer diameter as small as possible	0	Spur gears need large outer diameters
small bearing area	1	More bearings are needed
axially parallel axis	4	No problems
continuous movement	4	No problems
driving in both directions	4	No problems
low weight	0	More wheels are needed

able to transmit high torques	4	Due to load sharing
high gear ratio	1	Due to the small diameters which are needed it is not possible
load dispersal to multiple teeth	4	Due to load sharing
high efficiency while operation	4	As it was shown it is possible to perform with efficiency higher as 90%
uncomplicated self-locking	4	Self-locking behavior works well
no additional cooling system	4	As it was shown lubrication is splash lubrication is possible
no extra sensors	4	Self-locking works without additional signal
with standardized methods	2	Either rack cutters are defined or CNC machines are needed
no extra lamination	1	Due to the high torques it seems to be not possible
easy assembling and disassembling	3	Due to multiple bodies it is more complicated
silent operation	4	No problems
low abrasion	3	Lower Hertzian pressure leads to reduced pitting
low maintenance	3	Due to pitting

Subject 4: Planetary gear with improved connection

This model is shown in figure 5p. **Table 7.8** shows the assessment and the motivation for the values which are assigned.

Table 7.8: Evaluation of the planetary gear with improved connection

criteria	assessment	motivation
outer diameter as small as possible	1	As shown smallest diameters are not possible
small bearing area	2	Multiple bearings are needed
axially parallel axis	4	No problems
continuous movement	4	No problems
driving in both directions	4	No problems
low weight	1	Many parts are needed
able to transmit high torques	3	Complex arrangement
high gear ratio	1	Limited by efficiency
load dispersal to multiple teeth	3	Due to internal load sharing
high efficiency while operation	4	As it was shown it is possible to perform with efficiency higher as 90%
uncomplicated self-locking	4	Self-locking behavior works well
no additional cooling system	4	As it was shown lubrication is splash lubrication is possible
no extra sensors	4	Self-locking works without additional signal
with standardized methods	4	Due to usage of standardized teeth
no extra lamination	1	Due to the high torques it seems to be not possible
easy assembling and disassembling	1	Due to an complex arrangement and bearing areas
silent operation	4	No problems
low abrasion	2	Lower Hertzian pressure leads to reduced pitting
low maintenance	2	Due to pitting

Subject 5: Optimized planetary gear in parallel connection

This model is shown in figure 5q. **Table 7.9** shows the assessment and the motivation for the values which are assigned.

Table 7.9: Evaluation of the optimized planetary gear in parallel connection

criteria	assessment	motivation
outer diameter as small as possible	2	Smaller diameters as in subject 3
small bearing area	2	Multiple bearings are needed
axially parallel axis	4	No problems
continuous movement	4	No problems
driving in both directions	4	No problems
low weight	2	Many parts are needed
able to transmit high torques	3	Complex arrangement
high gear ratio	0	Limited by efficiency; increasing only with additional stages
load dispersal to multiple teeth	3	Due to internal load sharing
high efficiency while operation	4	As it was shown it is possible to perform with efficiency higher as 90%
uncomplicated self-locking	4	Self-locking behavior works well
no additional cooling system	4	As it was shown lubrication is splash lubrication is possible
no extra sensors	4	Self-locking works without additional signal
with standardized methods	4	Due to usage of standardized teeth
no extra lamination	1	Due to the high torques it seems to be not possible
easy assembling and disassembling	2	Due to an complex arrangement and bearing areas
silent operation	4	No problems
low abrasion	3	Lower Hertzian pressure leads to reduced pitting
low maintenance	3	Due to pitting

Subject 6: Planetary gear in parallel connection with Cyclo gear

This model is shown in figure 5r. **Table 7.10** shows the assessment and the motivation for the values which are assigned.

Table 7.10: Evaluation of the planetary gear in parallel connection with Cyclo gear

criteria	assessment	motivation
outer diameter as small as possible	3	Smaller diameters as in subject 3 and 4
small bearing area	3	Multiple bearings are needed
axially parallel axis	4	No problems
continuous movement	4	No problems
driving in both directions	4	No problems
low weight	3	Less parts are needed
able to transmit high torques	4	No problems
high gear ratio	0	Limited by efficiency; increasing only with additional stages
load dispersal to multiple teeth	4	Due to internal load sharing and cyclone shape

high efficiency while operation	4	As it was shown it is possible to perform with efficiency higher as 90%
uncomplicated self-locking	4	Self-locking behavior works well
no additional cooling system	4	As it was shown lubrication is splash lubrication is possible
no extra sensors	4	Self-locking works without additional signal
with standardized methods	3	Due to usage of cyclone shape
no extra lamination	1	Due to the high torques it seems to be not possible
easy assembling and disassembling	2	Due to complex bearing areas
silent operation	4	No problems
low abrasion	4	Due to cyclone shape
low maintenance	4	Due to low abrasion

Subject 7: Linkage drive

This model is shown in figure 6c. **Table 7.11** shows the assessment and the motivation for the values which are assigned.

Table 7.11: Evaluation of the Linkage drive

criteria	assessment	motivation
outer diameter as small as possible	4	Smallest diameter of all the models
small bearing area	2	Multiple bearings are needed; determine the outer diameter
axially parallel axis	4	No problems
continuous movement	4	No problems
low weight	3	Less parts are needed
able to transmit high torques	4	No problems
high gear ratio	1	Limited by the outer diameter; increasing only with additional stages
load dispersal to multiple teeth	4	Due to internal load sharing and cyclone shape
high efficiency while operation	4	As it was shown it is possible to perform with efficiency higher as 90%
uncomplicated self-locking	4	Self-locking behavior works well
no additional cooling system	4	As it was shown lubrication is splash lubrication is possible
no extra sensors	4	Self-locking works without additional signal
with standardized methods	3	Due to usage of cyclone shape
no extra lamination	1	Due to the high torques it seems to be not possible
easy assembling and disassembling	3	Due to easy design
silent operation	4	No problems
low abrasion	4	Due to cyclone shape
low maintenance	4	Due to low abrasion

7) Calculation of the total utility

To find out which of the models above fulfills the requirement list best, it is necessary to calculate the total efficiency of all these models.

Table 7.12 shows the outcome of this last step in the procedure.

As it can be seen in table 7.12, the highest rated model is the 'Linkage drive', followed by the 'Planetary gear in parallel connection with the Cyclo gear' and the 'Optimized planetary gear in parallel connection'. Furthermore it can be seen that the models 'Planetary gear with improved connection' and the 'Wildhaber/Novikov self-locking helical gear' have almost the same total utility. Although the self-locking behavior of the 'Wildhaber/Novikov self-locking helical gear' is not entirely clear, the evaluation shows that, whether the self-locking occurs or not, this concept is not able to fulfill the requirement list as well as the 'Linkage drive'. It is only a little bit better than the other 'Involute self-locking helical gear'. Hence this concept does not have to be further investigated.

In addition to the results of table 7.12, **figure 7b** shows the profiles of the evaluation. On the ordinate all criteria and on the abscissa the weighted assessments are plotted.

Ideally, a profile of a well rated solution has a balanced assessment in all criteria. As it is shown in figure 7b, no concept has such a balanced assessment. This is due to the different properties of the criteria and the models. It can be seen that in some criteria, e.g. 'continuous movement', silent operation' all models have the same assessment. Furthermore it can be seen that the high benefit value of the 'Linkage drive' is mainly due to the small diameter, which is not reached by any other concept.

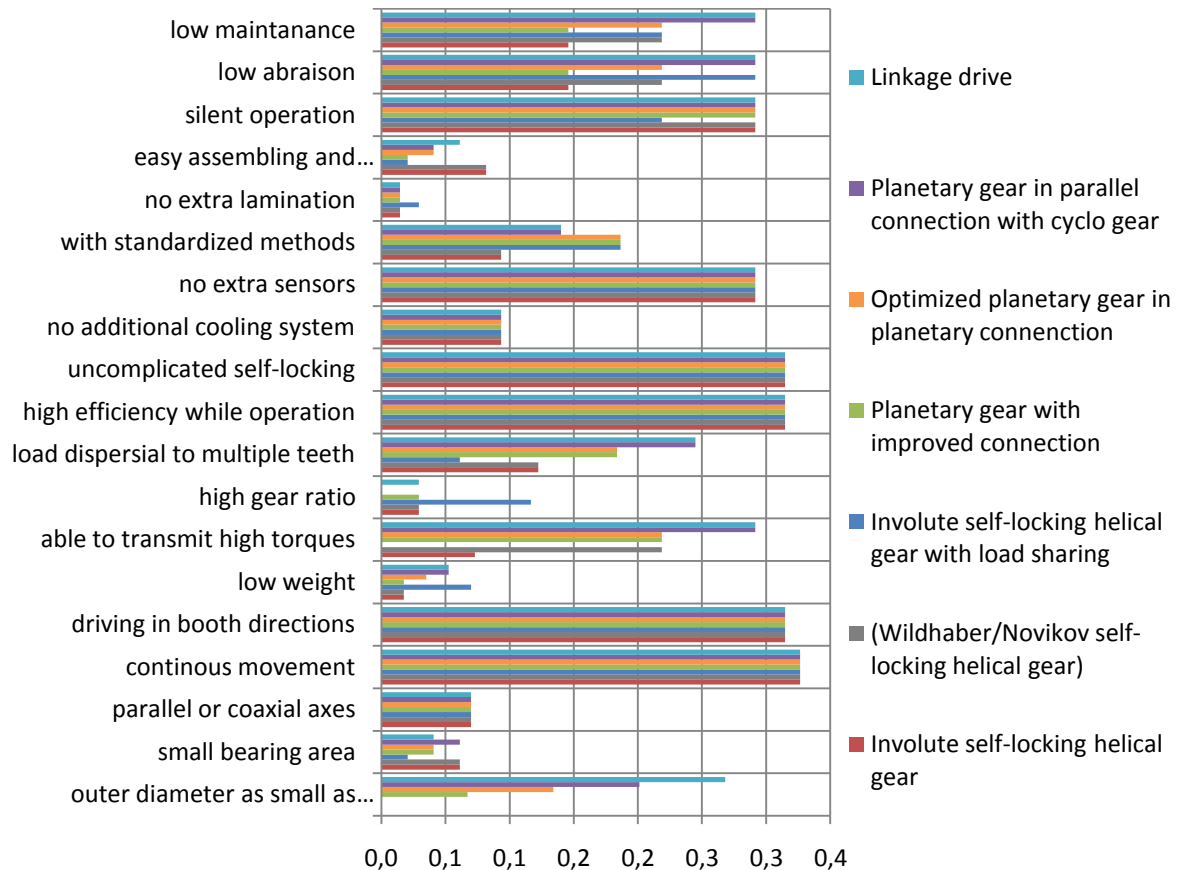


Figure 7b: Summary of the evaluation

Table 7.12: Total utility of all concepts

		Involute self-locking helical gear		(Wildhaber/Novikov self-locking helical gear)		Involute self-locking helical gear with load sharing		Planetary gear with improved connection		Optimized planetary gear in planetary connection		Planetary gear in parallel connection with Cyclo gear		Linkage drive	
	weighting factor	assessment	weighted assessment	assessment	weighted assessment	assessment	weighted assessment	assessment	weighted assessment	assessment	weighted assessment	assessment	weighted assessment	assessment	weighted assessment
outer diameter as small as possible	0.067	0	0.00	0	0.00	0	0.00	1	0.07	2	0.13	3	0.20	4	0.27
small bearing area	0.020	3	0.06	3	0.06	1	0.02	2	0.04	2	0.04	3	0.06	2	0.04
parallel or coaxial axes	0.017	4	0.07	4	0.07	4	0.07	4	0.07	4	0.07	4	0.07	4	0.07
continuous movement	0.082	4	0.33	4	0.33	4	0.33	4	0.33	4	0.33	4	0.33	4	0.33
driving in both directions	0.079	4	0.31	4	0.31	4	0.31	4	0.31	4	0.31	4	0.31	4	0.31
low weight	0.017	1	0.02	1	0.02	4	0.07	1	0.02	2	0.03	3	0.05	3	0.05
able to transmit high torques	0.073	1	0.07	3	0.22	0	0.00	3	0.22	3	0.22	4	0.29	4	0.29
high gear ratio	0.029	1	0.03	1	0.03	4	0.12	1	0.03	0	0.00	0	0.00	1	0.03
load dispersal to multiple teeth	0.061	2	0.12	2	0.12	1	0.06	3	0.18	3	0.18	4	0.24	4	0.24
high efficiency while operation	0.079	4	0.31	4	0.31	4	0.31	4	0.31	4	0.31	4	0.31	4	0.31
uncomplicated self-locking	0.079	4	0.31	4	0.31	4	0.31	4	0.31	4	0.31	4	0.31	4	0.31
no additional cooling system	0.023	4	0.09	4	0.09	4	0.09	4	0.09	4	0.09	4	0.09	4	0.09
no extra sensors	0.073	4	0.29	4	0.29	4	0.29	4	0.29	4	0.29	4	0.29	4	0.29
with standardized methods	0.047	2	0.09	2	0.09	4	0.19	4	0.19	4	0.19	3	0.14	3	0.14
no extra lamination	0.015	1	0.01	1	0.01	2	0.03	1	0.01	1	0.01	1	0.01	1	0.01
easy assembling and disassembling	0.020	4	0.08	4	0.08	1	0.02	1	0.02	2	0.04	2	0.04	3	0.06
silent operation	0.073	4	0.29	4	0.29	3	0.22	4	0.29	4	0.29	4	0.29	4	0.29
low abrasion	0.073	2	0.15	3	0.22	4	0.29	2	0.15	3	0.22	4	0.29	4	0.29
low maintenance	0.073	2	0.15	3	0.22	3	0.22	2	0.15	3	0.22	4	0.29	4	0.29
total utility		2.80		(3.09)		2.96		3.09		3.31		3.65		3.74	

8 Conclusion of the master thesis

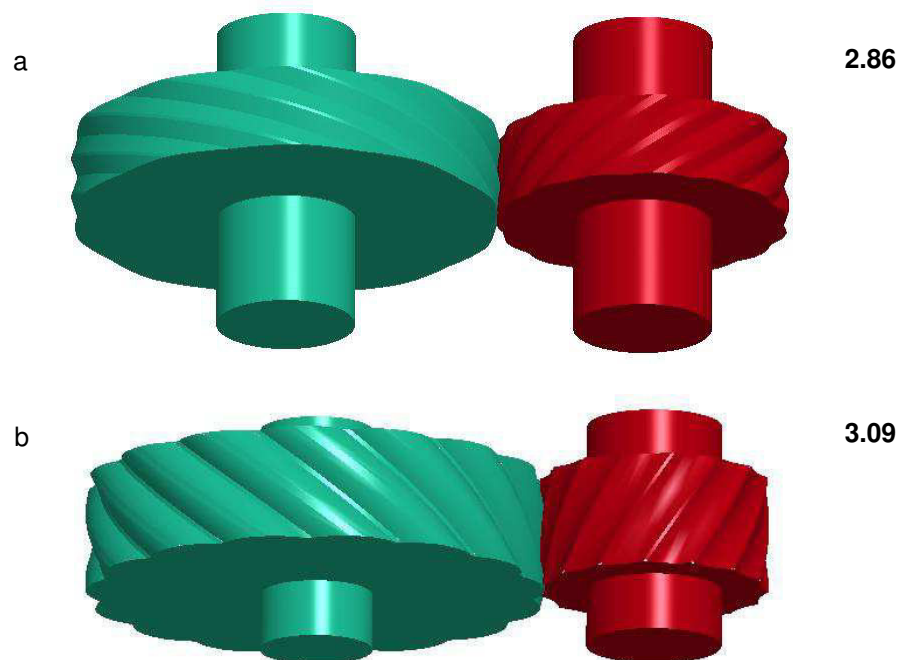
In this master thesis the possibility for self-locking on selected gears had been studied. This was done to fulfill a given requirement list. This list includes typical demands of mechanical engineering.

One very special requirement was that no additional device should be used for triggering self-locking. Other demands in this thesis were

- outer diameter as small as possible,
- driving in both directions,
- high gear ratio (around 100),
- uncomplicated self-locking behavior and
- high efficiency while normal operation.

Based on the state of the art, some kinds of gears were selected due to their potential for self-locking. These gears were the self-locking helical gear, the planetary gears in parallel connection and the linkage drive. Subsequently, these gears were calculated with Mathcad and modeled with Pro/Engineer. In which it must be mentioned that the efficiency and the geometry were only calculated for the involute self-locking helical gear and the planetary gears in parallel connection. At the linkage drive only the geometry of the meshes is calculated. After a multi body dynamics simulation, these models were analyzed. Whereat it must be mentioned that the simulation was not done by the author of this thesis; therefore it was not part of it.

After the analysis of the models, it was attempted to eliminate the disadvantages of them. This leads to new models. This new models were modeled and evaluated accordingly to VDI 2225. A summary of all subjects of evaluation is shown in the next **figure 8a**.



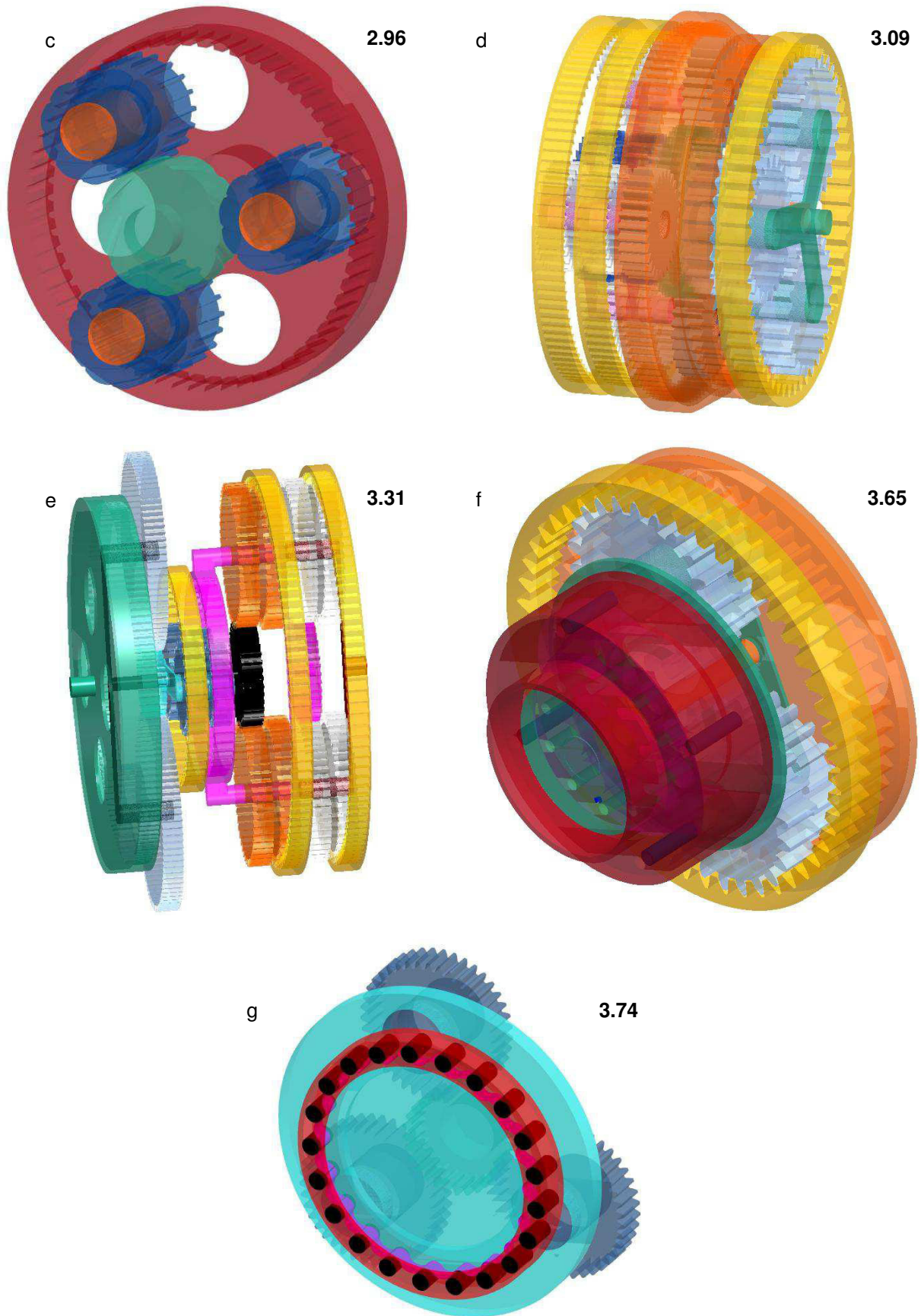


Figure 8a: Evaluated models: Involute self-locking helical gear (a), Wildhaber/Novikov self-locking helical gear (b), Self-locking helical gear with load sharing (c), Planetary gear with improved connection (d), Optimized planetary gear (e), Planetary gear in parallel connection with a Cyclo gear (f) and Linkage drive (g)

In figure 8a, the models were ranked by the occurrence in this thesis. Top right in each picture the figure also includes the benefit values of the concepts.

As it is visible the 'Involute self-locking helical gear' was assessed lowest. This is due to the geometry and the resulting disadvantages. As a result this kind of gear is unsuitable to transmit high torques. Due to the convex-concave contact surfaces the 'Wildhaber/Novikov self-locking helical gear' is able to transmit higher torques. The self-locking behavior of this concept was not proved in the multi body simulation. It is expected that this is due to a low state of information. But the evaluation was showing that there is no need to investigate this model in more detail because it was rated only a little bit higher as the 'Involute self-locking helical gear'. The main disadvantage of both models was that it is not possible to realize smallest diameters.

The outcome of the research of the planetary gears in parallel connection was that it is not possible to realize high ratios and high efficiency with smallest diameters. Because of the high base ratios of these gears, this can be explained as a technical contradiction. Thus models with lower gear ratio were created. Of these concepts only the gear planetary gear in parallel connection with the Cyclo gear was able to realize smallest diameters.

In contrast the concept with the linkage drive is able to fulfill more demands of the requirement list. Due to the infinite forces in the joints close to the dead-center position this gear is able to support self-locking. This gear is able to perform with high efficiency and acceptable gear ratio in smallest diameters.

Accordingly to the general steps of a systematic design procedure, the recommendation is made to prepare this solution in more detail.

Literature

- Bhushan, B. (2011) *Principles and applications of tribology* (2nd ed.). New Delhi: 2013
- Bouchè, B. *Selbsthemmende Planetengerieße*. in: VDI report 672. (1988), Düsseldorf: VDI, p.141÷161,
- Bouchè, B. *Selbsthemmende Antriebselemente mit hohem Wirkungsgrad im Vortrieb*. in: VDI report 905. (1998) Düsseldorf: VDI, p.57÷69
- Harnoy, A. (2003) *Bearing Design in Machinery Engineering Tribology and Lubrication*. New York: Marcel Dekker
- Hiersig, H.M. (1995) *Maschinenbau Lexikon*. Düsseldorf: VDI Verlag
- Hinrichsen, L. (2007) *Zustandsübergänge selbsthemmender Getriebe im Ratterbetrieb*. Kassel: university press, Dissertation 2007
- Kapelevich, A.L. (2013) *Direct Gear Design*. Boca Raton: CRC Press
- Künne, B. (2001) *Einführung in die Maschinenelemente* (2nd ed.). Dortmund: Teubner
- Lehmann, M. *Berechnung und Messung der Kräfte in einem Zykloiden-Kurvenscheiben-Getriebe*. Dissertation TU München 1976
- Looman, J. (2009) *Zahnradgetriebe Grundlagen, Konstruktionen, Anwendungen in Fahrzeugen* (3rd ed.). Berlin: Springer
- Müller, H.W., Glover, J.H. (ed.) (1982) *Epicyclic drive trains*. Detroit: Wayne State University
- Müller, H.W. (1998) *Die Umlaufgetriebe: Auslegung und vielseitige Anwendungen* (2nd ed.). Berlin: Springer
- Niemann, G., Winter, H. (2003) *Maschinenelemente Band 2: Getriebe allgemein, Zahnradgetriebe, Stirnradgetriebe* (2nd ed.). Berlin: Springer
- Pahl, G. Beitz, W., Feldhusen, J., Grote, K.H. (2007) *Pahl/Beitz Konstruktionslehre Grundlagen* (7th ed.). Berlin: Springer
- Phillips, J. (2003) *General Spatial Involute Gearing*. Sydney: Springer
- Perović, B. (2002) *Berechnung von Maschinenelementen: Grundlagen-Formelsammlung-Berechnungsbeispiele* (2nd ed.). Renningen: expertVerlag
- property right DE 3442138 A1 (22.05.1986), Reihn-Getriebe GmbH. Pr.: DE 3442138 17.11.1984 –Selbsthemmendes Schneckengetriebe
- priority right DE 10127676 A1 (12.11.2002), Strach, L., Pr.: DE 10127676 10.06.2001
- priority right DE 10261588 A1 (15.07.2004), Strach, L., Pr.: DE 10261588 24.12.2008 – Selbsthemmendes Zahnrad-Kreisschub-Getriebe mit maximalem Überdeckungsgrad
- priority right DE 19515132 A1 (16.11.1995), Brosowitsch, J., Pr.: DE 19515132 25.04.1995

- priority right GB 266163 A (not specified) , Wildhaber, E., Pr.: GB 26613 24.02.1927 – Improvements in or relating to toothed Gearing
- Radzevich, S.P., Dudley, D.W. (2012) *Handbook of practical gear design and manufacture* (2nd ed.). Boca Raton: CRC Press
- Ravi, V. (2011) *Theory of Machines (Kinematics)*. New Delhi: PHI Learning
- Rohloff AG. <http://www.rohloff.de/index.php?id=1429>. called on: 25.08.2013
- Tabor, D., Winer, W.D. *Lubrication of Metals with Silicones at High Pressures and Low Sliding speed*. in: The Institute of Petroleum (1966) *Gear Lubrication*. Amsterdam: Elsevier Publishing
- Volmer, J. (1978a) *Getriebetechnik Lehrbuch*. Karl-Marx-Stadt: VEB
- Volmer, J. (1978b) *Getriebetechnik Umlaufrädergetriebe*. Karl-Marx-Stadt: VEB
- Wittel, H., Muhrs, D., Jannasch, D., Voßiek, J. (2011) *Roloff/Matek Maschinenelemente* (20th ed.). Wiesbaden: Vieweg+Teubner
- Wyndorps, P. (2004) *3D-Konstruktion mit Pro/Engineer–Wildfire* (2nd ed.). Haan-Gruiten: Europa-Lehrmittel

Appendix

A -Creating a cad-model

In the following it is described how to create an exact model of a helical gear in 3-dimensional cad software (e.g. Pro/Engineer).

There are several possibilities to create such a model. In the literature (Wyndorps, 2004) some of them are given to create standardized helical gears. These models are not useful in this thesis. This results because the self-locking helical gear needs very high x-shift modifications and helix angles. The corresponding calculation procedure is described in chapter 4.2.2. In the following it is specified how to create such a self-locking helical gear with involute teeth. This model is done in Pro/Engineer. In its core the ideas of this approach are also useful for other spur or helical gears and also for other software which is similar to Pro/Engineer.

The following **figure 9a** shows the assembling of a possibly arrangement. As it can be seen this model has an extreme x-shift.

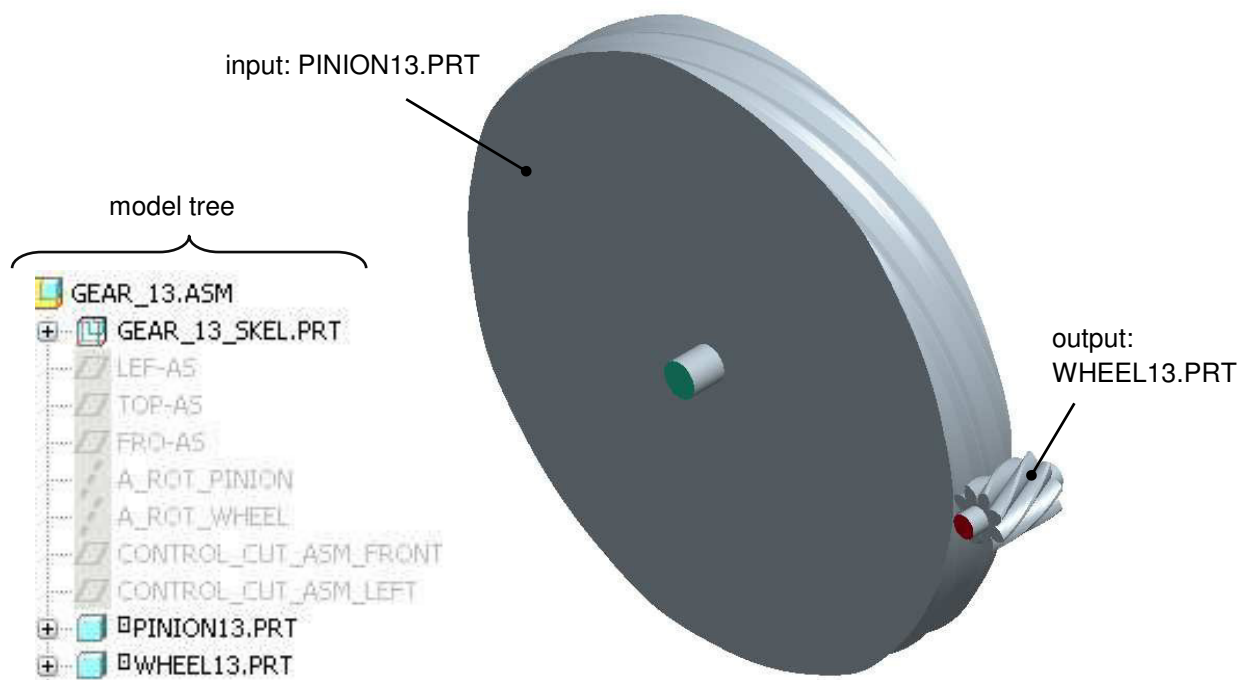


Figure 9a: Assembling

In the model tree the structure of the model is shown. The assembling consists of a skeleton part (GEAR_13_SKEL.PRT) which contains the main information. After the skeleton part some standard planes are defined (LEF-AS, TOP-AS and FRO-AS). Additionally the rotational axes of the two bodies are added (A_ROT_PINION and A_ROT_WHEEL). The planes 'CONTROL_CUT_ASM_FRONT' and 'CONTROL_CUT_ASM_LEFT' are defined to view the mesh in different sections.

Figure 9b(right) shows the model tree of the skeleton part. This part only consists of lines, planes and sketches. The first feature which is implemented is a Mathcad data file

(MCAD01_ANALYSIS). This file includes the calculation approach like it is described in chapter 4.2.2. The results of the calculation procedure are sent to Pro/Engineer. With this data, it is possible to create a plane for the wheel (RIGHT_WHEEL) and the axes for pinion and wheel (A_P and A_W). After defining two cylindrical coordinate systems (C_PIONION and C_WHEEL) and a sketch which includes the main diameters (DIAMETERS), two equations are implemented (PINION_HELP and WHEEL_HELP).

These equations define lines of the involute functions whereat these lines are ending at any point. But it is suitable that these lines intersecting the plane TOP with their endpoint. Hence it is necessary to rotate the involute functions. To determine the inclination of the rotation, a sketch (MEASUREMENT) is implemented (figure 9c). In this sketch the angel between the actual endpoint and the plane TOP is measured. With this inclination the set of equations to define the exact involute shape of the teeth is modified. The new set of equations can be presented as

$$\left. \begin{aligned} \varphi &= t * \sqrt{\left(\frac{d_a^2}{4 * r_b^2} - 1\right)} \\ r &= r_b * \sqrt{1 + \varphi^2} \\ \theta &= \frac{180}{\pi} * \left(\varphi - \frac{\pi}{180} * \text{atan}(\varphi)\right) - \left[\alpha + \frac{S_a}{d_a} * \frac{180}{\pi}\right] \end{aligned} \right\} (9-1)$$

Wherein φ describes any angel, t an internal parameter of Pro/Engineer, d_a the addendum diameter of the body, r_b the radii of the base diameter, r the radii of the involute function, θ the inclination of the involute function, α the inclination of the endpoint (result of the measurement) and S_a the tooth width at the addendum diameter.

In the set of equations (9-1) that term in the last equation, which is in square brackets, identifies the term which is indicated by the measurement. With this term it is possible to rotate the involute function to the correct endpoint.

After that, equations for the pinion and the wheel tooth shape (drive and coast side) are defined (PINION_DRIVE, PINION_COAST, WHEEL_DRIVE and WHEEL_COAST). This gives the exact shape of the teeth with the endpoint at the plane TOP.

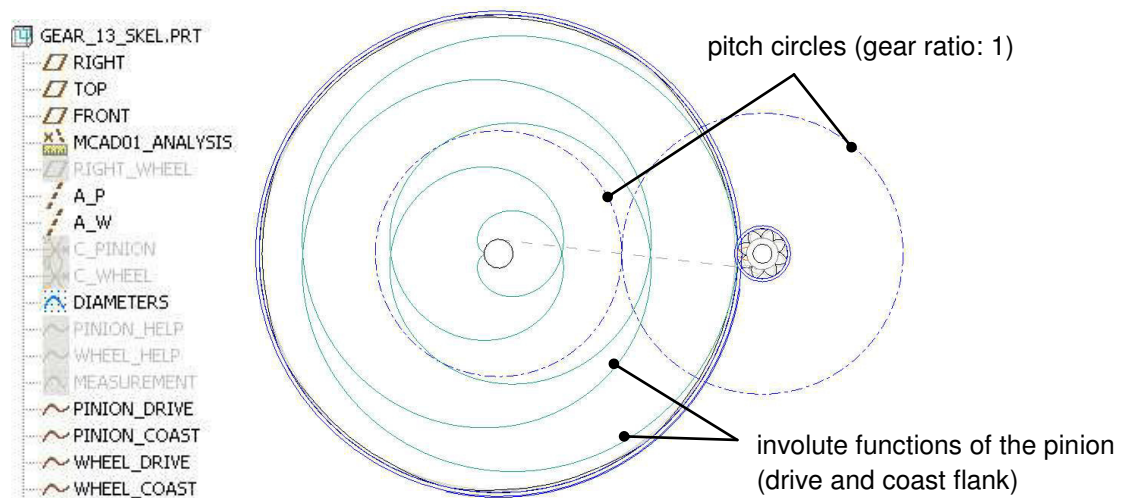


Figure 9b: Model tree of the skeleton part (right) and skeleton part (left)

Figure 9c shows the measurement which is necessary to determine the inclination.

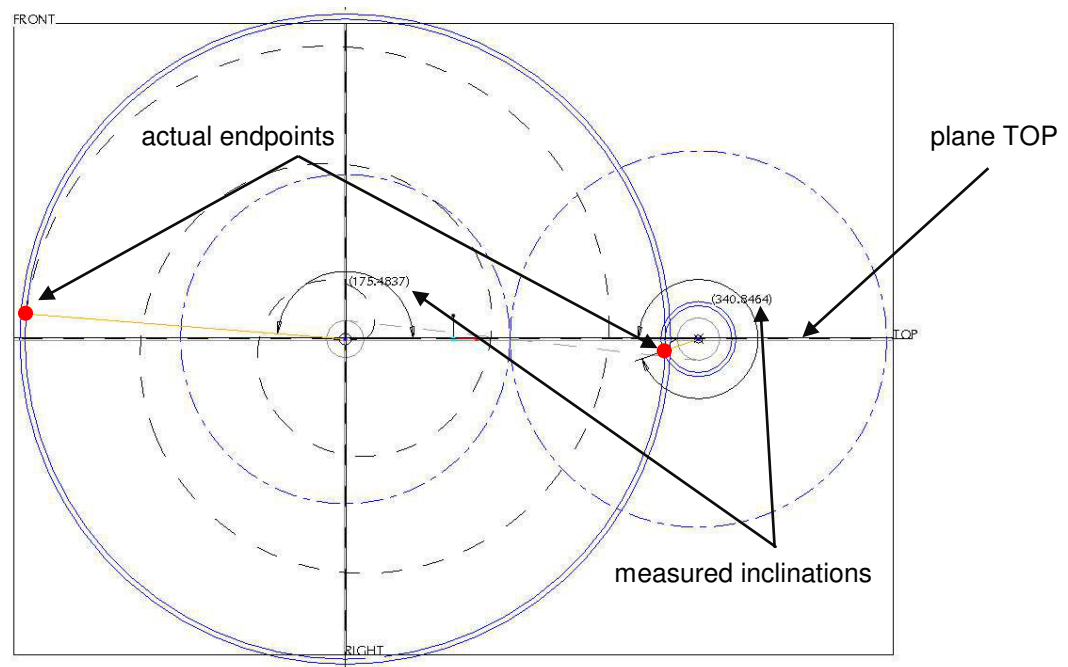


Figure 9c: Sketch of the measurement

Figure 9d shows the pinion of that gear arrangement. The structure of the pinion and the wheel is the same, therefore only one body is described in detail. The outcome of the Mathcad file is also used in these parts. After implementing a tangential plane (TANG, tangential to the addendum diameter), a sketch including a straight line is defined. This line is inclined with the helix angle at the addendum diameter (STRAIGHT_LINE). The next step is to extrude a surface for the addendum diameter (EXTRUDE_ADDENDUM_DIAMETER). After that step, the former implemented straight line is wrapped around the addendum diameter (GUIDELINE). This line is needed as guideline to drag the tooth profile (TOOTH_PROFILE). One of these profiles is defined with the variable sweep tool of Pro/Engineer and then it is patterned around the axis of revolution (ROT_PINION). After defining the tooth profiles the remaining body is rotated (BODY). In essence, this body consists of a cylinder with the root diameter as outer diameter.

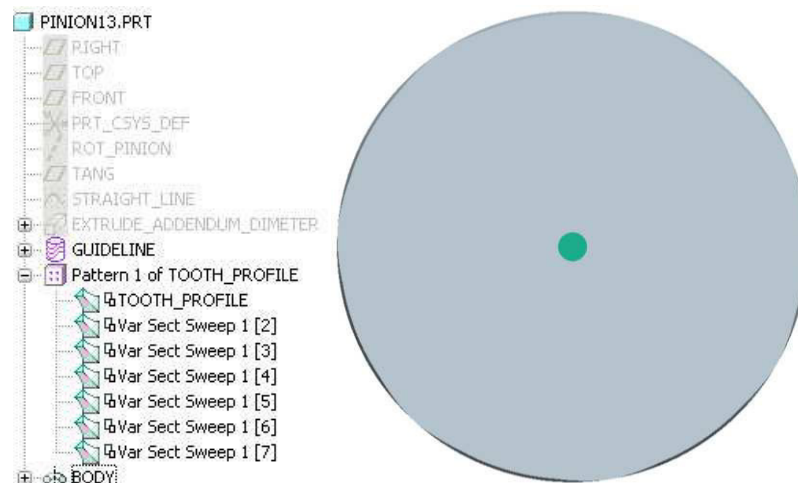


Figure 9d: Pinion of the arrangement

B –Source code of the Matlab plot

To analyze the behavior of the planetary gears, the self-locking condition is plotted. The result shows figure 5h. The figure shows the efficiency in driving situation over a base ratio - base efficiency plane. This diagram is special, because it only represents gears which are self-locking. If a measurement of any point is taken, the designer knows which base efficiency and base ratio would be needed to perform self-locking. Moreover if the considerations of chapter 3.2.3 are taken into account, the designer can imagine the principle gear structure quickly. Therefore figure 5h seems to be suitable for gear designers. In the following it is described in more detail how the figure is plotted. The description of each line is given after the %-sign.

```

step1=0.01;           %Definition of the increment for counting the base efficiency
I0=[]; Eta0=[]; Eta0_1=[]; colCount=[]; I0_mod=[]; %Initialization of some matrices
col=1; row=1;         %Initialization of counting variables

for eta0=0:step1:1      %Starting a for-loop for the base efficiency
    eta0_1=1/eta0;      %Calculating the reciprocal of the base efficiency
    Eta0=[Eta0,eta0];   %Saving the actual base efficiency
    Eta0_1=[Eta0_1,eta0_1]; %Saving the actual reciprocal of the base efficiency
    step2=abs(eta0_1-eta0)*step1; %Calculation of another increment for counting the
                                base ratio as a multiple of the first increment
    for i0=eta0:step2:eta0_1 %Starting a for-loop for the base ratio
        I0(col,row)=i0;    %Saving the actual base ratio
        col=col+1;         %Increase the counter of the columns
    end                    %Finishing the for-loop of the base ratio
    row=row+1;             %Increase the counter of the rows
end                        %Finishing the for-loop of the base efficiency

for row=1:1:size(I0,2) %Starting a for-loop in order to initialize a counter variable for the rows
    for col=1:1:size(I0,1) %Starting a for-loop in order to initialize a counter variable for
                            the columns
        if I0(col,row) ~= 0
            colCount=[colCount,col]; %If the actual base ratio is not equal to zero the
                                      actual value of the column is saved and the
                                      %Counting is stopped
            break
        end %Finishing the if block
    end %Finishing the for-loop of the columns
end %Finishing the for-loop of the rows

for row=1:1:size(I0,2) %Starting a for-loop in order to initialize a counter variable for the rows
    for col=1:1:size(I0,1) %Starting a for-loop in order to initialize a counter variable for
                            the columns
        if I0(col,row) ~= 0 %If the actual base ratio is not equal to zero a for-loop is
                              started to convert the base ratio to a new matrix
            for k=0:1:size(Eta0,2)-1
                I0_mod(k+1,row)=I0(colCount(row)+k,row);
            end %Finishing the for-loop to convert the values
        end %Finishing the if block
    end %Finishing the for-loop of the columns
end %Finishing the for-loop of the rows

for col=1:1:size(Eta0,2)-1 %Starting a for-loop to shift the values to suitable positions
                            inside the matrix
    Eta0(col+1,:)=Eta0(col,:);

```



```

    Eta0_1(col+1,:)=Eta0_1(col,:);
end
I0_mod(:,end+1)=ones(size(I0_mod,1),1);    %Changing the last column of the modified
                                           base ratios to one
I0_mod(:,1)=I0(1,1);    %Changing the first column of the modified base ratios
for row=1:1:size(I0_mod,2)    %Starting a for-loop in order to initialize a counter variable for
                               the rows
    for col=1:1:size(I0_mod,1)    %Starting a for-loop in order to initialize a counter
                                  variable for the columns
        if I0_mod(col,row)>=2    %If block in order to restrict the base ratio with two
            I0_mod(col,row)=2;
        end    %Finishing the if block
    end    %Finishing the for-loop of the columns
end    %Finishing the for-loop of the rows

for row=1:1:size(I0_mod,2)    %Starting a for-loop in order to initialize a counter variable for
                               the rows
    for col=1:1:size(I0_mod,1)    %Starting a for-loop in order to initialize a counter
                                  variable for the columns
        if I0_mod(col,row)<1    %Calculating the efficiency in case of a base ratio
                                smaller than one
            sig=1;
            EtaU(col,row)=(I0_mod(col,row)-
1)/(I0_mod(col,row)*(Eta0(col,row)^sig)-1);
        elseif I0_mod(col,row)>1    &Calculation the efficiency in case of a base ratio
                                    larger than one
            sig=-1;
            EtaU(col,row)=(I0_mod(col,row)-
1)/(I0_mod(col,row)*(Eta0(col,row)^sig)-1);
        end    %Finishing the if block
    end    %Finishing the for-loop of the columns
end    %Finishing the for-loop of the rows

EtaU(:,size(EtaU,1))=ones(size(EtaU,1),1);    %Setting the last column of the
                                           efficiency to one
surf(Eta0,I0_mod,EtaU,'DisplayName','Eta0,I0_mod,EtaU');    %Plotting the surface
figure(gcf);    %Creating a figure
grid on    %Creating a grid in the figure

```